Journal of Medicinal Chemistry

Article

pubs.acs.org/jmc

Discovery and Optimization of Novel Antagonists to the Human Neurokinin-3 Receptor for the Treatment of Sex-Hormone Disorders (Part I)

Hamid R. Hoveyda,* Graeme L. Fraser, Marie-Odile Roy, Guillaume Dutheuil, Frédéric Batt, Mohamed El Bousmaqui, Julien Korac, François Lenoir, Alexey Lapin, Sophie Noël, and Sébastien Blanc

Euroscreen SA, 47 Rue Adrienne Bolland, 6041 Gosselies, Belgium

Supporting Information

ABSTRACT: Neurokinin-3 receptor (NK_3R) has recently emerged as important in modulating the tonic pulsatile gonadotropin-releasing hormone (GnRH) release. We therefore decided to explore NK_3R antagonists as therapeutics for sex-hormone disorders that can potentially benefit from lowering GnRH pulsatility with consequent diminished levels of plasma luteinizing hormone (LH) and correspondingly attenuated levels of circulating androgens and estrogens. The discovery and lead optimization of a novel *N*-acyl-triazolopiperazine NK_3R antagonist chemotype achieved through bioisosteric lead change from the high-throughput screening (HTS) hit is described. A concomitant improvement in the antagonist bioactivity and ligand lipophilic efficiency (LLE) parameter were the principal guidelines in the lead optimization efforts. Examples of advanced lead analogues to demonstrate the amenability of this chemotype to achieving a suitable pharmacokinetic (PK) profile are provided as well as pharmacokinetic−pharmacodynamic (PKPD) correlations to analyze the trends observed for LH inhibition in castrated rats and monkeys that served as preliminary in vivo efficacy models.

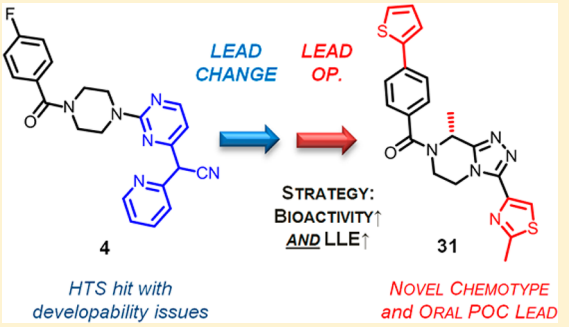

INTRODUCTION

The neurokinin-3 receptor (NK_3R) is a class A GPCR preferentially activated by neurokinin B (NKB) peptide, which together with senktide (a synthetic peptide) are the only known potent and selective agonists at NK_3R.[1] Early studies indicated that NK_3R plays a seminal role in dopaminergic function in the midbrain. As excessive dopaminergic function was conjectured to be responsible for some of the symptoms of schizophrenia, a "hyperdopaminergic hypothesis" was put forth implicating neurokinins in the pathophysiology of cognitive disorders.[2] Consequently, in the past two decades, the main drive for the development of NK_3R antagonists has been their perceived potential as antipsychotics. However, this premise remains unsubstantiated to date, as no clear demonstration of efficacy on cognitive end points were obtained in phase II human clinical trials of compounds **1**, **2a**, and **2b** (Figure 1).[3] Recently, a compelling body of studies clarifies the role of NKB/NK_3R signaling in reproductive neuroendocrinology instead, which forms the basis of the approach for the work described herein.[4]

Reproductive function invokes a plethora of central and peripheral signals that are orchestrated through the hypothalamic pituitary gonadal (HPG) axis that controls the tonic pulsatile GnRH release from puberty onward (Figure 2). Episodic GnRH release coordinates the release of gonadotrophs (i.e., LH and FSH), which in turn stimulate the gonads to produce gametes and ultimately steroidal sex hormones. Signaling through NKB/NK_3R is in fact considered a principal regulatory component of the HPG axis that together with downstream signaling of kisspeptin/GPR54 modulates the so-called GnRH pulse generator (Figure 2).[5] NK_3R is expressed on the so-called **k**isspeptin-**N**KB-**Dy**n (dynorphin A) neurons (KNDy neurons for short)[6] located in the hypothalamic arcuate nucleus (ARC). Under conditions that favor an increase in GnRH, binding of NKB to NK_3R (on KNDy neurons) induces kisspeptin secretion, which acts on GPR54 (on GnRH neurons) with attendant impact on the GnRH pulse regulator (Figure 2). A stimulatory role of NKB on LH release has been reported in several animal models including rodents and monkeys, with a potential interplay in relation to circulating levels of steroid hormones such as estradiol also noted.[7] We have elsewhere reported that compound **3**[8] (Figure 1), the initial proof-of-concept (POC) compound in this project as discussed further below, antagonized senktide but *not* kisspeptin, hence supporting the conclusion that the foregoing lead structures act specifically at the NK_3R level and not further downstream.[9] In 2009, Topaloglu et al. reported that patients with loss-of-function mutations in the genes encoding either NKB or NK_3R exhibit hypogonadotropic hypogonadism and

Received: November 10, 2014

DOI: 10.1021/jm5017413
J. Med. Chem. XXXX, XXX, XXX−XXX

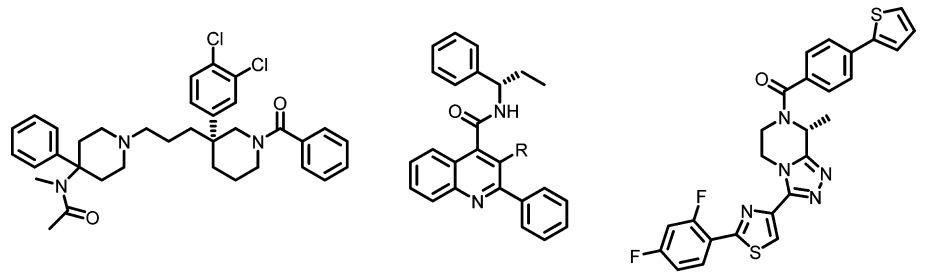

Figure 1. Structures of the two well-known NK_3R antagonist chemotypes (**1**–**2**) and the initial POC candidate from the novel *N*-acyl-triazolopiperazine chemotype discussed herein (**3**).

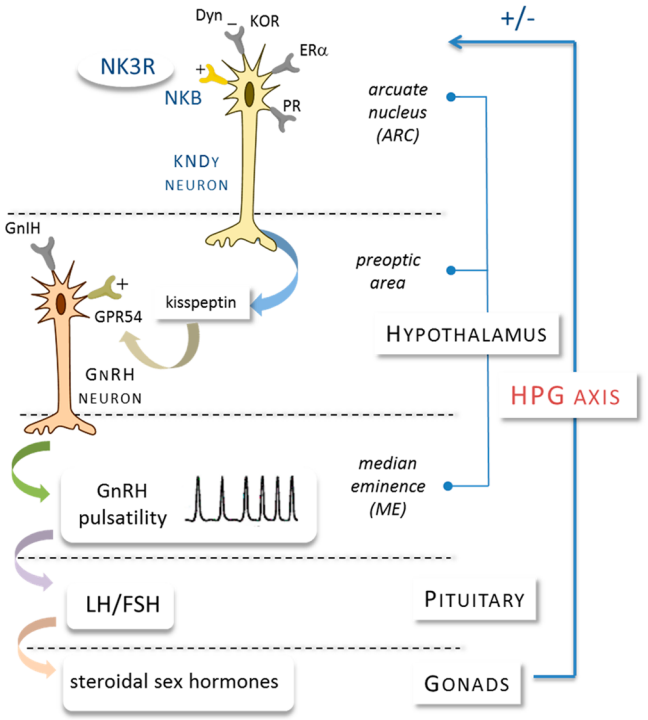

Figure 2. HPG axis and neuroanatomical hierarchy of NKB/kisspeptin/GnRH (+ and − symbols refer to stimulatory and inhibitory feedback effects).

infertility.[10] Importantly, no phenotype of abnormal cognitive behavior was reported in such patients contrary to the expectations from the aforesaid "hyperdopaminergic hypothesis". Moreover, re-examination of the NK_3R knockout mice following Topaloglu's seminal report revealed several common features with the human loss-of-function phenotype, thus supporting the relevance of the rodent in vivo model as a starting point in the project.[11]

Pulsatile GnRH secretion is critical for many physiological processes, notably in the female menstrual cycle. GnRH peptide and synthetic variants have been used through intravenous (iv) or continuous infusion administration to treat a range of sex-hormone disorders such as breast and prostate carcinoma, endometriosis, uterine fibroids (UF),[12] and precocious puberty, as well as for in vitro fertilization (IVF).[13] Whereas GnRH-R agonists cause receptor desensitization, its antagonists competitively block the receptor.[14] Whether as agonists or antagonists, GnRH-R ligands produce the same final outcome: the blockade of the transmission of the GnRH pulse signal and consequent preclusion of FSH and LH secretion. However, the persistent abrogation of gonadotropin secretion causes a hypoestrogenic state that in turn results in bone mineral density (BMD) loss, a notable side effect and a limiting factor regulating the duration of clinical use of GnRH ligands.[15] As an alternative treatment of last resort for endometriosis and UF, for example, surgical intervention is also employed, but such hysterectomies are also not without perils.[16] Therefore, there is clearly a need for novel and safer alternative therapeutic approaches to treat sex-hormone disorders, which is what we believe selective NK_3R antagonists can potentially offer as discussed below.

GnRH pulse frequency controls the selectivity of LH versus FSH induction such that high frequency pulses stimulate LH release as opposed to low frequency pulses that favor FSH induction.[17] Furthermore, a report by Francou et al. in 2011 indicated that patients with a loss of function mutation in NK_3R expressed a phenotype of normosomic congential hypogonadotropic hypogonadism, low plasma LH, and attendant low LH/FSH levels. It was demonstrated that a LH/FSH ratio in normal ranges could be restored with exogenous pulsatile GnRH administration.[18] This biology collectively forms the basis of our NK_3R therapeutic approach toward the treatment of such sex-hormone disorders as polycystic ovarian syndrome (PCOS),[19] a disease with a "neuroendocrine hallmark" of a persistently rapid GnRH pulse favoring pituitary synthesis of LH over FSH and contributing as such to increased plasma LH and attendant high plasma LH/FSH levels.[20] Therefore, antagonism of NK_3R may offer an alternative therapeutic approach for PCOS and related sex-hormone disorders, such as UF and endometriosis, where a decreased GnRH pulse frequency is desirable.[21] We believe that a key potential advantage offered by NK_3R antagonists lies in their capacity to *selectively modulate* the HPG axis, thereby *slowing the GnRH pulse frequency rather than abrogating* it altogether (as is the case with GnRH ligands) and thus obviate the BMD side effect.

The field of nonpeptide NK_3R antagonists was pioneered nearly two decades ago through the discovery of osanetant **1**[22] and talnetant **2a**[23] (Figure 1) and has since been further exploited by various groups.[24] As noted above, their utility as potential antipsychotics (**1**, **2a**, and **2c**) remains unsubstantiated to date. However, recent in vivo results on these compounds suggest efficacy in modulating sex hormones instead, an observation retrospectively justifiable through the proposed HPG axis mode-of-action (Figure 2). For example, **2b** (AZD2624) was reported to cause a dose-dependent decrease of testosterone in healthy human volunteers in a phase 1 study,[25] and talnetant (**2a**) is reported to reduce LH levels in

DOI: 10.1021/jm5017413
J. Med. Chem. XXXX, XXX, XXX−XXX

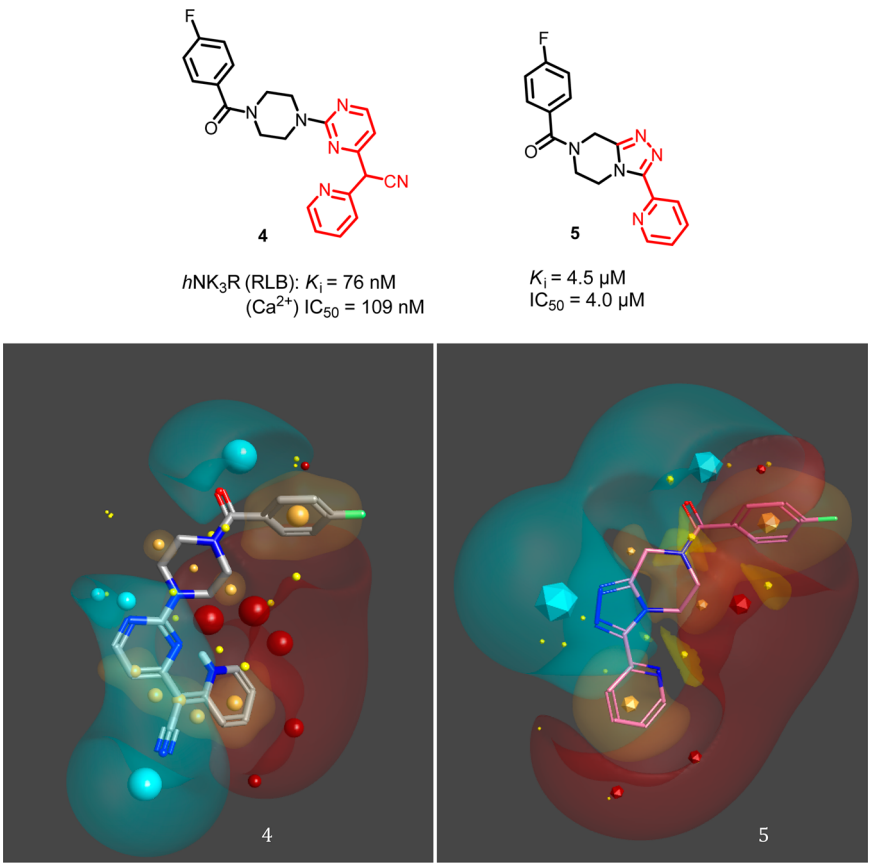

Figure 3. (top panels) HTS hit series prototype structure (**4**)[28] and its bioisosteric modification that served as the starting point for a new NK_3R antagonist scaffold (**5**). (bottom panels) Comparative analysis of 3D electrostatic potential field points (red and blue, positive and negative fields; yellow and gold, van der Waals and hydrophobic fields) using Forge v.10.3 (Cresset Biomolecular Discovery, UK)[29] showing ≥70% similarity in terms of shape and field similarities between the two structures.

Scheme 1. Synthesis of Analogues[a]

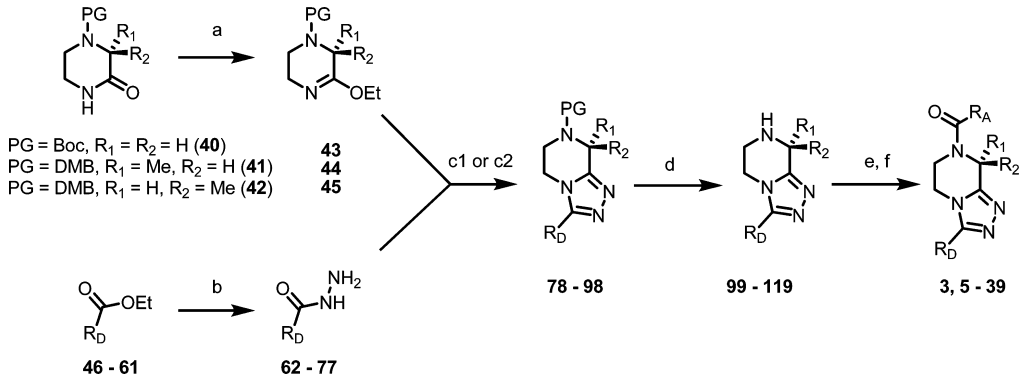

[a]Reagents and conditions: (a) Et_3OBF_4/Na_2CO_3 (ca. 1:2 equiv), CH_2Cl_2, 45−60 min, 67−88%; (b) hydrazine, ethanol, 3−14 h, 64%; (c1) PG = Boc:neat, 100−130 °C, 14−24 h, 70%; (c2) PG = DMB:anhydrous methanol or ethanol, 70 °C, 8 h, 84%; (d) TFA or HCl, 86−89%; (e) acid chloride, *N*-methylmorpholine, CH_2Cl_2, 15 min; (f) silica gel chromatography and/or crystallization, 49−55% (2 steps).

male dogs.[24] As part of our ongoing interest in NK_3R antagonists, and cognizant of the lead development pitfalls in the two reference chemotypes exemplified by osanetant (**1**) and talnetant (**2a**),[26] we deemed it necessary to find novel starting point(s) for this project.[26] The HTS campaign was performed using the aequorin Ca^{2+} bioluminescence assay[27] on human NK_3R, followed by an initial round of validation/optimization leading to the identification of **4** as a representative analogue of a hit series characterized by the presence of the 4-pyrimidinyl-2-pyridinyl-acetonitrile moiety (Figure 3).[28] Several shortcomings in this series, such as poor solubility, microsomal stability, and off-target safety profile led to our decision to abandon this chemotype due to a low probability of it generating a successful advanced lead. Instead, we used the accumulated SAR insights in the initial hit validation work (data not presented) to test several bioisosteric modifications to steer away from the HTS hit chemotype **4**. These efforts ultimately led to the discovery of **5** as a potential novel starting point. Posthoc computational molecular field alignment[29] analysis revealed that **5** displays ≥70% resemblance in shape and field similarity to **4** (Figure 3,

DOI: 10.1021/jm5017413
J. Med. Chem. XXXX, XXX, XXX−XXX

Table 1. SAR at Ring A

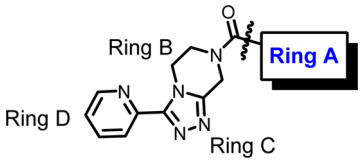

cpd	Ring A	pK_i	pIC_{50}	LLE[a]	clogP (log$D_{7.4}$)[b]	Solubility (μM)[c]
4	see Fig 3	7.1	7.0	(3.6)	(3.4)[28]	1.3
5	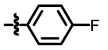	5.3	5.5	4.5 (4.25)	0.8 (1.1)	≥ 200
6	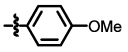	< 4.5	< 4.5	< 3.7	0.8	194
7		5.3	5.2	4.5	0.8	199
8		< 4.5	< 4.5	< 3.7	0.8	196
9		< 4.5	< 4.5	< 3.7	0.8	≥ 200
10		< 4.5	< 4.5	< 3.7	0.8	≥ 200
11	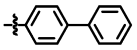	5.9	5.8	3.4	2.5	28
12	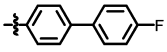	5.7	5.8	3.0	2.7	10
13	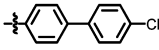	5.3	5.4	2.0	3.2	5.3
14	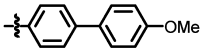	< 4.5	< 4.5	< 2	2.5	6.4
15	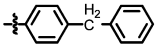	< 4.5	< 4.5	< 1.8	2.7	169
16	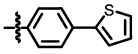	6.3	6.2	3.9	2.4	12
17	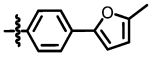	4.8	5.0	2.4	2.4	71
18	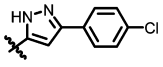	5.8	5.8	3.7	2.2	1.4

[a]LLE = pK_i − clogP. Parenthesized LLE based calculated using log $D_{7.4}$. [b]log $D_{7.4}$ values in parentheses: N = 3 and %RSD ≤ 5. [c]pH 7.4 PBS buffer, N = 3 and %RSD ≤ 5.

bottom panels). Rather gratifyingly, this novel *N*-acyl-triazolopiperazine chemotype (e.g., **5**) contrasted sharply against the HTS hit chemotype (e.g., **4**) as it displayed a much improved off-target and PK-ADME profiles although significantly right-shifted in antagonist NK_3R bioactivity. For example, **5** displayed a clean CYP profile (IC_{50} >10 μM for 3A4, 2D6, 1A2, 2C9, and 2C19 isoforms), excellent rat and human miscrosomal stability (RLM and HLM $T_{1/2}$ > 240 min) as well as oral availability (%F = 108 in rat), a significantly improved shake-flask solubility of ≥200 μg/mL (at pH 7.4) consistent with its balanced log $D_{7.4}$ = 1.1. Conversely, **4** displayed a poor CYP profile (<5 μM for 2D6, 2C9, 2C19, and 1A2), rather limited rat microsomal stability ($T_{1/2}$ = 13 min), and solubility at 1.3 μg/mL, consistent with its relatively high log $D_{7.4}$ = 3.4.[28] Nevertheless, in adopting **5** as the starting lead, it was crucial to rapidly address the 2-log right-shift in bioactivity against **4** (Figure 3). We herein report the optimization of **5** that resulted in several in vivo POC lead structures (based on the HPG axis mode-of-action, Figure 2). Further efforts that culminated in the ESN364 clinical candidate (currently in phase 2 human clinical trials) will be presented as a sequel to this report.[30]

RESULTS AND DISCUSSION

Synthesis. The preparative route used to access the foregoing *N*-acyl-triazolopiperazine NK_3R antagonists is illustrated in Scheme 1. This methodology relies on a cyclodehydration reaction between the piperazinoimidate (**43**−**45**) and the acyl hydrazide (**62**−**77**) to form the fused triazolopiperazine core, i.e., the key intermediates **78**−**98**.

DOI: 10.1021/jm5017413
J. Med. Chem. XXXX, XXX, XXX−XXX

Table 2. SAR at Rings B and D (R_A = 4-Fluorophenyl)

Cpd	Structure	pK_i	pIC_{50}	LLE[a]	clogP (log$D_{7.4}$)[b]	Solubility (μM)[c]	CYP panel IC_{50} (μM)[d]
5	See Fig 3	5.3	5.5	4.5 (4.2)	0.8 (1.1)	≥ 200	>100, 15, 66, 14, 27
19	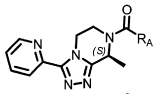	5.1	5.1	3.7	1.4	≥ 200	-
20	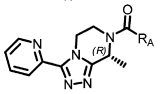	6.1	6.1	4.7	1.4	≥ 200	-
21	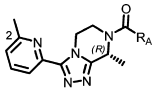	7.2	7.1	5.4 (5.6)	1.8 (1.6)	197	-
22	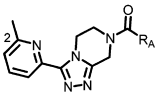	6.3	6.3	5.0 (4.9)	1.3 (1.4)	≥ 200	>100, >100, >100, 48, 69
23	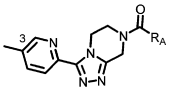	5.8	5.6	4.4	1.3	≥ 200	-
24	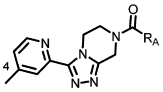	5.2	5.2	3.9	1.3	≥ 200	-
25	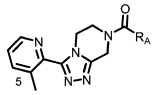	< 4.5	< 4.5	< 3.5	1.0	≥ 200	-
26	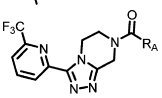	6.4	6.4	4.6	1.8	193	>100, >100, >100, >100, 21
27	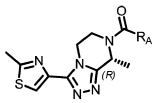	7.0	6.8	5.4 (5.7)	1.6 (1.3)	≥ 200	63, >100, 56, 44, >100
28	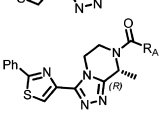	7.6	7.8	4.4 (4.2)	3.2 (3.4)	179	67, 54, 19, 19, 25

[a]LLE = pK_i − clogP. Parenthesized LLE based calculated using log $D_{7.4}$. [b]log $D_{7.4}$ values in parentheses: N = 3 and %RSD ≤ 5. [c]pH 7.4 PBS buffer, N = 3 and %RSD ≤ 5. [d]Values for CYP 3A4, 2D6, 2C9, 2C19, and 1A2, respectively.

While this synthetic approach is well-documented in the literature,[31] we were unable to find procedures whereby chiral intermediates ($R_1 \neq R_2$) can be prepared reproducibly and with acceptable chiral purity. To this effect, our investigations revealed several crucial factors in minimizing racemization especially in steps (a) and (c). The use of buffered Meerwein condition is precedented in the literature, particularly in the context of chiral substrates.[32] We also observed that buffered Meerwein conditions can help limit racemization during the imidate formation step (a), specifically by employing a mild base additive (Na_2CO_3 proved optimal) in conjunction with freshly prepared Meerwein reagent (Et_3OBF_4).[33] Another significant factor in obtaining high chiral purity in the final product was the choice of protective group used in the chiral piperazinone building block (i.e., PG in **40**−**42**). In particular, N−Csp^3 protective groups such as 2,4-dimethoxybenzyl (DMB) proved far superior to N−Csp^2 protective groups, e.g., *tert*-butyl carbamate (Boc), in limiting racemization. Somewhat unexpectedly, with DMB-protected substrates, step (c) proceeded to completion more rapidly than when Boc-protected substrates were used. This improved reaction kinetics in step (c), afforded through the use of the DMB protective group, is at least partly the reason for the improved product chiral purity. By employing both buffered Meerwein (Et_3OBF_4) conditions and the DMB-protective group strategy, it was entirely feasible to reproducibly limit racemization, in steps (a) and (c), to ≤1% with respect to the chiral purity in **41** or **42**. Acidolytic cleavage of the protective group (**78**−**98**), followed by acylation of the deprotected amine (**99**−**119**), afforded the final product. Purification was performed by either silica gel flash column chromatography or through crystallization in the case of the more advanced leads (e.g., **31**). In the case of analogue **31**, crystallization from hot ethyl acetate/*tert*-butyl methyl ether aided in enhancing both the chemical and the enantiomeric purity to >99%.

Bioactivity, Solubility, and Off-Target Safety (CYP, hERG) SAR. The initial bioactivity SAR was established using radioligand binding (RLB) through displacement of [^{3}H]-labeled **2c**[23] from recombinant human NK_3R in CHO cells. RLB assays were also conducted using human NK_1R and NK_2R subtypes in order to establish the receptor subtype selectivity profile (Table 4). Transfected cloned NK_1R and NK_2R were employed together with [^{3}H]-labeled Substance P and [^{125}I]-labeled neurokinin A, respectively, as their cognate radioligands.

DOI: 10.1021/jm5017413
J. Med. Chem. XXXX, XXX, XXX−XXX

Table 3. Further SAR on Advanced Leads ($R_{A'}$ = 4-(Thiophen-2-yl)phenyl)

cpd	structure	pK_i	pIC_{50}	LLE [a]	clogP (log$D_{7.4}$) [b]	Solub (μM) [c]	CYP panel IC_{50} (μM) [d]	hERG IC_{50} (μM)
29	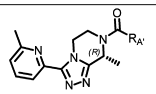	8.0	8.0	4.6 (4.6)	3.4 (3.4)	110	45, 86, 18, 26, 57	7.3
30	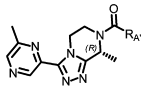	7.9	7.7	5.5 (5.2)	2.4 (2.7)	160	2, >100, 17, 39, 50	4.7
3	see Fig 1	8.7	7.7	3.6 (3.7)	5.1 (5.0)	0.4	19, 7, 3, 4, 21	1.4
31	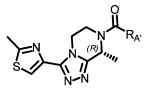	7.9	7.8	4.7 (4.8)	3.2 (3.1)	118	50, >100, 21, 34, 26	24
32	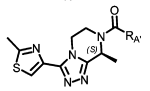	6.5	6.3	3.3 (3.4)	3.2 (3.1)	-	-	-
33	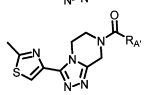	7.1	7.1	4.4 (4.2)	2.7 (2.9)	172	30, >100, 19, 15, 19	27
34	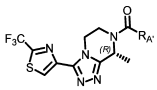	7.1	7.2	3.4 (3.3)	3.7 (4.1)	11	>100, >100, 5, 18, 8	-
35	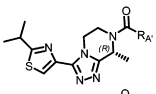	8.6	8.4	4.5 (4.2)	4.1 (4.4)	25	35, 27, 4, 12, 17	-
36	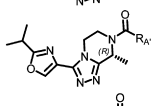	8.5	8.4	5.0 (5.2)	3.5(3.3)	119	43, 65, 14, 22, 81	7.3
37	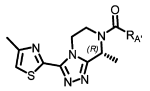	8.2	8.1	5.0 (5.3)	3.2 (2.9)	50	11, 42, 8, 18, 8	17
38	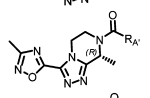	7.6	7.6	5.4 (5.4)	2.2 (2.2)	185	55, >100, 40, 54, 32	5.1
39	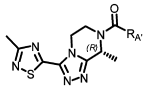	8.5	8.4	6.1 (5.5)	2.4 (3.0)	93	80, 39, 13, 19, 67	8.0

[a] LLE = pK_i − clogP. Parenthesized LLE based calculated using log $D_{7.4}$. [b] log $D_{7.4}$ values in parentheses: N = 3 and %RSD ≤ 5. [c] pH 7.4 PBS buffer, N = 3 and %RSD ≤ 5. [d] Values for CYP 3A4, 2D6, 2C9, 2C19, and 1A2, respectively.

Confirmation of NK_3R antagonist activity was made through aequorin Ca^{2+} bioluminescence functional assay measuring inhibition of NKB-induced Ca^{2+} signaling in CHO cells expressing recombinant human NK_3R.[27] The functional assay data established the foregoing compounds as antagonists of the human NK_3R receptor as with the reference compound **2c**. Linear regression analysis for RLB versus aequorin functional data displayed an excellent fit with r^2 = 0.98. The RLB (pK_i) and functional aequorin Ca^{2+} (pIC_{50}) data herein (Tables 1−3) were obtained with the assays performed on each compound at least in triplicate with standard deviation ≤0.3.

As was alluded to previously, upon adopting analogue **5** as the initial lead, a primary project goal became that of significantly enhancing the NK_3R antagonist bioactivity (ΔpK_i and ΔIC_{50} ≥ 2 vs **5**) but in a lipophilically efficient manner. The emphasis on lipophilicity reduction is primarily from the viewpoint of minimizing the potential for toxicological risk rather than from the Lipinski rule-of-five[34] concern with limited oral availability. Increased risk of adverse safety has been correlated in several studies to high lipophilicity,[35] as reflected in such empirical recent paradigms as Pfizer's 3/75 rule[36] or GSK's 4/400 rule.[37] In addition, off-target promiscuity and organ toxicity have also been reported by several groups to correlate to compound lipophilicity and hence to clinical attrition rate.[38] A metric that helps capture the risk−reward balance of improved bioactivity against lipophilicity is the ligand lipophilic efficiency: LLE = pK_i − clogP (or log $D_{7.4}$).[39] In this regard, we aimed for ΔLLE ≥ 0 vis-à-vis **5** (i.e., LLE ≥ 4.25) concurrent to the goal of ≥2-log improved bioactivity (ΔpK_i, pIC_{50} ≥ 2). Other ligand metrics, in particular, ligand efficiency (LE = (1.37/HAC) × pK_i, where HAC denotes the number of non-hydrogen atoms)[39] and fraction sp^3 (Fsp^3 = number of sp^3 hybridized carbons/total carbon count)[40] were also tracked throughout although not the primary focus herein. LE and Fsp^3 ligand metrics will be revisited in the conclusion to this report. Moderate solubility (>10 μM) was also considered as an important practical target, particularly given the severe solubility issues encountered with the HTS hit chemotype (**4**, Table 1).[41] We sought to achieve these goals through a detailed knowledge of the bioactivity SAR, which is highlighted below (Tables 1−3).

DOI: 10.1021/jm5017413
J. Med. Chem. XXXX, XXX, XXX−XXX

To help make informed decisions during lead progression, off-target safety profiles were also monitored alongside (Tables 2,3). This included but was not limited to the major cytochrome P450 (CYP) isoforms in drug metabolism that are therefore critical in terms of drug−drug interaction concerns, i.e. CYP3A4, 2D62, 2C9, 2C19, and 1A2. As well, due to its role in repolarization of the cardiac action potential and its attendant impact on cardiosafety, human ether-a-go-go-related gene (hERG) K^+-channel interaction was also tracked, in the more advanced analogues, through electrophysiological patch-clamp measurements.

For brevity, each of the four (hetero)aryl rings in the lead structures herein, exemplified by **5**, is annotated alphabetically (Rings A−D) as indicated in the illustration to Table 1. These annotations are used consistently throughout.

Ring A SAR. The Ring A in vitro bioactivity SAR (Table 1) was extensively explored at the outset because it was readily amenable to rapid analoguing through parallel synthesis, i.e., *N*-acylation of the triazolopiperazines (**99**−**119** in Scheme 1). A predilection for *para* or *meta* phenyl substitution with electron withdrawing groups, e.g., fluorophenyl substitutions in **5** and **7**, was evident. An electronic SAR effect was also apparent as the electron-donating substituents, e.g., methoxy group, eroded bioactivity at both the *para* (**6**) and the *ortho* aryl ring positions (**8**). Substitution at the *ortho* aryl position was disfavored irrespective of the electronic nature of the substituent (**9** and **10**), likely due to conformational effects that are unfavorable to receptor interaction when this position is substituted. With 1,4-biphenyl Ring A derivatives (**11**−**14**), bioactivity SAR mirrored the substitution pattern and electronic requirements seen before. Hence, whether unsubstituted (**11**) or *para* fluorophenyl substituted (**12**), a 0.3−0.6 log improved potency vis-à-vis **5** resulted, whereas with electron-donating *para* substitution bioactivity was abrogated (**14**), analogous to the effect of introducing a rotatable bond in the 1,4-biphenyl moiety (**15**). Because the gain in potency through the biaryl GPCR privileged structure[42] was greatly offset by a deterioration of LLE and solubility (**11** vs **5**), we explored the use of heteroaryl rings to try to reconcile these opposing tendencies. After extensive analoguing, the 4-(thiophen-2-yl)phenyl group in **16** emerged as the most effective in terms of improved bioactivity (ΔpK_i = 1, ΔpIC_{50} = 0.7 vs **5**), although with an undesirable impact on both LLE[43] (ΔLLE_{clogP} = −0.6) and solubility (12 μM as compared to ≥200 μM in **5**) (Table 1). The utility of the 4-(thiophen-2-yl)phenyl moiety will be revisited below.

Ring B and Ring D SAR: "Magic Methyl Effects". Highlights of Ring B and Ring D SAR in terms of bioactivity and off-target safety profiling are presented in Tables 2−3. Early in the lead optimization efforts, a so-called magic methyl effect[44] was discovered in both Ring B and Ring D bioactivity SAR (see below) that proved to be a key factor in the lead optimization goal of combined bioactivity and LLE improvements.

Modifying the initial lead **5** to **20** (Table 2) resulted in 0.6−0.8 log improvement in bioactivity (ΔpK_i = 0.8, ΔpIC_{50} = 0.6) due to the (*R*)-Me substitution on Ring B piperazine (the Ring B magic methyl). That the improved potency in **20** came at no detriment to the LLE (ΔLLE_{clogP} = 0.5 vs **5**), or solubility (≥200 μM just as with **5**), was a significant result. Moreover, a stereochemical SAR in Ring B methyl substitution was evident with the order of antagonist bioactivity as follows: (*R*)-Me (**20**) ≫ des-Me Ring B (**5**) > (*S*)-Me (**19**). This SAR is revisited further below based on X-ray structural studies (Figure 4) on advanced congeners.

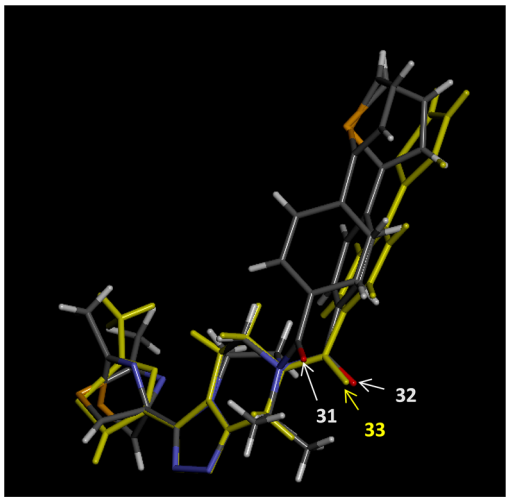

Figure 4. Superposition of the three X-ray crystal structures based on an alignment of the core triazolopiperazine ring system for compounds **31**−**33** as indicated (arrows pointing to the position of the carbonyl amide oxygen).

A Ring D magic methyl effect was also apparent in the early lead structures, i.e. placing a methyl group *ortho* to the pyridine nitrogen in Ring D rendered **22** (Table 2) one-log more potent compared to its des-methyl Ring D congener **5** (ΔpK_i = 1, ΔpIC_{50} = 0.8). Moreover, combining the Ring B (**20**) and Ring D magic methyl effects (**22**) in the same structure, **21**, resulted in a rather significant cumulative improvement in bioactivity (ΔpK_i = 1.9, ΔpIC_{50} = 1.6) and LLE (ΔLLE = 1.4) against the initial lead **5**, without any serious adverse impact on solubility (Table 2). Hence, the bioactivity and LLE trends in the foregoing congeners were as follows: **21** > **20** ≈ **22**. Furthermore, a regiospecific SAR in the Ring D magic methyl effect was apparent given the order of decreasing antagonist bioactivity (and LLE) among the following congeners: **22** (2-Me) > **23** (3-Me) > **24** (4-Me) ≈ **5** (des-Me) > **25** (5-Me) (Table 2). No electronic SAR was detected at this stage because the trifluoromethyl congener to **22**, i.e., compound **26**, elicited a similar bioactivity (ΔpK_i, ΔpIC_{50} = 0.1). Nevertheless, based on LLE considerations, the *ortho* methyl substitution was retained (ΔLLE_{clogP} = −0.4, **22** vs **26**). On the whole, these results suggested that modulation of the pyridine basicity in the Ring D position is not critical in impacting bioactivity.[45] This observation then prompted us to widen the search for alternative heteroaryl rings as highlighted below. For instance, analogue **27** containing a 2-methylthiazole as Ring D displayed similar antagonist bioactivity and LLE to its 2-methylpyridine congener **21**, whereas **28** bearing the bulkier and more lipophilic 2-phenylthiazole proved appreciably more potent against **21** (ΔpK_i = 0.4, ΔpIC_{50} = 0.7). Additional improved bioactivity compared to **28** (Table 2) was achieved by modifications that further increased lipophilicity at both Ring D and Ring A positions, culminating in **3**[8] (Figure 1, Table 3) as a highly potent NK_3R antagonist (pK_i = 8.7, pIC_{50} = 7.7). On the basis of these SAR data, it can be surmised that the receptor binding pocket surrounding Ring A and Ring D can accommodate additional $\pi-\pi$ or hydrophobic interactions. Although highly potent, it came as no surprise that **3** displayed a significantly deteriorated LLE (ΔLLE = −0.55 vs **5**), in step

DOI: 10.1021/jm5017413
J. Med. Chem. XXXX, XXX, XXX−XXX

with its poor shake-flask solubility (0.4 μM against $\geq$200 μM in **5**) as well as its subpar CYP profile (IC_{50} < 10 μM for 2D6, 2C9, 2C19 isoforms) and an abysmal hERG IC_{50} = 1.4 μM (Table 3). This global profile curbed any further consideration of compound **3** beyond the initial POC studies (see below). At this point, we decided to retain the lipophilic 4-(thiophen-2-yl)phenyl group but endeavored to optimize the Ring D heteroaryl moiety to address the LLE objective overall (i.e., ΔLLE > 0 vs **5**).

Further SAR on Advanced Leads. Presented in Table 3 is a selection of additional Ring D SAR explorations. This was undertaken as a means of addressing the LLE objective despite retaining the lipophilic 4-(thiophen-2-yl)phenyl moiety (i.e., $R_{A'}$ in Table 3) that significantly improved antagonist bioactivity. Thus, as with the earlier leads (**5** vs **16**), in the advanced leads as well the aforesaid heterobiaryl moiety afforded a nearly one-log improved potency (ΔpK_i = 0.8 and ΔpIC_{50} = 0.9, **29** vs **21**) albeit with an equivalent loss in LLE (ΔLLE = −1.0) due to the replacement of 4-fluorophenyl Ring (R_A in **21**, Table 2) with 4-(thiophen-2-yl)phenyl group ($R_{A'}$ in **29**, Table 3).

Turning our attention to Ring D, 2-methylpyrazine combined with 4-(thiophen-2-yl)phenyl, i.e., **30** (Table 3), proved initially promising as it was nearly equipotent (ΔpK_i = −0.1, ΔpIC_{50} = −0.3) to its 2-methylpyridine congener (**29**) although with a 0.6-log improved LLE, also reflected in its comparatively lower log $D_{7.4}$ (Δlog $D_{7.4}$ = −0.7) and higher solubility. Despite this, however, **30** displayed a poor off-target safety profile, i.e., hERG IC_{50} = 4.7 μM (vs 7.3 μM in **29**) and CYP3A4 IC_{50} = 2.2 μM (vs 45 μM in **29**). The hERG SAR will be discussed further below.

Thiazole Ring D analogues, e.g., **31** (Table 3), ultimately proved more successful than the pyridine or pyrazine congeners in reaching the dual project objectives as discussed below. Unlike the aforementioned case with pyridine Ring D analogues (e.g., **21** vs **26**, Table 2), with the congeneric thiazole structures an electronic SAR was noted in terms of Ring D magic methyl effect. For instance, 2-methylthiazole Ring D analogue **31** proved 0.6−0.8 log more potent vis-à-vis its trifluoromethyl congener **34** (ΔpK_i = 0.8, ΔpIC_{50} = 0.6). Importantly, the impact of the Ring B magic methyl effect on bioactivity and LLE (see above), including its stereochemical SAR, was maintained with the Ring D thiazole congeners as well: (*R*)-Me (**31**) ≫ des-Me Ring B (**33**) > (*S*)-Me (**32**). Moreover, higher alkyl substituents than methyl in Ring D thiazole series further enhanced the bioactivity, e.g., 2-isopropylthiazole (**35**) was 0.6−0.7 log left-shifted against **31** (Table 3). Nonetheless, this gain was outweighed by the higher lipophilicity (Δlog $D_{7.4}$ = 1.3) and poorer solubility in spite of the improved LLE in **35** compared to **31** (ΔLLE = 0.6). These observations combined with the poor CYP 2C9 safety threshold (IC_{50} = 4 μM, Table 3) led to the dismissal of the higher alkyl homologues in the 2-substituted thiazole Ring D lead series. In attempting to improve lipophilicity in the foregoing structures, the oxazole congener to **35**, i.e., **36** (Δlog $D_{7.4}$ = −1.1) was prepared and profiled. While **36** proved valuable in terms of improvements in solubility, CYP 2C9 (IC_{50} = 14 μM) and LLE (ΔLLE = 1.0 vs **36** and 0.4 vs **31**), it proved suboptimal in hERG (IC_{50} = 7.3 μM). Alternatively, the Ring D thiazole regioisomer to **31**, i.e., **37**, provided another means of improving both bioactivity (ΔpK_i = 0.3, ΔpIC_{50} = 0.3) and LLE profiles (ΔLLE = 0.5 vs **31**) (Table 3). Despite this, based on the comparison of off-target safety profile, i.e., hERG and CYP values (3A4, 2C9 and 1A2), **31** proved clearly superior to its regioisomeric congener, **37** (Table 3). Additional noteworthy Ring D variants to the 2-methylthiazole in **31** were the oxadiazole (**38**) and thiadiazole (**39**) congeners. The 3-methyl-1,2,4-thiadiazole analogue **39** (Δlog $D_{7.4}$ = −0.1 vs **31**) in particular displayed a significant combined improvement in bioactivity (ΔpK_i = 0.6, ΔpIC_{50} = 0.6) and LLE (ΔLLE = 0.8) vs **31**, while retaining an acceptable solubility and CYP profile. By comparison, the less lipophilic 3-methyl-1,2,4-oxadiazole congener **38** (Δlog $D_{7.4}$ = −0.9 vs **31**) proved less bioactive than **31** (ΔpK_i = −0.3, ΔpIC_{50} = −0.2) but with improved solubility and LLE profile (ΔLLE = 0.7 vs **31**). However, both **38** and **39** were subpar to **31** due to their inadequate hERG safety threshold (IC_{50} < 10 μM). Therefore, compound **31** proved the best lead candidate at this juncture in terms of its overall bioactivity and safety profiles and it helped achieve the two-pronged objective of significantly improving *both* the LLE (ΔLLE = 0.5) *and* the antagonist bioactivity vis-à-vis the initial lead **5** (ΔpK_i = 2.6, ΔpIC_{50} = 2.3). That said, a selection of leads, including **3**, **36**, **38**, and **39**, in addition to osanetant (**1**) and talnetant (**2a**) as NK_3R gold standards, were taken through additional selectivity profiling as well as in vivo PK and brain uptake characterization in order to help establish PKPD correlations with respect to the initial in vivo efficacy results as discussed further below.

X-ray Analyses Related to Ring B Magic Methyl Effect. Single crystal X-ray crystallographic analysis on congeners **31**−**33** revealed differences in the relative orientation of the amide carbonyl oxygen due to the local conformational effects in the piperazine Ring B (Figure 4). It is possible that the Ring B magic methyl effect is at least partially due to the role of (*R*)-Me piperazine Ring B substitution in influencing the carbonyl amide orientation toward its bioactive conformation. The indispensability of the tertiary amide functionality for bioactivity was established earlier (data not presented).

hERG SAR. Modulation of pK_a and control of lipophilicity are among well-known strategies for hERG optimization.[46] The lipophilicity reduction strategy is supported by hERG homology models and mutagenesis studies that substantiate the existence of a lipophilic binding site. In addition, π−cation interactions within the hERG K^+-channel offer a rationale for the pK_a modulation strategy, e.g., compounds possessing basic nitrogen site(s) that can be protonated at physiological pH. However, pK_a modulation is not relevant here because the basicity of Ring D heteroaryl rings are outside the physiologically relevant range.[47]

Returning to the hERG SAR, the improved hERG in **31** (IC_{50} = 24 μM, Table 3), with 2-methylthiazole at Ring D, against the congeneric 2-methylpyridine analogue (**29**) mirrored the reduced lipophilicity trend in this analogy (Δlog $D_{7.4}$ = −0.3). Other Ring D methyl-substituted thiazole analogues similar to **31** (log $D_{7.4}$ = 3.1), such as **33** (log $D_{7.4}$ = 2.9) and **37** (log $D_{7.4}$ = 2.9), also displayed a generally improved hERG safety (IC_{50} ≥ 17 μM) consistent with the improved lipophilicity trends (Table 3). A reverse case in point was the previously noted example of analogue **3** (log $D_{7.4}$ = 5.0) that displayed the worst hERG profile (IC_{50} = 1.4 μM), consistent with it being the most lipophilic analogue in this report.

However, some of the hERG SAR was not consistent with the reduced lipophilicity trends. For example analogue **30**, i.e., 2-methylpyrazine Ring D congener, deviated from the latter trend with hERG IC_{50} = 4.7 μM, i.e., worse than both **31** and **29** despite being noticeably less lipophilic than either congeners

DOI: 10.1021/jm5017413
J. Med. Chem. XXXX, XXX, XXX−XXX

Table 4. Selectivity Profile Data for Advanced Lead and Reference Compounds (1, 2a)[a]

	NK_3R (pK_i)			hNK_2R		hNK_1R		(% binding inhibition at 10 μM)			
cpd	*h*-	*mk*-	*r*-	pK_i	Δ	pK_i	Δ	GPR54	KOR	GnRH-R	NPFF1 (GnIH)
NKB	9.1	ND	ND	7.8	1.3	6.3	2.8	-	-	-	-
senktide	8.5	ND	ND	<5	>3.5	<5	>3.5	-	-	-	-
1	8.8	ND	7.3	7.1	1.7	6.4	2.4	-	100	-	-
2a	8.1	ND	6.7	5.4	2.7	4.9	2.9	-	12	-	-
3	8.7	8.4	7.9	6.1	2.6	5.9	2.8	−21	−14	35	−14
31	7.8	7.7	7.1	4.9	2.9	4.9	2.9	−29	25	30	18
36	8.5	8.2	7.5	5.0	3.5	5.1	3.4	-	41	-	-
38	7.6	7.6	6.9	-	-	-	-	-	23	-	-
39	8.4	8.2	7.7	4.9	3.5	4.9	3.5	−17	42	35	24

[a]The pK_i values for NK_nR (n = 1−3) data are reported as mean of at least three independent measurements (N = 3) with SD ≤ 0.2. Values for the NKB and senktide peptides are taken from Sarau et al. (ref 23). Designations *h*-, *mk*-, and *r*- refer to human, monkey, and rat orthologues of NK_3R. Δ = pK_i NK_3R − pK_i NK_nR (n = 1, 2).

Table 5. Plasma Protein Binding, Caco-2 Permeability, and PK Data in Rats[a] for Reference Compounds (1, 2a) and Advanced Lead Analogues

		P_{app}[b] (nm/s)		rat PK (iv dose 1 mg/kg; oral dose 3 mg/kg)							
cpd	plasma f_u (rat)	AB	BA	iv CL_T (mL/min/kg)	iv V_{ss} (L/kg)	iv $T_{1/2}$ (min)	iv AUC_u (μM·min)[c]	oral AUC_u (μM·min)[c]	oral T_{max} (min)	oral $C_{max,u}$ (nM)	%*F*
1[d]	0.006	-	-	57	8.7	121	0.2	0.1	45	0.42	17
2a[d]	0.0003	872	985	2.0	1.5	448	0.5	0.7	60	2.65	47
3[e]	0.0008	-	-	8.9	4.1	321	0.2	0.1	45	0.14	17
31[f]	0.055	482	529	7.4	1.4	126	16.9	60.3	45	443	119
36[f]	0.036	464	438	8.2	2.6	210	9.3	13.6	68	58.7	49
38[f]	0.108	574	604	11.3	1.0	62	23.3	46.3	35	272	66
39[f]	0.065	609	628	7.3	2.8	267	32.7	-	-	-	-

[a]Mean values presented for N = 3−4 rats per group. [b]Caco-2 P_{app} values obtained in the presence of 0.1% bovine serum albumin; for reference, propranolol a high permeability compound displays Caco-2 flux values of ≥450 nm/s with efflux ratio (P_{AB}/P_{BA}) = 1. [c]AUC_u = unbound AUC = $AUC_{total} \times f_u$. [d]PK formulation: 1% DMSO, 9% hydroxypropyl-β−cyclodextrin in 0.9% NaCl. [e]PK formulation: 4:5:1 DMA/PEG-400/physiological saline. [f]PK formulation: 9% hydroxypropyl-β−cyclodextrin.

in question (Δlog $D_{7.4}$ = −0.4 vs **31** and −0.7 vs **29**). Likewise, the 3-methyl-1,2,4-oxadiazole Ring D congener **38**, despite being significantly less lipophilic than **31** (Δlog $D_{7.4}$ = −0.9), displayed the second worst hERG value at 5.1 μM (Table 3). These observations suggest that in addition to lipophilicity as a correlative factor to the hERG SAR, likely a hydrogen bond donor/acceptor (HBD/A) interaction is also involved between the Ring D heteroaryl moiety and the hERG channel. It is well-known that a divalent sulfur atom is a much weaker hydrogen bond acceptor (HBA) than an oxygen or nitrogen atom.[48] Therefore, the increase in the number of HBA atoms (i.e., N + O) in the Ring D heteroaryl correlates with the decreasing trend in hERG IC_{50} among the following congeners: **31** (thiazole, N) > **39** (thiadiazole, N + N) > **38** (oxadiazole, N + N + O).

In conclusion, the hERG SAR in the foregoing structures can be understood through the interplay between the compound lipophilicity and the number of HBA atoms (N+O) in the heteroaryl Ring D. These findings were exploited in further advanced lead optimization efforts that will be published as a sequel to this report.[30]

Neurokinin Receptor Selectivity. As stated at the outset, NKB[1] is both a potent and a selective agonist to the NK_3R (pK_i = 9.1), with >1-log selectivity against NK_2R and nearly 3-log selectivity against the NK_1R subtype (Table 4), consistent with the relative similarity of these receptor subtypes based on their sequence homology.[49] Senktide is less potent but more selective than NKB.[23] A goal in this project was target selectivity toward NK_3R to minimize off-target effects. As shown in Table 4, the foregoing advanced leads were all similar to NKB (or better) insofar as their NK_3R subtype selectivity is concerned, and they proved superior to both osanetant (**1**) and talnetant (**2a**) in this regard.

In terms of species orthologue selectivity, radioligand binding potencies were more right-shifted at rodent NK_3R as compared to human or monkey NK_3R values, i.e., 0.9-log unit right-shifts on average in rat against human NK_3R as compared to 0.2-log in the monkey against human NK_3R analogy. This is not surprising given the previously reported pharmacology data[26] and based on sequence alignment and phylogenetic analysis of NK_3R in different genomes showing that the rat and mouse sequences cluster together and are set apart from the primate receptor cluster.[49]

Finally, additional receptors that are related to the HPG axis pathway (Figure 2) are also noted in Table 4. These include KOR (or κ-opioid receptor), GPR54 (or KiSS1R), GnRH receptor, and the more recently discovered gonadotropin inhibitory hormone receptor, GnIH-R,[50] also known as the neuropeptide FF receptor, NPFF1. The inhibition binding data at 10 μM indicated that the foregoing lead structures act selectively on NK_3R without any detectable activity against any of the said receptors, in contrast to osanetant (**1**), for example, that displayed poor selectivity against KOR (100% inhibition at 10 μM and 75% at 1 μM). In fact, compound **31** was devoid of off-target effects in the broad CEREP ExpresSProfile screen as well, underscoring the general superiority of this novel NK_3

DOI: 10.1021/jm5017413
J. Med. Chem. XXXX, XXX, XXX−XXX

Table 6. Physicochemical Properties, Brain Fraction Unbound, and Brain Exposure Data in Rat for Reference Compounds (1, 2a) and Advanced Lead Analogues[a]

cpd	MW	TPSA	clogP	log $D_{7.4}$	brain f_u (bf_u)	$(B/P)_u$ at 10 min[a]	$(B/P)_u$ at 60 min[a]	$C_{brain,u}$ at 10 min (nM)[a]	$C_{brain,u}$ at 60 min (nM)[a]
1[b]	606.6	44	5.7	3.4	0.001	0.12	0.12	0.15	0.09
2a[b]	382.4	62	7.4	-	0.010	2.9	3.2	4.74	1.68
3[c]	519.6	64	5.1	5.0	0.001	1.9	2.5	1.08	0.89
31[d]	421.5	64	3.2	3.1	0.028	0.2	0.1	13.3	7.79
36[d]	433.5	77	3.5	3.3	0.016	0.2	0.2	11.8	5.42
38[d]	406.5	90	2.2	2.2	0.084	0.6	0.4	126	50.5
39[d]	422.5	77	2.4	3.0	0.031	0.7	0.7	60.9	39.2

[a]For brain in vivo studies, compounds dosed iv at 1 mg/kg. $(B/P)_u$ = unbound brain-to-plasma ratio = $C_{brain,u}/C_{plasma,u}$ with $C_{brain,u} = C_{brain,total} \times bf_u$ and $C_{plasma,u} = C_{plasma,total} \times f_u$. [b]In vivo formulation: 0.9% NaCl, 1% DMSO, 9% hydroxypropyl-β-cyclodextrin. [c]In vivo formulation: 4:5:1 DMA/PEG-400/water. [d]In vivo formulation: 9% hydroxypropyl-β-cyclodextrin.

antagonist chemotype as compared against those exemplified by osanetant (**1**) or talnetant (**2a**), commonly regarded as gold standards.[51]

Pharmacokinetics and Brain Exposure. The results of Caco-2 permeability, plasma fraction unbound as well as iv and oral PK parameters are summarized in Table 5. In Table 6, brain exposure data together with brain fraction unbound values are also provided. The in vivo PK and brain exposure data were obtained in male Sprague−Dawley rats at 1 mg/kg iv bolus and 3 mg/kg oral (gavage) in suitable formulations as specified (Tables 5−6). On the whole, the advanced leads in question, i.e., **3**, **31**, **36**, **38**, and **39**, displayed favorable rat PK profiles, with total systemic clearance (CL_T) levels (7.3−11.3 mL/min/kg range) significantly lower than hepatic blood flow (55 mL/min/kg),[52] distribution volumes ca. 2−7-fold that of total body water, plasma half-life ($T_{1/2}$) values ranging from 1.0 to >5.3 h, and absolute oral bioavailability (%F) >20% . The improved oral bioavailability in **3** vis-à-vis **31** is globally consistent with the Lipinski rule-of-five,[34] given the clogP reduction to below 5 and MW reduction to below 500 in the said comparison (Table 6). The lipophilicity reduction in the latter analogy (Δlog $D_{7.4}$ = −1.9) is also in step with the reduced volume of distribution trend (ΔV_{ss} = −2.7 L/kg). Compound **31** displayed a high Caco-2 permeability and plasma f_u combined with low CL and reasonably short oral T_{max}. In addition, **31** displayed complete oral absorption reflected in the high oral AUC and %F = 119 (Table 5). Absolute oral bioavailability values of >100% have been reported in the literature due to various possible contributing causes.[53] Because after three and one-third half-lives 90% of the dose would be eliminated,[54] based on the relatively short half-life of **31** (oral $T_{1/2} \approx$ iv $T_{1/2}$ = 2.1 h), approximately 7 h postdosing it should be essentially cleared. In keeping with this, following a 5-day twice daily (BID) oral dosing at 30 mg/kg in rats, no accumulation of **31** and no hepatotoxicity indications were noted (i.e., ALT, AST, and bilirubin levels were normal). Similarly to analogue **31**, compounds **36**, **38**, and **39** that are rule-of-five compliant and generally consistent with the physicochemical attributes of successful CNS drugs[55] (despite slight violations in TPSA < 60−70 Å^2 rule) also displayed good systemic and brain exposure levels in rats.

The free drug hypothesis is a useful principle for PKPD analyses (see next section) and it postulates that the unbound, or free fraction, rather than total drug is the responsible agent for eliciting a pharmacological or toxicological response.[56] Therefore, crucial to a proper evaluation of the PK data, whether in systemic or brain studies, is a consideration of the pertinent in vivo parameters as unbound values. This enables an evaluation of the dynamic physiological effects such as metabolism, transport, permeability, movement between cellular and tissue compartments in the context of free plasma, and brain levels of the compound that is otherwise erroneously ignored, or misinterpreted, as cautioned by several recent reports on the subject.[57] To this end, measurements of free drug fraction in plasma (f_u) and in brain tissue (bf_u) were carried out in vitro (Tables 5 and 6, respectively) and the relevant in vivo PK parameters cited using calculated unbound values as specified. Although lipophilicity alone generally does not correlate well to albumin binding, in a congeneric series the lipophilicity trends are often apparent, as is the case here.[58] Accordingly, among the lead structures **3**, **31**, **36**, **38**, and **39**, the following increasing trend in f_u (Table 5) and bf_u (Table 6) was noted: **3** < **36** < **31** < **39** < **38**, which matches the decreasing order of lipophilicity based on clogP and measured log $D_{7.4}$ values (Table 6). However, as noted above, for the increased free fraction to translate into increased unbound plasma and/or brain levels, additional factors such as permeability rates, intrinsic clearance and transporter activity need to be in step as well. Overall, the total clearance levels (CL_T) varied by 1.5-fold (**38** vs **39** as extrema) compared to 135-fold variation in plasma f_u (**39** vs **3** as extrema). Given the latter and the fact that the foregoing structures were not permeability limited, or affected by efflux, as inferred from the Caco-2 results (Table 5), the improved f_u and bf_u trends are consistent with improved unbound plasma and brain levels, respectively.

Unbound brain-to-plasma ratios, i.e., $(B/P)_u$ measured at 10 and 60 min post iv dosing, are provided in Table 6. However, it is rather misleading to evaluate $(B/P)_u$ values without a parallel consideration of the unbound brain concentration levels.[59] For example, whereas osanetant (**1**) as well as analogues **31** and **36** have comparable $(B/P)_u$ at 0.1−0.2, the free brain concentration of **1** (0.1−0.2 nM) is significantly lower than that in **31** and **36** (5−13 nM).[60] Conversely, while analogues talnetant (**2a**) and **3** have $(B/P)_u > 1$,[61] the free brain concentrations are rather low in the 1−5 nM range. It is also worth noting that analogues **38** (LLE = 5.4) and **39** (LLE = 5.5), i.e., the highest LLE analogues herein, displayed the highest unbound brain concentrations (Table 6). Therefore, the general strategy of achieving a balanced lipophilicity (improved LLE) was also fruitful in the context of unbound plasma and brain exposure levels, with attendant impact on in vivo efficacy data as discussed below.

LH Inhibition in Vivo Efficacy Data. LH is frequently used as a biomarker for determination of the potential inhibitory effects of compounds on the sex-hormone axis.

DOI: 10.1021/jm5017413
J. Med. Chem. XXXX, XXX, XXX−XXX

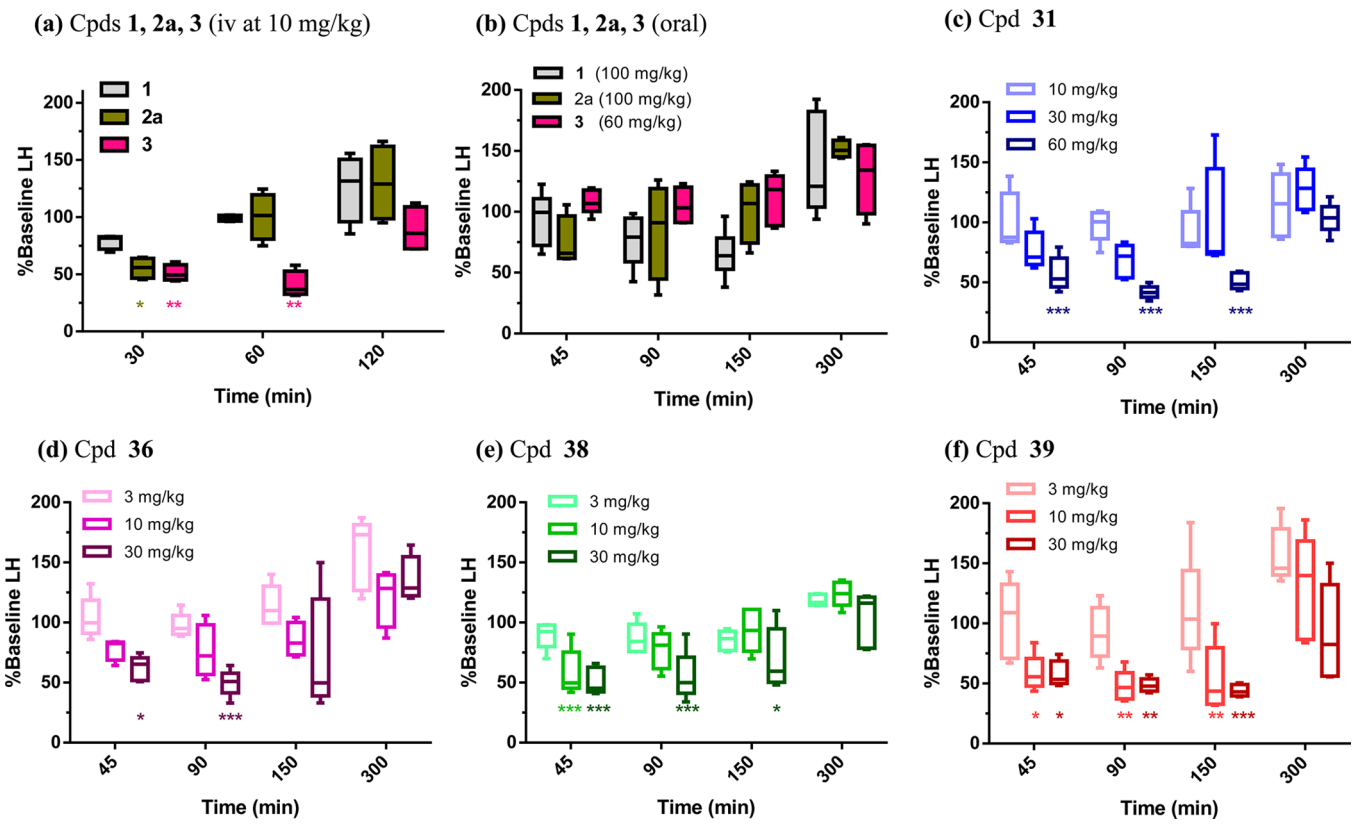

Figure 5. LH inhibition efficacy studies in castrate male rats (N = 4−6/group): (a) iv at 10 mg/kg (DMA/PEG400/H_2O, 4:5:1) and (b−e) oral at doses indicated (0.5% methylcellulose/water). LH reported at indicated time points as decrease relative to the baseline value for each group. Statistical analysis performed by 2-way ANOVA followed by Bonferroni's posthoc analysis: ***p < 0.001, **p < 0.01, *p < 0.05. Box-and-whisker plots: box represents 25th−75th percentiles; whiskers represent minima and maxima.

Table 7. PKPD Correlations in the Oral LH Inhibition Studies in Castrated Male Rats[a]

			3 mg/kg		10 mg/kg		30 mg/kg		60 mg/kg		100 mg/kg	
cpd	rat K_i (nM)[b]	LLE[c]	$C_{plasma,u}/K_i$	$C_{brain,u}/K_i$	$C_{plasma,u}/K_i$	$C_{brain,u}/K_i$	$C_{plasma,u}/K_i$	$C_{brain,u}/K_i$	$C_{plasma,u}/K_i$	$C_{brain,u}/K_i$	$C_{plasma,u}/K_i$	$C_{brain,u}/K_i$
1	56	3.9	-	-	-	-	-	-	-	-	0.07	0.01
2a	193	−0.7	-	-	-	-	-	-	-	-	0.03	0.10
3	13	2.9	-	-	-	-	-	-	0.01	0.02	-	-
31	76	4.0	-	-	4.3	0.6	7.0	1.0	**10.4**	**1.5**	-	-
36	32	4.2	0.9	0.2	4.5	0.8	**11.1**	**1.9**	-	-	-	-
38	116	4.7	2.3	1.0	**7.7**	**3.4**	**11.9**	**5.3**	-	-	-	-
39	22	4.7	2.7	1.8	**7.6**	**5.1**	**8.3**	**5.6**	-	-	-	-

[a]Values shown in bold font represent statistically significant LH inhibition effects as depicted in Figure 5. In vivo plasma concentration data obtained directly from the castrated rats used in the LH inhibition study albeit only at the general LH-nadir time point of 45 min. Unbound plasma and brain values were calculated as follows: $C_{plasma,u} = C_{plasma,total} \times f_u$ and $C_{brain,u} = C_{plasma,total} \times (B/P)_{total,60\ min} \times bf_u$. [b]RLB K_i values against rat NK_3R with mean of at least 3 independent measurements reported; SD ≤ 0.2 for all compounds. [c]LLE = pK_i (rat NK_3R) − log $D_{7.4}$ (or clogP, in the case of **2a**).

Castrated animals are often used in these in vivo efficacy experiments because their persistently elevated LH levels afford a wide dynamic range that facilitates measurements.[62] The in vivo efficacy studies were initially performed in castrate male rats following iv dosing given that the oral PK profile for the most advanced lead at the time, i.e., **3** (Figure 1), was deemed inadequate. Consequently, **3** and gold standards **1** and **2a** were dosed intravenously at the highest formulable concentration, i.e., 10 mg/kg. Statistically significant effects (≈ 50% inhibition) were observed in the initial iv POC studies with **3** (Figure 5a). We note in passing that LH measurements are reported as a decrease relative to the baseline LH level for each group of rats (N = 4−6 rats per group). With the initial POC established through lead structure **3**, and given the development of compounds with improved oral PK and brain uptake profiles (such as **31**, **36**, **38**, and **39**), we next focused on oral efficacy studies instead (Figure 5b−f and Table 7). It is noteworthy that in oral LH inhibition studies, the iv POC lead **3** proved altogether ineffective (up to 60 mg/kg) just as the gold standards osanetant and talnetant (**1** and **2a**, respectively, tested at up to 100 mg/kg). The improved leads **31**, **36**, **38**, and **39**, however, were all proven orally efficacious at 30 mg/kg, with **38** and **39** displaying oral efficacy in LH inhibition with doses as low as 10 mg/kg (Figure 5e,f). These results can be rationalized through PK and PKPD (Table 7) considerations as elaborated below.

The total plasma readouts at various administered doses in the same in vivo LH inhibition efficacy assays were used to

DOI: 10.1021/jm5017413
J. Med. Chem. XXXX, XXX, XXX−XXX

Table 8. PK Data and PKPD Correlations for Compound 31 in Castrated Male Cynomolgus Monkey LH Inhibition Studies[a]

dose route	dose (mg/kg)	$C_{max,u}$ (nM)	CL_T (mL/min/kg)	V_{ss} (L/kg)	$T_{1/2}$ (min)	T_{max} (min)	AUC_u (nM·h)	$C_{plasma,u}/K_i$	%F
iv	10	-	16.5	1.52	210	-	1055	-	-
po	5	17.9	-	-	-	90	64.6	1.0	12
po	20	237	-	-	-	60	526	9.4	25

[a]Mean values presented $N = 4$ monkeys per group. AUC_u = unbound AUC = $AUC_{total} \times f_u$ (monkey plasma $f_u = 0.043$).

construct PKPD correlations (Table 7). To recall, NK_3R is expressed on the KNDy neuron dendrites located in the ARC region of hypothalamus (Figure 2). Recent reports suggest that the ARC falls into the category of circumventricular organs (CVO),[63] i.e., regions of the brain that lack blood−brain barrier (BBB) and are exposed to blood solutes, an arrangement believed to be part of a neuroendocrine control system for maintaining hormone levels among other factors.[64] Therefore, unbound fractions in *both* plasma *and* brain tissue would be relevant for consideration in the PKPD analysis. Using the total B/P ratios as well as f_u and corresponding bf_u parameters discussed above, unbound plasma and brain concentrations ($C_{plasma,u}$ and $C_{brain,u}$, respectively) were calculated as footnoted in Table 7. Thereafter, the ratio of the unbound plasma and brain concentrations with respect to rat NK_3R radioligand binding K_i were calculated at each dose. Two caveats to this data analysis are as follows: (i) only the 45 min plasma readout was used in the PK sampling for this PKPD analysis, and (ii) the brain-to-plasma ratio at 60 min was used to convert 45 min plasma readouts. Although the latter may cause an underestimation, given the B/P ratio stability at 10 and 60 min time points (Table 6), this adjustment is unlikely to alter the overall interpretation of the data. Despite these caveats, the $C_{plasma,u}/K_i$ and $C_{brain,u}/K_i$ ratios served as insightful PKPD parameters for the analysis of the in vivo oral efficacy data.

The PKPD analysis revealed that in all cases where statistically significant LH inhibition was observed in castrated male rats, $C_{plasma,u}/K_i \geq 7.6$ and $C_{brain,u}/K_i > 1$ were attained. The larger plasma ratio against that in the brain is consistent with the localization of the receptor within neurons in the hypothalamic ARC. In addition, these PKPD parameters make it abundantly clear that the previously stated absence of oral efficacy with either the iv POC lead **3** ($C_{plasma,u}/K_i$ and $C_{brain,u}/K_i \leq 0.02$, at 60 mg/kg), or with the gold standards **1** and **2a** ($C_{plasma,u}/K_i \leq 0.07$ and $C_{brain,u}/K_i \leq 0.1$, even at 100 mg/kg), is due to their rather low unbound plasma and brain exposure levels. Moreover, with the improved LLE analogues, the in vivo efficacy was left-shifted, driven by the improved in vivo exposure as indicated by the PKPD parameters. Recall that the LLE values relevant here are based on the rat NK_3R pK_i data (Table 7), which parallel human NK_3R LLE values but are underestimated for human due to the right-shifted rodent bioactivity values. Therefore, with LLE ≥ 4.2 for **36**, **38**, and **39**, the oral efficacy was reached at 30 mg/kg as compared to **31** with LLE = 4.0 that reached oral efficacy at 60 mg/kg. In fact, only the highest LLE analogues, i.e., **38** and **39**, managed to reach oral efficacy at 10 mg/kg. Overall, the PKPD parameters discussed embody the dual project goals of improved LLE, which in turn led to an improved in vivo exposure and enhanced bioactivity. The eventual recovery of LH values to basal levels (at 300 min) is consistent globally with the PK profile (e.g., $T_{1/2} < 300$ min) as well as consideration of the homeostatic regulation of the HPG axis.[65]

In vivo efficacy was also established in castrated cynomolgus monkeys (*Macaca fascicularis*), chosen because this "old world" primate best resembles humans in their sex-hormone physiology. As noted earlier, monkey NK_3R is the most germane to its human counterpart, also mirrored in the comparison of relative shifts in the RLB K_i data against human NK_3R as compared to the rat NK_3R data (Table 4). Compound **31** was nominated for these initial monkey LH inhibition studies based on the considerations of acceptable LLE = 4.5 (based on monkey NK_3R pK_i), bioactivity and, importantly, its superior off-target safety profiles (hERG and CYP) relative to the other advanced leads herein. Last but not least, the monkey PK profile of analogue **31** was supportive of undertaking this additional in vivo efficacy study (Table 8). In castrated monkeys, an oral dose of **31** at 20 mg/kg (in 0.5% methylcellulose/water) significantly decreased plasma LH levels by ≈40% (at nadir, time = 90 min postdosing, Figure 6), with

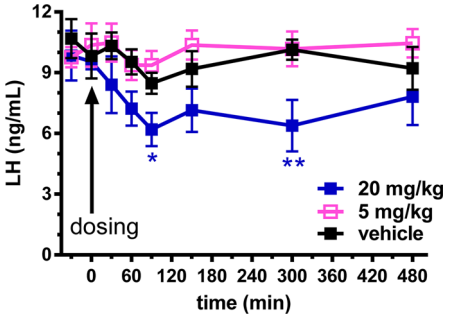

Figure 6. LH inhibition in castrate male cynomolgus monkeys ($N = 4$ per group) following oral administration of compound **31** in 0.5% methylcellulose/water. Data ± SEM provided. Oral monkey PK results summarized in Table 8 correspond to plasma samples from this study. Statistical analysis performed by 2-way ANOVA followed by Dunnet's comparison to vehicle group, $*p < 0.05$; $**p < 0.01$).

LH inhibition persisting from 90−300 min and with recovery apparent at 480 min postdosing. Consistent with the plasma PKPD relationship in rats, efficacy in monkeys corresponded to $C_{plasma,u}/K_i = 9.4$ ($C_{brain,u}$ not determined).

CONCLUSIONS

A global objective of the initial phase of this project was to establish the amenability of the novel NK_3R antagonist *N*-acyl-triazolopiperazine chemotype (**5**) toward lead optimization. This novel chemotype was discovered through a bioisosteric lead change from the HTS hit series (**4**) that was deemed unlikely to succeed in advanced lead optimization irrespective of its excellent in vitro bioactivity. While the "scaffold hop" from **4** to **5** paid immediate dividends from the point of view of LLE, PK, and off-target safety profiles, it also necessitated a significant improvement in the NK_3R antagonist bioactivity profile against compound **5** ($pK_i = 5.3$, $pIC_{50} = 5.5$). Mindful of the increased safety risks that correlate with high lipophilicity compounds, we sought to improve the bioactivity profile (i.e., pK_i, $\Delta pIC_{50} > 2$) in a lipophilically efficient manner (i.e., ΔLLE ≥ 0 vs **5**) (Figure 7). Compound **3** (Figure 1) furnished the

DOI: 10.1021/jm5017413
J. Med. Chem. XXXX, XXX, XXX−XXX

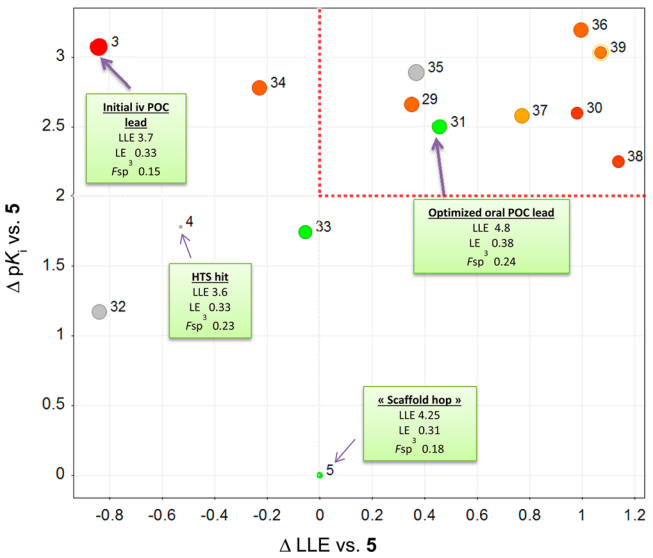

Figure 7. Lead optimization progress as a plot of ΔpK_i = pK_i(compd *x*) − pK_i(compd **5**) versus ΔLLE = LLE(compd *x*) − LLE(compd **5**). The pK_i values refer to hNK$_3$R RLB data and LLE = pK_i(hNK$_3$R) − log $D_{7.4}$. The highlighted red box indicates the quadrant where the project targets of ΔLLE > 0 and ΔpK_i > 2 vs compd **5** are achieved. Coloring scheme of the dots denotes hERG IC_{50} values: red <10 μM, green >20 μM, and gray implies not determined. LE = (1.37/HAC) × pK_i, where HAC denotes the number of non-hydrogen atoms;[39] Fsp^3 = number of sp^3 hybridized carbons/total carbon count.[40]

initial in vivo POC analogue through LH inhibition in castrated male rats via iv administration. Despite a notable improvement in bioactivity against **5** (ΔpK_i = 3.07, ΔpIC_{50} = 2.2), compound **3** fell drastically short of the LLE target (ΔLLE = −0.55 vs **5**), consistent with its rather poor aqueous solubility and off-target safety profile (CYP and hERG). Further efforts resulted in identifying advanced leads that fulfilled both enhanced bioactivity and improved LLE (the highlighted red box in Figure 7). While these advanced leads displayed an attractive oral and brain PK as well as off-target selectivity and solubility profiles, the hERG safety SAR distinguished **31** as the best overall candidate at this stage of the lead optimization program. Moreover, compound **31** (ΔLLE = 0.55, ΔpK_i = 2.6, ΔpIC_{50} = 2.3) also showed improved ligand efficiency[39] (ΔLE = 0.07) and fraction sp^3 content[40] (ΔFsp^3 = 0.06) vis-à-vis **5**. Importantly, in comparing congeneric analogues, the improved LLE trend correlated with an increase in the unbound levels both in plasma ($C_{plasma,u}$) and in the brain tissue ($C_{brain,u}$). In addition, oral efficacy was achieved through LH inhibition in castrated rats when $C_{plasma,u}/K_i \geq 7.6$ and $C_{brain,u}/K_i > 1$ levels were attained, as demonstrated using several advanced analogues, and, in the case of **31**, in castrated monkeys as well ($C_{plasma,u}/K_i$ = 9.4). The PKPD analysis suggested that in vivo efficacy correlates with adequate unbound levels of these analogues in both plasma ($C_{plasma,u}$) and brain ($C_{brain,u}$), consistent with the neuroanatomy of the NK$_3$R that is part of the CVO region in the brain and therefore exposed to the blood solutes as well.

While we have not demonstrated in vivo data either in female species or in relation to GnRH pulsatility in this report, such data have been preliminarily disclosed elsewhere[62] and will also be the subject of further disclosures in the near future.[66] In a sequel to this report,[30] we will also disclose additional optimization on analogue **31** that culminated in ESN364 as the clinical candidate (currently in phase 2 human trials).[67]

EXPERIMENTAL SECTION

General Information. Solvents and reagents were of reagent grade and were used as supplied by the manufacturer. All reactions were performed under a N_2 atmosphere unless otherwise noted. Piperazinone starting materials **40** and **41** (Scheme 1) as well as (*S*)-ent-**42** were procured from a commercial vendor (J&W PharmLab, PA, USA). Chromatography refers to flash chromatography using silica gel. NMR spectra were recorded on Bruker ARX spectrometer (300 MHz) at room temperature. Chemical shifts are expressed in parts per million δ relative to residual solvent as an internal reference. Peak multiplicities are expressed as follows: singlet (s), doublet (d), triplet (t), quartet (q), heptuplet (h), multiplet (m), and broad singlet (bs). HPLC purity analysis of compounds was carried out using one of the following methods. Method A: LC/diode array detector/evaporative light scattering detector coupled to single quadrupole mass spectrometry (LC/UV/ELSD/MS); column, Chromolith SpeedROD Rp-18 4.6 × 50 mm; mobile phase A, 0.1% TFA in water/acetonitrile (95:5 v/v); mobile phase B, 0.1% TFA in acetonitrile (v/v); gradient begins at 0% B increasing to 95% B over 2.3 min, hold at 95% B until 2.8 min; flow rate, 3.75 mL/min. Method B: LC/diode array detector coupled to single quadrupole mass spectrometry (LC/UV/MS); column, Sunfire C18 3 μm 3.0 mm × 50 mm; mobile phase A, 0.1% TFA in water (v/v); mobile phase B, 0.1% TFA in acetonitrile (v/v); gradient begins at 5% B, hold 0.2 min at 5% B, increasing to 95% B over 6.0 min, hold at 95% B until 7.75 min; flow rate, 1.0 mL/min. Method C: LC/diode array detector coupled to single quadrupole mass spectrometry (LC/UV/MS); column, Sunfire C18 3 μm 3.0 mm × 50 mm; mobile phase A, 0.1% TFA in water (v/v); mobile phase B, 0.1% TFA in acetonitrile (v/v); gradient begins at 5% B, hold 0.2 min at 5% B, increasing to 95% B over 2.0 min, hold at 95% B until 3.75 min; flow rate, 1.0 mL/min. Enantiomeric excess of chiral compounds and intermediates was carried out using one of the following methods. Method D: column, Chiralpak IA 5.0 μm C18 4.6 mm × 250 mm; mobile phase, 0.1% DEA in TBME (v/v); flow rate, 1.0 mL/min; UV absorbance at 280 nm. Method E: column, Chiralpak IA 5.0 μm C18 4.6 mm × 250 mm; mobile phase, 0.1% DEA in EtOAc/hexane (7:3 v/v); flow rate, 1.5 mL/min; UV absorbance at 280 nm. Method F: column, Chiralpak IC 5.0 μm C18 4.6 mm × 250 mm; mobile phase, 0.1% DEA in EtOH/hexane (1:1 v/v); flow rate, 1.0 mL/min; UV absorbance at 280 nm. Method G: column, Chiralpak IA 5.0 μm C18 4.6 mm × 250 mm; mobile phase, 0.1% DEA in EtOAc (v/v); flow rate, 1.0 mL/min; UV absorbance at 280 nm. Method H: column, Chiralpak IC 5.0 μm C18 4.6 mm × 250 mm; mobile phase, 0.1% DEA in EtOAc/hexane (1:1 v/v); flow rate, 1.5 mL/min; UV absorbance at 280 nm. Method I: column, Chiralpak ID 5.0 μm C18 4.6 mm × 250 mm; mobile phase, 0.1% DEA in hexane/DCM/IPA (3:1:1 v/v); flow rate, 1.0 mL/min; UV absorbance at 280 nm. Method J: column, Chiralpak IA 5.0 μm C18 4.6 mm × 250 mm; mobile phase, 0.1% DEA in EtOAc (v/v); flow rate, 1.5 mL/min; UV absorbance at 280 nm. Method K: column, Chiralpak IB 5.0 μm C18 4.6 mm × 250 mm; mobile phase, 0.1% DEA in hexane/DCM/EtOAc (135:5:60 v/v); flow rate, 1.5 mL/min; UV absorbance at 280 nm. Method L: column, Chiralpak IA 5.0 μm C18 4.6 mm × 250 mm; mobile phase, 0.1% DEA in hexane/DCM/IPA (3:1:1 v/v); flow rate, 1.0 mL/min; UV absorbance at 280 nm. Method M: column, Chiralpak IC 5.0 μm C18 4.6 mm × 250 mm; mobile phase, 0.1% DEA in TBME/MeOH (92:2 v/v); flow rate, 1.0 mL/min; UV absorbance at 280 nm. Nomenclature of compounds below was achieved using Beilstein AutoNom feature accessible within ChemBioDraw Ultra, version 12. Reference compounds **1** and **2a** were accessed as indicated previously.[26]

Synthesis. *Step a_1: tert-Butyl 5-Ethoxy-3,6-dihydropyrazine-1(2H)-carboxylate (**42**).* To a premade solution of Et_3OBF_4 (2.3 g, 12.1 mmol, 1.4 equiv) in CH_2Cl_2 (20 mL) was added **40** (2 g, 8.8 mmol, 1.0 equiv) at 0 °C. After the addition was completed, the reaction mixture was allowed to warm to room temperature and stirred

DOI: 10.1021/jm5017413
J. Med. Chem. XXXX, XXX, XXX−XXX

for an additional hour. A saturated solution of $NaHCO_3$ (500 mL) was slowly added to the reaction mixture, and it was stirred for 5 min. The organic layer was separated, and the aqueous layer was further extracted with CH_2Cl_2 (200 mL). The combined organic layers were subsequently washed with brine, dried over $MgSO_4$, filtered, and dried in vacuo to dryness to obtain **43** as viscous yellow oil (2.03 g, 88%). LCMS (method C) m/z 246 (M + H_2O + 1). HPLC purity >90% (254 nm). ^1H NMR ($CDCl_3$): δ 4.1 (q, J = 7.1 Hz, 2H), 3.85 (s, 2H), 3.5 (m, 1H), 3.35 (t, J = 5.1 Hz, 2H), 1.45 (s, 9H), 1.3 (t, J = 7.1 Hz, 3H).

*Step a_2: (R)-1-(2,4-Dimethoxybenzyl)-5-ethoxy-6-methyl-1,2,3,6-tetrahydropyrazine (**44**).* To a solution of (*R*)-4-(2,4-dimethoxybenzyl)-3-methylpiperazin-2-one, **41** (20 g, 76 mmol, 1 equiv) in CH_2Cl_2 (250 mL) was added, at 15 °C, Na_2CO_3 (18 g, 170 mmol, 2.25 equiv), followed by Et_3OBF_4[33] (18 g, 95 mmol, 1.25 equiv) over 10 min, whereupon a slight exotherm was noted (15 to 21 °C). After stirring the reaction mixture 45 min further at room temperature, it was quenched with brine (340 mL), the organic layer separated, dried ($MgSO_4$), filtered, and concentrated in vacuo (1−2 mbar, 30 °C) to afford the crude product as a yellow oil. Purification by silica gel flash chromatography (EtOAc/MeOH: 99/1) afforded pure **44** as a yellow oil (14.75 g, 67%). (NB: This product was stored at −20 °C under Ar and typically used for the subsequent reaction within a day of its preparation.) LCMS (method C) m/z 311 (M + H_2O + 1). HPLC purity 96% (280 nm). Chiral LC (method D): 98.8% ee ($t_{R(S)}$ = 4.4 min, $t_{R(R)}$ = 10.7 min). ^1H NMR ($CDCl_3$): δ 7.23 (d, J = 8.8 Hz, 1H), 6.48 (d, J = 8.8 Hz, 1H), 6.44 (s, 1H), 4.02 (m, 2H), 3.92 (s, 3H), 3.91 (s, 3H), 3.86 (d, $J_{AB}J_{AB}$ = 14.0 Hz, 1H), 3.46 (d, J_{AB} = 14.0 Hz, 1H), 3.44 (m, 2H), 3.10 (m, 1H), 2.79 (m, 1H), 2.32 (m, 1H), 1.35 (d, J = 6.8 Hz, 3H), 1.24 (t, J = 6.0 Hz, 3H). ^{13}C NMR ($CDCl_3$): δ 164.5, 160.1, 158.9, 131.1, 118.8, 104.1, 98.6, 60.4, 55.5, 55.4, 55.1, 51.4, 45.8, 45.6, 16.1, 14.5.

*(S)-1-(2,4-Dimethoxybenzyl)-5-ethoxy-6-methyl-1,2,3,6-tetrahydropyrazine (**45**).* Prepared similarly to **44** but starting from the (*S*)-form of the chiral ketopiperazine precursor **42** (390 mg, 71%). LCMS (method C) m/z 311 (M + 1 + H_2O). HPLC purity >95% (254 nm). Chiral LC (method D): 99.5% ee ($t_{R(S)}$ = 4.4 min, $t_{R(R)}$ = 10.7 min).

*Step b: General Procedure A for the Synthesis of Intermediates **62**−**77**, Exemplified with 2-Methylthiazole-4-carbohydrazide (**62**).* Ethyl 2-methylthiazole-4-carboxylate **46** (10 g, 58.4 mmol) was dissolved in anhydrous EtOH (25 mL) and treated with hydrazine monohydrate (17.0 mL, 354.4 mmol, 6 equiv) at room temperature, whereupon the reaction mixture was heated to reflux for 14 h. Upon allowing the reaction mixture to reach room temperature, it was concentrated in vacuo and the obtained oil was coevaporated with CH_2Cl_2:MeOH (1:1, 3 × 200 mL) and recrystallized (hot EtOH, 60 mL) to obtain **62** as a pale-orange solid (5.85 g, 64%). LCMS (method C) m/z 158 (M + 1). ^1H NMR ($CDCl_3$): δ 8.32 (br, 1H), 7.96 (s, 1H), 4.07 (br, 2H), 2.70 (s, 3H). ^{13}C NMR ($CDCl_3$): δ 166.6, 161.9, 148.1, 123.4, 19.2.

*6-Methylpyrazine-2-carbohydrazide (**67**).* Starting from commercially available methyl 6-(trifluoromethyl)picolinate **51** as per general procedure A to obtain 290 mg (66%). LCMS (method C) m/z 153 (M + 1). HPLC purity >95% (254 nm). This intermediate (**67**) was used to ultimately prepare compd **25**.

*6-(Trifluoromethyl)picolinohydrazide (**68**).* Starting from commercially available methyl 6-(trifluoromethyl)picolinate **52** as per general procedure A to obtain 506 mg (100%). LCMS (method C) m/z 206 (M + 1). HPLC purity >95% (254 nm). This intermediate (**68**) was used to ultimately prepare compd **26**.

*2-(2,4-Difluorophenyl)thiazole-4-carbohydrazide (**71**).* Starting from ethyl 2-(2,4-difluorophenyl)thiazole-4-carboxylate **55** as per general procedure A to obtain 10.7 g (72%). LCMS (method C) m/z 256 (M + 1). HPLC purity >95% (254 nm). ^1H NMR ($CDCl_3$): δ 10.07 (s, 1H), 8.33 (s, 1H), 8.20 (m, 1H), 7.00 (m, 2H). This intermediate (**71**) was used to ultimately prepare compd **3**.

*2-(Trifluoromethyl)thiazole-4-carbohydrazide (**72**).* Starting from commercially available ethyl 2-(trifluoromethyl)thiazole-4-carboxylate **56** as per general procedure A to obtain 550 mg (quant). LCMS (method C) m/z 212 (M + 1). HPLC purity >95% (254 nm). This intermediate (**72**) was used to ultimately prepare compd **34**.

*2-Isopropylthiazole-4-carbohydrazide (**73**).* Starting from commercially available ethyl 2-isopropylthiazole-4-carboxylate **57** as per general procedure A to obtain 405 mg (87%). LCMS (method C) m/z 186 (M + 1). HPLC purity 96% (254 nm). ^1H NMR ($CDCl_3$): δ 8.00 (s, 1H), 4.03 (br, 2H), 3.28 (h, J = 6.9 Hz, 1H), 1.39 (d, J = 6.9 Hz, 6H). This intermediate (**73**) was used to ultimately prepare compd **35**.

*2-Isopropyloxazole-4-carbohydrazide (**74**).* Starting from methyl 2-isopropyloxazole-4-carboxylate **58** as per general procedure A to obtain 250 mg (98%). LCMS (method C) m/z 170 (M + 1). HPLC purity 98% (254 nm). This intermediate (**74**) was used to ultimately prepare compd **36**.

*4-Methylthiazole-2-carbohydrazide (**75**).* Starting from commercially available methyl 2-isopropyloxazole-4-carboxylate **59** as per general procedure A to obtain 159 mg (82%). LCMS (method C) m/z 158 (M + 1). HPLC purity 98% (254 nm). This intermediate (**75**) was used to ultimately prepare compd **37**.

*3-Methyl-1,2,4-oxadiazole-5-carbohydrazide (**76**).* Starting from ethyl 3-methyl-1,2,4-oxadiazole-5-carboxylate as per general procedure A to obtain 2.23 g (81%). LCMS (method C) m/z 143 (M + 1). HPLC purity >95% (254 nm). ^1H NMR ($CDCl_3$): δ 8.22 (br, 1H), 4.21 (br, 2H), 2.48 (s, 3H). This intermediate (**76**) was used to ultimately prepare compd **38**.

*3-Methyl-1,2,4-thiadiazole-5-carbohydrazide (**77**).* Starting from methyl 3-methyl-1,2,4-thiadiazole-5-carboxylate as per general procedure A to obtain 398 mg (quant). LCMS (method C) m/z 159 (M + 1). HPLC purity >95% (254 nm). ^1H NMR ($CDCl_3$): δ 8.40 (br, 1H), 4.13 (br, 2H), 2.71 (s, 3H). This intermediate (77) was used to ultimately prepare compd **39**.

*Step c1: General Procedure B for the Synthesis of Intermediates **78**−**84**, Exemplified with tert-Butyl-3-(2-methylthiazol-4-yl)-5,6-dihydro-[1,2,4]triazolo[4,3-a]pyrazine-7(8H)-carboxylate (**84**).* **43** (1.1 g, 4.8 mmol, 1 equiv) was dissolved in anhydrous EtOH (20 mL), to which was added **62** (0.75 g, 4.8 mmol, 1 equiv) in one portion. The resulting solution was stirred under reflux overnight. The reaction mixture was allowed to reach room temperature, whereupon the solvent was removed under reduced pressure. The crude compound was then purified on silica gel (CH_2Cl_2/MeOH: 99/1 to 98/2) to afford the desired product **85** as white solid (1.1 g, 70%). LCMS (method C) m/z 321 (M + 1). HPLC purity 95% (254 nm). ^1H NMR ($CDCl_3$): δ 7.95 (s, 1H), 4.87 (s, 2H), 4.47 (t, J = 5.4 Hz, 2H), 3.84 (t, J = 5.4 Hz, 2H), 2.70 (s, 3H), 1.47 (s, 9H). This intermediate (**85**) was used to ultimately prepare compd **33**.

*tert-Butyl 3-(Pyridin-2-yl)-5,6-dihydro-[1,2,4]triazolo[4,3-a]-pyrazine-7(8H)-carboxylate (**78**).* Starting from **43** and commercially available picolinohydrazide **63** as per general procedure B to obtain 1.1 g (86%). LCMS (method C) m/z 302 (M + 1). HPLC purity >90% (254 nm). ^1H NMR ($CDCl_3$): δ 8.60 (d, J = 4.6 Hz, 1H), 8.30 (d, J = 8.0 Hz, 1H), 7.81 (m, 1H), 7.32 (ddd, J = 1.0, 4.9, 7.6 Hz, 1H), 4.91 (s, 2H), 4.63 (t, J = 5.4 Hz, 2H), 3.86 (t, J = 5.4 Hz, 2H), 1.49 (s, 9H). This intermediate (**78**) was used to ultimately prepare compds **5**−**18**.

*tert-Butyl 3-(6-Methylpyridin-2-yl)-5,6-dihydro-[1,2,4]triazolo-[4,3-a]pyrazine-7(8H)-carboxylate (**79**).* Starting from **43** and commercially available 6-methylpicolinohydrazide **64** as per general procedure B to obtain 2.7 g (98%). LCMS (method C) m/z 316 (M + 1). HPLC purity >95% (254 nm). This intermediate (**79**) was used to ultimately prepare compd **22**.

*tert-Butyl 3-(5-Methylpyridin-2-yl)-5,6-dihydro-[1,2,4]triazolo-[4,3-a]pyrazine-7(8H)-carboxylate (**80**).* Starting from **43** and commercially available 5-methylpicolinohydrazide **65** as per general procedure B to obtain 64 mg (61%). LCMS (method C) m/z 316 (M + 1). HPLC purity >90% (254 nm). ^1H NMR ($CDCl_3$): δ 8.43 (s, 1H), 8.19 (d, J = 8.1 Hz, 1H), 7.63 (m, 1H), 4.91 (s, 2H), 4.61 (t, J = 5.4 Hz, 2H), 3.86 (t, J = 5.4 Hz, 2H), 2.41 (s, 3H), 1.50 (s, 9H). This intermediate (**80**) was used to ultimately prepare compd **23**.

*tert-Butyl 3-(4-Methylpyridin-2-yl)-5,6-dihydro-[1,2,4]triazolo-[4,3-a]pyrazine-7(8H)-carboxylate (**81**).* Starting from **43** and commercially available 4-methylpicolinohydrazide **66** as per general procedure B to obtain 200 mg (96%). LCMS (method C) m/z 316

DOI: 10.1021/jm5017413
J. Med. Chem. XXXX, XXX, XXX−XXX

(M + 1). HPLC purity >90% (254 nm). ^{1}H NMR ($CDCl_3$): δ 8.46 (d, J = 5.0 Hz, 1H), 8.15 (s, 1H), 7.15 (d, J = 5.0 Hz, 1H), 4.92 (s, 2H), 4.62 (t, J = 5.4 Hz, 2H), 3.86 (t, J = 5.4 Hz, 2H), 2.42 (s, 3H), 1.50 (s, 9H). This intermediate (**81**) was used to ultimately prepare compd **24**.

*tert-Butyl 3-(3-Methylpyridin-2-yl)-5,6-dihydro-[1,2,4]triazolo-[4,3-a]pyrazine-7(8H)-carboxylate (**82**).* Starting from **43** and commercially available 3-methylpicolinohydrazide **67** as per general procedure B to obtain 160 mg (77%). LCMS (method C) m/z 316 (M + 1). HPLC purity >90% (254 nm). ^{1}H NMR ($CDCl_3$): δ 8.50 (m, 1H), 7.69 (m, 1H), 7.26 (m, 1H), 4.95 (s, 2H), 4.39 (t, J = 5.4 Hz, 2H), 3.85 (t, J = 5.4 Hz, 2H), 2.70 (s, 3H), 1.47 (s, 9H). This intermediate (**82**) was used to ultimately prepare compd **25**.

*tert-Butyl 3-(6-(Trifluoromethyl)pyridin-2-yl)-5,6-dihydro-[1,2,4]-triazolo[4,3-a]pyrazine-7(8H)-carboxylate (**83**).* Starting from **43** and **68** as per general procedure B to obtain 256 mg (96%). LCMS (method C) m/z 370 (M + 1). HPLC purity >95% (254 nm). This intermediate (**83**) was used to ultimately prepare compd **26**.

*Step c2: General Procedure C for the Synthesis of Intermediates **85**–**98**, Exemplified with (R)-4-(7-(2,4-Dimethoxybenzyl)-8-methyl-5,6,7,8-tetrahydro-[1,2,4]triazolo[4,3-a]pyrazin-3-yl)-2-methylthiazole (**85**).* **44** (15.9 g, 51.2 mmol, 1 equiv) was dissolved in anhydrous methanol (51 mL) under Ar, to which was added **62** (8.05 g, 51.2 mmol, 1.0 equiv) in one portion. The resulting solution was stirred at 60–70 °C for 8 h, whereupon it was allowed to reach room temperature and volatiles removed in vacuo (1–2 mbar, 30 °C). The residue obtained was then dissolved in EtOAc (250 mL), washed with NaOH (1 M, 2 × 110 mL), and after separation the organic layer was dried ($MgSO_4$), filtered, and volatiles removed (1–2 mbar, 30 °C) to obtain viscous orange oil (18.04 g, 91%). LCMS (method C) m/z 386 (M + H). HPLC purity 89% (280 nm). This oil was purified by silica gel flash chromatography (gradient: 1–5% MeOH in CH_2Cl_2) to obtain **85** as a pale-yellow solid (16.7 g, 84%). LCMS (method C) m/z 386 (M + H). HPLC purity 98% (280 nm). Chiral LC (method E) 97.6% ee ($t_{R(R)}$ = 14.1 min, $t_{R(S)}$ = 20.2 min). ^{1}H NMR ($CDCl_3$): δ 7.88 (s, 1H), 7.23 (s, 1H), 6.44 (m, 2H), 4.45 (dt, J = 4.5, 13.2 Hz, 1H), 4.19 (m, 1H), 4.01 (q, J = 4.6 Hz, 1H), 3.90 (d, J_{AB} = 13.6 Hz, 1H), 3.78 (s, 3H), 3.77 (s, 3H), 3.56 (d, J_{AB} = 13.6 Hz, 1H), 3.17 (dt, J = 4.7, 13.0 Hz, 1H), 2.70 (s, 3H), 2.68 (m, 1H), 1.69 (d, J = 6.6 Hz, 3H). ^{13}C NMR ($CDCl_3$): δ 166.2, 160.2, 158.8, 154.6, 148.1, 143.2, 130.9, 118.8, 118.2, 104.2, 98.5, 60.4, 55.2, 53.9, 50.2, 45.8, 44.2, 19.2, 17.7. $[\alpha]^{D}_{Na}$ = +6.2° (10.3 mg/mL in $CHCl_3$, 95.1% ee). This intermediate (**85**) was used to ultimately prepare compds **27** and **31**.

*(S)-7-(2,4-Dimethoxybenzyl)-8-methyl-3-(pyridin-2-yl)-5,6,7,8-tetrahydro-[1,2,4]triazolo[4,3-a]pyrazine (**86**).* Starting from **45** and commercially available picolinohydrazide **63** as per general procedure C to obtain 390 mg (80%). LCMS (method C) m/z 366 (M + 1). HPLC purity >95% (254 nm). This intermediate (**86**) was used to ultimately prepare compd **19**.

*(R)-7-(2,4-Dimethoxybenzyl)-8-methyl-3-(pyridin-2-yl)-5,6,7,8-tetrahydro-[1,2,4]triazolo[4,3-a]pyrazine (**87**).* Starting from **44** and commercially available picolinohydrazide **63** as per general procedure C to obtain 120 mg (48%). LCMS (method C) m/z 366 (M + 1). HPLC purity >95% (254 nm). This intermediate (**87**) was used to ultimately prepare compd **20**.

*(R)-7-(2,4-Dimethoxybenzyl)-8-methyl-3-(6-methylpyridin-2-yl)-5,6,7,8-tetrahydro-[1,2,4]triazolo[4,3-a]pyrazine (**88**).* Starting from **44** and commercially available 6-methylpicolinohydrazide **64** as per general procedure C to obtain 190 mg (76%). LCMS (method C) m/z 380 (M + 1). HPLC purity >95% (254 nm). This intermediate (**88**) was used to ultimately prepare compds **21** and **29**.

*(R)-4-(7-(2,4-Dimethoxybenzyl)-8-methyl-5,6,7,8-tetrahydro-[1,2,4]triazolo[4,3-a]pyrazin-3-yl)-2-phenylthiazole (**89**).* Starting from **44** and commercially available 2-phenylthiazole-4-carbohydrazide **69** as per general procedure C to obtain 230 mg (50%). LCMS (method C) m/z 448 (M + 1). HPLC purity 88% (215 nm). ^{1}H NMR ($CDCl_3$): δ 8.10 (s, 1H), 7.94 (m, 2H), 7.44 (m, 3H), 7.29 (d, J = 8.1 Hz, 1H), 6.50 (m, 2H), 4.60 (dt, J = 4.6, 13.2 Hz, 1H), 4.34 (m, 1H), 4.07 (q, J = 6.5 Hz, 1H), 3.96 (d, J = 13.5 Hz, 1H), 3.81 (2s, 6H), 3.59 (d, J = 13.5 Hz, 1H), 3.25 (dt, J = 4.6, 13.2 Hz, 1H), 2.75 (m, 1H), 1.76 (d, J = 6.6 Hz, 3H). This intermediate (**89**) was used to ultimately prepare compd **28**.

*(R)-7-(2,4-Dimethoxybenzyl)-8-methyl-3-(6-methylpyrazin-2-yl)-5,6,7,8-tetrahydro-[1,2,4]triazolo[4,3-a]pyrazine (**90**).* Starting from **44** and **70** as per general procedure C to obtain 370 mg (51%). LCMS (method C) m/z 381 (M + 1). HPLC purity >95% (254 nm). This intermediate (**90**) was used to ultimately prepare compd **30**.

*(R)-2-(2,4-Difluorophenyl)-4-(7-(2,4-dimethoxybenzyl)-8-methyl-5,6,7,8-tetrahydro-[1,2,4]triazolo[4,3-a]pyrazin-3-yl)thiazole (**91**).* Starting from **44** and **71** as per general procedure C to obtain 15 mg (3%). LCMS (method C) m/z 484 (M + 1). HPLC purity >95% (254 nm). Chiral LC (method D) 99.2% ee ($t_{R(S)}$ = 4.3 min, $t_{R(R)}$ = 10.2 min). This intermediate (**91**) was used to ultimately prepare compd **3**.

*(S)-4-(7-(2,4-Dimethoxybenzyl)-8-methyl-5,6,7,8-tetrahydro-[1,2,4]triazolo[4,3-a]pyrazin-3-yl)-2- methylthiazole (**92**).* Starting from **45** and **62** as per general procedure C to obtain 36 mg (59%). LCMS (method C) m/z 386 (M + 1). HPLC purity >95% (254 nm). Chiral LC (method E) 94.2% ee ($t_{R(R)}$ = 14.1 min, $t_{R(S)}$ = 20.2 min). This intermediate (**92**) was used to ultimately prepare compd **32**.

*(R)-4-(7-(2,4-Dimethoxybenzyl)-8-methyl-5,6,7,8-tetrahydro-[1,2,4]triazolo[4,3-a]pyrazin-3-yl)-2-(trifluoromethyl)thiazole (**93**).* Starting from **44** and **72** as per general procedure C to obtain 400 mg (77%). LCMS (method C) m/z 440 (M + 1). HPLC purity >90% (254 nm). This intermediate (**93**) was used to ultimately prepare compd **34**.

*(R)-4-(7-(2,4-Dimethoxybenzyl)-8-methyl-5,6,7,8-tetrahydro-[1,2,4]triazolo[4,3-a]pyrazin-3-yl)-2-isopropylthiazole (**94**).* Starting from **44** and **73** as per general procedure C to obtain 210 mg (30%). LCMS (method C) m/z 414 (M + 1). HPLC purity >95% (254 nm). ^{1}H NMR ($CDCl_3$): δ 7.97 (s, 1H), 7.31 (d, J = 8.0 Hz, 1H), 6.52 (m, 1H), 6.49 (s, 1H), 4.43 (m, 1H), 4.32 (m, 1H), 4.10 (m, 1H), 3.97 (m, 1H), 3.83 (s, 3H), 3.82 (s, 3H), 3.68 (m, 1H), 3.17 (h, J = 6.9 Hz, 1H), 3.25 (m, 1H), 2.77 (m, 1H), 1.78 (d, J = 6.1 Hz, 3H), 1.42 (d, J = 6.9 Hz, 6H). This intermediate (**94**) was used to ultimately prepare compd **35**.

*(R)-4-(7-(2,4-Dimethoxybenzyl)-8-methyl-5,6,7,8-tetrahydro-[1,2,4]triazolo[4,3-a]pyrazin-3-yl)-2-isopropyloxazole (**95**).* Starting from **44** and **74** as per general procedure C to obtain 333 mg (79%). LCMS (method C) m/z 398 (M + 1). HPLC purity 93% (254 nm). This intermediate (**95**) was used to ultimately prepare compd **36**.

*(R)-2-(7-(2,4-Dimethoxybenzyl)-8-methyl-5,6,7,8-tetrahydro-[1,2,4]triazolo[4,3-a]pyrazin-3-yl)-4-methylthiazole (**96**).* Starting from **44** and **75** as per general procedure C to obtain 299 mg (77%). LCMS (method C) m/z 386 (M + 1). HPLC purity 95% (254 nm). This intermediate (**96**) was used to ultimately prepare compd **37**.

*(R)-5-(7-(2,4-Dimethoxybenzyl)-8-methyl-5,6,7,8-tetrahydro-[1,2,4]triazolo[4,3-a]pyrazin-3-yl)-3-methyl-1,2,4-oxadiazole (**97**).* Starting from **44** and **76** as per general procedure C to obtain 543 mg (87%). LCMS (method C) m/z 371 (M + 1). HPLC purity >98% (254 nm). ^{1}H NMR ($CDCl_3$): δ 7.25 (d, J = 8.4 Hz, 1H), 6.48 (d, J = 8.4 Hz, 1H), 6.47 (s, 1H), 4.43 (dt, J = 13.3, 4.6 Hz, 1H), 4.28 (m, 1H), 4.10 (q, J = 6.7 Hz, 1H), 3.94 (t, J = 13.6 Hz, 1H), 3.80 (2s, 6H), 3.63 (t, J = 13.6 Hz, 1H), 3.25 (dt, J = 13.1, 4.9 Hz, 1H), 2.77 (m, 1H), 2.49 (s, 3H), 1.74 (d, J = 6.6 Hz, 3H). This intermediate (**97**) was used to ultimately prepare compd **38**.

*(R)-5-(7-(2,4-Dimethoxybenzyl)-8-methyl-5,6,7,8-tetrahydro-[1,2,4]triazolo[4,3-a]pyrazin-3-yl)-3-methyl-1,2,4-thiadiazole (**98**).* Starting from **44** and **77** as per general procedure C to obtain 315 mg (64%). LCMS (method C) m/z 387 (M + 1). HPLC purity 91% (254 nm). Chiral LC (method M) 94.1% ee ($t_{R(R)}$ = 25.1 min, $t_{R(S)}$ = 27.9 min). ^{1}H NMR ($CDCl_3$): δ 7.26 (d, J = 8.4 Hz, 1H), 6.48 (d, J = 8.4 Hz, 1H), 6.47 (s, 1H), 4.50 (m, 1H), 4.30 (m, 1H), 4.09 (q, J = 6.6 Hz, 1H), 3.94 (t, J = 13.6 Hz, 1H), 3.80 (s, 6H), 3.61 (t, J = 13.6 Hz, 1H), 3.22 (m, 1H), 2.75 (m, 1H), 2.69 (s, 3H), 1.72 (d, J = 6.5 Hz, 3H). This intermediate (**98**) was used to ultimately prepare compd **39**.

*Step d: General Procedure D for the Synthesis of Intermediates **99**–**119**, Exemplified with (R)-2-Methyl-4-(8-methyl-5,6,7,8-tetrahydro-[1,2,4]triazolo[4,3-a]pyrazin-3-yl)thiazole (**108**) (Free Base or Hydrochloride Salt).* To a solution of **85** (12 g, 31.1 mmol, 1 equiv) in CH_2Cl_2 (150 mL) at 0 °C was added TFA (23 mL, 233 mmol, 7.5 equiv) in one portion. The ice bath was removed after 10 min and the reaction mixture stirred at room temperature for 15 min, whereupon

DOI: 10.1021/jm5017413
J. Med. Chem. XXXX, XXX, XXX–XXX

water (100 mL) was added, the suspension stirred for 30 min, and filtered. The aqueous layer was adjusted to pH 14 by addition of NaOH (4M, 150 mL) and further extracted with CH_2Cl_2 (2 × 100 mL). The combined organic layers were dried ($MgSO_4$), filtered, and volatiles removed to afford the title product in the free base form as a white solid (6.67 g, 91%). LCMS (method C) m/z 236 (M + 1). HPLC purity 91% (280 nm). To convert the free based **108** to the HCl salt form, HCl (5−6 M) in isopropyl alcohol (125 mL, 623 mmol, 20 equiv based on 5 M solution) was added at 0 °C over 10 min to a solution of **108** in isopropyl alcohol (0.2 M, 140 mL). After stirring the mixture for a further 15 min at 0 °C, TBME (350 mL) was added in one portion, stirred at 0 °C (15 min), and filtered, and the white precipitate was washed with TBME (2 × 80 mL) to afford **108**·HCl an off-white solid. Additional product was recovered from the filtrate by removing the volatiles and treating the residue with isopropyl alcohol (20 mL) and TBME (300 mL) at 0 °C to obtain more white precipitate that was filtered and dried in vacuo. The combined dried batches afforded 7.5 g (89%) of **108**·HCl as a white solid, which was used without further purification in the next step. LCMS (method C) m/z 236 (M + 1). HPLC purity 94% (280 nm). Chiral LC (method F) 97.9% ee ($t_{R(S)}$ = 9.4 min, $t_{R(R)}$ = 10.6 min). ^{1}H NMR (CD_3OD): δ 5.08 (m, 2H), 4.79 (m, 2H), 4.04 (m, 1H), 3.90−3.82 (m, 2H), 2.83 (s, 3H), 1.91 (d, J = 6.6 Hz, 3H). This intermediate (**108**) was used to ultimately prepare compds **27** and **31.**

*3-(2-Pyridyl)-5,6,7,8-tetrahydro-[1,2,4]triazolo[4,3-a]pyrazine (**99**).* Starting from **78** as per general procedure D to obtain 350 mg (46%). LCMS (method C) m/z 202 (M + 1). HPLC purity >95% (254 nm). ^{1}H NMR ($CDCl_3$): δ 8.61 (m, 1H), 8.31 (d, J = 8.0 Hz, 1H), 7.80 (td, J = 1.8, 8.0 Hz, 1H), 7.31 (m, 1H), 4.56 (t, J = 5.6 Hz, 2H), 4.33 (s, 2H), 3.27 (t, J = 5.6 Hz, 2H). This intermediate (**99**) was used to ultimately prepare compds **5**−**18**..

*(S)-8-Methyl-3-(pyridin-2-yl)-5,6,7,8-tetrahydro-[1,2,4]triazolo-[4,3-a]pyrazine (**100**).* Starting from **86** as per general procedure D to obtain 90 mg (40%). LCMS (method C) m/z 216 (M + 1). HPLC purity >95% (254 nm). This intermediate (**100**) was used to ultimately prepare compd **19**.

*(R)-8-Methyl-3-(pyridin-2-yl)-5,6,7,8-tetrahydro-[1,2,4]triazolo-[4,3-a]pyrazine (**101**).* Starting from **87** as per general procedure D to obtain 47 mg (66%). LCMS (method C) m/z 216 (M + 1). HPLC purity >95% (254 nm). This intermediate (**101**) was used to ultimately prepare compd **20**..

*(R)-8-Methyl-3-(6-methylpyridin-2-yl)-5,6,7,8-tetrahydro-[1,2,4]-triazolo[4,3-a]pyrazine (**102**).* Starting from **88** as per general procedure D to obtain 110 mg (96%). LCMS (method C) m/z 230 (M + 1). HPLC purity >95% (254 nm). This intermediate (**102**) was used to ultimately prepare compds **21** and **29**.

*3-(6-Methylpyridin-2-yl)-5,6,7,8-tetrahydro-[1,2,4]triazolo[4,3-a]-pyrazine Dihydrochloride (**103**).* Starting from **79** as per general procedure D to obtain 1.33 g (quant). LCMS (method C) m/z 216 (M + 1). HPLC purity >90% (254 nm). This intermediate (**103**) was used to ultimately prepare compd **22**.

*3-(5-Methyl-2-pyridyl)-5,6,7,8-tetrahydro-[1,2,4]triazolo[4,3-a]-pyrazine (**104**).* Starting from **80** as per general procedure D to obtain 43 mg (98%). LCMS (method C) m/z 216 (M + 1). HPLC purity >95% (254 nm). ^{1}H NMR ($CDCl_3$): δ 8.45 (d, J = 5.0 Hz, 1H), 8.14 (s, 1H), 7.13 (d, J = 5.0 Hz, 1H), 4.58 (t, J = 5.6 Hz, 2H), 4.35 (2H), 3.30 (t, J = 5.6 Hz, 2H), 2.42 (s, 3H). This intermediate (**104**) was used to ultimately prepare compd **23**.

*3-(4-Methyl-2-pyridyl)-5,6,7,8-tetrahydro-[1,2,4]triazolo[4,3-a]-pyrazine (**105**).* Starting from **81** as per general procedure D to obtain 109 mg (quant). LCMS (method C) m/z 216 (M + 1). HPLC purity >95% (254 nm). ^{1}H NMR ($CDCl_3$): δ 8.44 (s, 1H), 8.18 (d, J = 8.1 Hz, 1H), 7.62 (m, 1H), 4.56 (t, J = 5.6 Hz, 2H), 4.34 (2H), 3.30 (t, J = 5.6 Hz, 2H), 2.39 (s, 3H). This intermediate (**105**) was used to ultimately prepare compd **24**.

*3-(3-Methyl-2-pyridyl)-5,6,7,8-tetrahydro-[1,2,4]triazolo[4,3-a]-pyrazine (**106**).* Starting from **82** as per general procedure D to obtain 60 mg (44%.). LCMS (method C) m/z 216 (M + 1). HPLC purity >95% (254 nm). ^{1}H NMR ($CDCl_3$): δ 8.50 (m, 1H), 7.67 (m, 1H), 7.25 (m, 1H), 4.36 (2H), 4.35 (t, J = 5.6 Hz, 2H), 3.28 (t, J = 5.6 Hz, 2H), 2.70 (s, 3H). This intermediate (**106**) was used to ultimately prepare compd **25**.

*3-(6-(Trifluoromethyl)pyridin-2-yl)-5,6,7,8-tetrahydro-[1,2,4]-triazolo[4,3-a]pyrazine Dihydrochloride (**107**).* Starting from **83** as per general procedure D to obtain 83 mg (35%). LCMS (method C) m/z 270 (M + 1). HPLC purity >95% (254 nm). This intermediate (**107**) was used to ultimately prepare compd **26**.

*(R)-4-(8-Methyl-5,6,7,8-tetrahydro-[1,2,4]triazolo[4,3-a]pyrazin-3-yl)-2-phenylthiazole (**109**).* Starting from **89** as per general procedure D to obtain 17 mg (8%). LCMS (method C) m/z 298 (M + 1). HPLC purity 90% (254 nm). ^{1}H NMR ($CDCl_3$): δ 8.09 (s, 1H), 7.95 (m, 2H), 7.46 (3, 3H), 4.73 (m, 1H), 4.30 (m, 2H), 3.47 (m, 1H), 3.21 (m, 1H), 1.68 (d, J = 6.7 Hz, 3H). This intermediate (**109**) was used to ultimately prepare compd **28**.

*(R)-8-Methyl-3-(6-methylpyrazin-2-yl)-5,6,7,8-tetrahydro-[1,2,4]-triazolo[4,3-a]pyrazine (**110**).* Starting from **90** as per general procedure D to obtain 175 mg (78%). LCMS (method C) m/z 231 (M + 1). HPLC purity >95% (254 nm). This intermediate (**110**) was used to ultimately prepare compd **30**.

*(R)-2-(2,4-Difluorophenyl)-4-(8-methyl-5,6,7,8-tetrahydro-[1,2,4]-triazolo[4,3-a]pyrazin-3-yl)thiazole (**111**).* Starting from **91** as per general procedure D to obtain 7 mg (98%). LCMS (method C) m/z 334 (M + 1). HPLC purity >95% (254 nm). This intermediate (**111**) was used to ultimately prepare compd **3**.

*(S)-2-Methyl-4-(8-methyl-5,6,7,8-tetrahydro-[1,2,4]triazolo[4,3-a]pyrazin-3-yl)thiazole (**112**).* Starting from **92** as per general procedure D to obtain 22 mg (quant). LCMS (method C) m/z 236 (M + 1). HPLC purity 95% (254 nm). This intermediate (**112**) was used to ultimately prepare compd **32**.

*2-Methyl-4-(8-methyl-5,6,7,8-tetrahydro-[1,2,4]triazolo[4,3-a]-pyrazin-3-yl)thiazole Hydrochloride (**113**).* Starting from **84** as per general procedure D to obtain 736 mg (86%). LCMS (method C) m/z 222 (M + 1). HPLC purity 97% (254 nm). This intermediate (**113**) was used to ultimately prepare compd **33**.

*(R)-4-(8-Methyl-5,6,7,8-tetrahydro-[1,2,4]triazolo[4,3-a]pyrazin-3-yl)-2-(trifluoromethyl)thiazole (**114**).* Starting from **93** as per general procedure D to obtain 250 mg (95%). LCMS (method C) m/z 290 (M + 1). HPLC purity >90% (254 nm). This intermediate (**114**) was used to ultimately prepare compd **34**.

*(R)-2-Isopropyl-4-(8-methyl-5,6,7,8-tetrahydro-[1,2,4]triazolo-[4,3-a]pyrazin-3-yl)thiazole (**115**).* Starting from **94** as per general procedure D to obtain 105 mg (79%). LCMS (method C) m/z 264 (M + 1). HPLC purity >98% (254 nm). This intermediate (**94**) was used to ultimately prepare compd **35**.

*(R)-2-Isopropyl-4-(8-methyl-5,6,7,8-tetrahydro-[1,2,4]triazolo-[4,3-a]pyrazin-3-yl)oxazole Hydrochloride (**116**).* Starting from **95** as per general procedure D to obtain 299 mg (quant). LCMS (method C) m/z 248 (M + 1). HPLC purity 96% (254 nm). This intermediate (**116**) was used to ultimately prepare compd **36**.

*(R)-4-Methyl-2-(8-methyl-5,6,7,8-tetrahydro-[1,2,4]triazolo[4,3-a]pyrazin-3-yl)thiazole (**117**).* Starting from **96** as per general procedure D to obtain 83 mg (45%). LCMS (method C) m/z 236 (M + 1). HPLC purity >95% (254 nm). This intermediate (**117**) was used to ultimately prepare compd **37**.

*(R)-3-Methyl-5-(8-methyl-5,6,7,8-tetrahydro-[1,2,4]triazolo[4,3-a]pyrazin-3-yl)-1,2,4-oxadiazole (**118**).* Starting from **97** as per general procedure D to obtain 389 mg (quant). LCMS (method C) m/z 221 (M + 1). HPLC purity >90% (254 nm). This intermediate (**97**) was used to ultimately prepare compd **38**.

*(R)-3-Methyl-5-(8-methyl-5,6,7,8-tetrahydro-[1,2,4]triazolo[4,3-a]pyrazin-3-yl)-1,2,4-thiadiazole hydrochloride (**119**).* Starting from **98** as per general procedure D to obtain 286 mg (quant). LCMS (method C) m/z 237 (M + 1). HPLC purity 95% (254 nm). Chiral LC (method H) 99.1% ee ($t_{R(R)}$ = 11.1 min, $t_{R(S)}$ = 12.7 min). ^{1}H NMR ($CDCl_3$): δ 4.66 (m, 1H), 4.33−4.21 (bm, 2H), 3.47 (m, 1H), 3.23 (m, 1H), 2.72 (s, 3H), 1.69 (d, J = 6.7 Hz, 3H). This intermediate (**119**) was used to ultimately prepare compd **39.**

*Steps e,f: General Procedure E for the Synthesis of Targets **3**, **5**−**39**, Exemplified with (R)-(8-Methyl-3-(2-methylthiazol-4-yl)-5,6-dihydro-[1,2,4]triazolo[4,3-a]pyrazin-7(8H)-yl)(4-(thiophen-2-yl)-phenyl)methanone (**31**).* To a 0 °C solution of **108**·HCl (8.76 g, 30.9

DOI: 10.1021/jm5017413
J. Med. Chem. XXXX, XXX, XXX−XXX

mmol, 96% purity, 1 equiv) in CH_2Cl_2 (300 mL) was added *N*-methylmorpholine (7.5 mL, 68.0 mmol, 2.2 equiv) over 30 min, and then 4-(thiophen-2-yl)benzoyl chloride (6.89 g, 30.9 mmol, 1.0 equiv) was added as solid portions over 10 min. The reaction mixture was stirred at room temperature for 10 min, quenched with addition of 1 M HCl (100 mL), and washed with CH_2Cl_2 (2 × 100 mL). The combined organic extracts were then washed with 1 M NaOH (200 mL), brine (200 mL), dried ($MgSO_4$), and evaporated to dryness. After purification by silica gel flash chromatography (eluent: EtOAc/MeOH: 98/2) **31** was obtained as a white solid (7.16 g, 55%). LCMS (method B) *m/z* 422 (M + H). HPLC purity 97% (280 nm). Chiral LC (method G) 97.9% ee. Elemental Analysis Calcd (found) for $C_{21}H_{20}N_5OS_2$: 59.83% (59.96%); H, 4.54% (4.42%); N, 16.61% (16.30%); S, 15.21% (14.99%). Crystallization from hot EtOAc/TBME (4:1, v/v) afforded the product in white crystalline form with an (unoptimized) recovery yield of 60−70%. HPLC purity 99.4% (280 nm, method B). Chiral LC (method G) 99.4% ee ($t_{R(S)}$ = 10.8 min, $t_{R(R)}$ = 14.7 min). HRMS calculated for $C_{21}H_{20}N_5OS_2$ 422.1109; found 422.1100. ^{1}H NMR ($CDCl_3$): δ 7.99 (s, 1H), 7.69 (d, *J* = 7.9 Hz, 2H), 7.47 (d, *J* = 7.9 Hz, 2H), 7.37 (m, 2H), 7.12 (m, 1H), 5.77 (m, 1H), 4.83 (dd, *J* = 3.4, 13.5 Hz, 1 H), 4.60 (m, 1H), 4.24 (dt, *J* = 4.2, 12.8 Hz, 1H), 3.50 (m, 1H), 2.70 (s, 3H), 1.73 (d, *J* = 6.7 Hz, 3H). ^{13}C NMR ($CDCl_3$): δ 170.6, 166.7, 152.3, 148.4, 143.2, 143.1, 136.9, 133.9, 128.4, 127.8, 126.3, 126.1, 124.3, 119.5, 119.4, 48.4, 45.2, 38.1, 20.0, 19.3.

[(8R)-3-[2-(2,4-Difluorophenyl)thiazol-4-yl]-8-methyl-6,8-dihydro-5H-[1,2,4]triazolo[4,3-a]pyrazin-7-yl]-[4-(2-thienyl)phenyl]-methanone (***3***). Starting from **111** and 4-(thiophen-2-yl)benzoyl chloride as per general procedure E to obtain 6 mg (63%). LCMS (method B) *m/z* 520 (M + 1). HPLC purity 98% (254 nm). Chiral LC (method G) 99.0% ee ($t_{R(S)}$ = 9.5 min, $t_{R(R)}$ = 11.8 min). ^{1}H NMR ($CDCl_3$): δ 8.26 (s, 1H), 7.71 (d, *J* = 8.2 Hz, 2H), 7.50 (d, *J* = 8.2 Hz, 2H), 7.37 (m, 3H), 7.13 (dd, *J* = 3.6, 5.0 Hz, 1H), 6.98−7.01 (m, 2H), 5.76 (m, 1H), 4.91 (dd, *J* = 3.2, 13.4 Hz, 1H), 4.65 (m, 1H), 4.39 (m, 1H), 3.56 (m, 1H), 1.78 (d, *J* = 6.9 Hz, 3H). ^{13}C NMR ($CDCl_3$): δ 169.2, 164.9 (d), 161.3 (dd), 159.4 (d), 158.0 (d), 125.3, 147.2, 142.5 (d), 135.2, 134.2, 130.3 (dd), 128.7, 127.9, 126.7, 125.4, 124.7, 121.2 (d), 117.1 (dd), 113.0 (dd), 44.8,[68] 19.1. ^{19}F NMR ($CDCl_3$): δ −102.9, −104.8. HRMS: calcd 520.1077, found 520.1065, $C_{26}H_{20}N_5OS_2F_2$.

(4-Fluorophenyl)(3-(pyridin-2-yl)-5,6-dihydro-[1,2,4]triazolo[4,3-a]pyrazin-7(8H)-yl)methanone (***5***). Starting from **99** and 4-fluorobenzoyl chloride as per general procedure E to obtain 179 mg. LCMS (method A) *m/z* 324 (M + 1). HPLC purity >98% (254 nm). ^{1}H NMR (DMSO-d_6): δ 8.62 (d, *J* = 4.6 Hz, 1H), 8.33 (d, *J* = 7.8 Hz, 1H), 7.84 (dt, *J* = 1.6, 7.8 Hz, 1H), 7.53 (m, 2H), 7.35 (m, 1H), 7.16 (t, *J* = 8.5 Hz, 2H), 5.09 (bs, 2H), 4.74 (t, *J* = 5.5 Hz, 2H), 4.07 (m, 2H). ^{13}C NMR ($CDCl_3$): δ 170.2, 165.8, 162.5, 151.5, 149.0, 147.6, 137.3, 130.1 (d), 129.9, 124.3, 122.1, 116.1 (d), 45.8.[68] ^{19}F-NMR ($CDCl_3$): −105.1. HRMS: calcd 324.1261, found 324.1248, $C_{17}H_{15}N_5OF$.

(4-Methoxyphenyl)(3-(pyridin-2-yl)-5,6-dihydro-[1,2,4]triazolo-[4,3-a]pyrazin-7(8H)-yl)methanone (***6***). Starting from **99** and 4-methoxybenzoyl chloride as per general procedure E to obtain 45 mg. LCMS (method A) *m/z* 336 (M + 1). HPLC purity 93% (254 nm). ^{1}H NMR (DMSO-d_6): δ 8.70 (d, *J* = 4.3 Hz, 1H), 8.17 (d, *J* = 8.9 Hz, 1H), 7.98 (dt, *J* = 1.8, 7.3 Hz, 1H), 7.52 (m, 3H), 7.04 (d, *J* = 8.7 Hz, 2H), 4.95 (bs, 2H), 4.59 (t, *J* = 5.4 Hz, 2H), 3.92 (bs, 2H), 3.82 (s, 3H). ^{13}C NMR (DMSO-d_6): δ 169.9, 160.8, 150.7, 149.2, 147.3, 137.6, 131.6, 129.4, 126.8, 124.4, 122.4, 113.8, 55.3, 45.4.[68] HRMS: calcd 336.1461, found 336.1455, $C_{18}H_{18}N_5O_2$.

(3-Fluorophenyl)(3-(pyridin-2-yl)-5,6-dihydro-[1,2,4]triazolo[4,3-a]pyrazin-7(8H)-yl)methanone (***7***). Starting from **99** and 3-fluorobenzoyl chloride as per general procedure E to obtain 40 mg. LCMS (method A) *m/z* 324 (M + 1). HPLC purity 94% (254 nm). ^{1}H NMR (DMSO-d_6): δ 8.69 (d, *J* = 4.3 Hz, 1H), 8.16 (d, *J* = 8.0 Hz, 1H), 7.98 (dt, *J* = 1.7, 7.6 Hz, 1H), 7.53 (m, 2H), 7.37 (m, 3H), 4.99 (m, 2H), 4.59 (t, *J* = 5.5 Hz, 2H), 3.85 (bm 2H). ^{13}C NMR (DMSO-d_6): δ 168.4, 163.5, 160.3, 150.7, 149.1, 147.3, 137.6, 137.2 (d), 130.9 (d), 124.4, 123.3, 122.4, 117.0 (d), 114.2 (d), 45.3, 43.9.[68] ^{19}F NMR (DMSO-d_6): −109.1. H HRMS: calcd 324.1261, found 324.1265, $C_{17}H_{15}N_5OF$.

(3-Methoxyphenyl)(3-(pyridin-2-yl)-5,6-dihydro-[1,2,4]triazolo-[4,3-a]pyrazin-7(8H)-yl)methanone (***8***). Starting from **99** and 3-methoxybenzoyl chloride as per general procedure E to obtain 42 mg. LCMS (method A) *m/z* 336 (M + 1). HPLC purity 96% (254 nm). ^{1}H NMR (DMSO-d_6): δ 8.89 (d, *J* = 4.5 Hz, 1H), 8.18 (d, *J* = 7.9 Hz, 1H), 7.99 (dt, *J* = 1.5, 7.7 Hz, 1H), 7.52 (m, 1H), 7.41 (m, 1H), 7.07 (m, 3H), 4.98 (m, 2H), 4.59 (t, *J* = 5.3 Hz, 2H), 3.85 (m, 2H). ^{13}C NMR (DMSO-d_6): δ 169.6, 159.2, 150.7, 149.2, 147.3, 137.6, 136.4, 129.9, 124.4, 122.4, 119.0, 115.9, 112.4, 55.3, 45.4, 43.8.[68] HRMS: calcd 336.1461, found 336.1469, $C_{18}H_{18}N_5O_2$.

(2-Fluorophenyl)(3-(pyridin-2-yl)-5,6-dihydro-[1,2,4]triazolo[4,3-a]pyrazin-7(8H)-yl)methanone (***9***). Starting from **99** and 2-fluorobenzoyl chloride as per general procedure E to obtain 59 mg (73%). LCMS (method A) *m/z* 324 (M + 1). HPLC purity 96% (254 nm). ^{1}H NMR ($CDCl_3$): 2 rotamers detected in a 55/45 ratio: δ 8.65 (m, 0.55H), 8.60 (m, 0.45H), 8.36 (m, 1H), 7.86 (dt, *J* = 1.7, 7.8 Hz, 1H), 7.48 (m, 2H), 7.38 (m, 1H), 7.23 (m, 1H), 7.17 (m, 1H), 5.30 (s, 1.1H), 4.93 (s, 0.9H), 4.79 (m, 2H), 4.27 (m, 1.1H), 3.82 (m, 0.9H). ^{13}C NMR ($CDCl_3$): δ 165.9, 159.9, 156.6, 151.5, 151.2, 148.9, 148.8, 147.5, 137.1, 132.5 (d), 132.3 (d), 129.6, 125.1, 124.2, 122.9, 122.3 (d), 116.3 (d), 115.9 (d), 46.0, 45.4, 44.2, 44.0, 40.2, 39.4. ^{19}F NMR ($CDCl_3$): −111.4. H HRMS: calcd 324.1261, found 324.1277, $C_{17}H_{15}N_5OF$.

(2-Methoxyphenyl)(3-(pyridin-2-yl)-5,6-dihydro-[1,2,4]triazolo-[4,3-a]pyrazin-7(8H)-yl)methanone (***10***). Starting from **99** and 2-methoxybenzoyl chloride as per general procedure E to obtain 49 mg. LCMS (method A) *m/z* 336 (M + 1). HPLC purity 98% (254 nm). ^{1}H NMR (DMSO-d_6): 2 rotamers detected in a 3/2 ratio: δ 8.72 (d, *J* = 4.6 Hz, 0.4H), 8.65 (d, *J* = 4.9 Hz, 0.6H), 8.16 (m, 1H), 7.99 (t, *J* = 7.7 Hz, 1H), 7.48 (m, 2H), 7.33 (dd, *J* = 1.1 7.3 Hz, 0.6H), 7.29 (dd, *J* = 0.8, 7.5 Hz, 0.4H), 7.13 (m, 1H), 7.04 (t, *J* = 7.3 Hz, 1H), 5.04 (m, 1H), 4.57 (m, 1H), 4.45 (t, *J* = 5.4 Hz, 1H), 4.09 (m, 1H), 3.81 (s, 1.8H). 3.63 (s, 1.2H), 3.63 (m, 1H). ^{13}C NMR (DMSO-d_6): 2 rotamers detected in a 3/2 ratio δ 167.4, 167.2, 155.1, 155.0, 150.7, 149.2, 149.1, 147.3, 137.6, 131.2, 131.0, 128.2, 128.0, 124.6, 124.4, 124.3, 122.5, 120.9, 120.8, 111.6, 111.5, 55.6, 55.5, 45.6, 45.1, 43.3, 43.1, 38.8, 38.4. HRMS: calcd 336.1461, found 336.1456, $C_{18}H_{18}N_5O_2$.

[1,1′-Biphenyl]-4-yl(3-(pyridin-2-yl)-5,6-dihydro-[1,2,4]triazolo-[4,3-a]pyrazin-7(8H)-yl)methanone (***11***). Starting from **99** and 4-phenylbenzoyl chloride as per general procedure E to obtain 62 mg (65%). LCMS (method A) *m/z* 382 (M + 1). HPLC purity 98% (254 nm). ^{1}H NMR ($CDCl_3$): δ 8.63 (d, *J* = 4.1 Hz, 1H), 8.35 (d, *J* = 8.0 Hz, 1H), 7.85 (dt, *J* = 1.8, 7.8 Hz, 1H), 7.79 (d, *J* = 8.4 Hz, 2H), 7.61 (m, 4H), 7.48 (m, 2H), 7.40 (m, 2H), 5.16 (bs, 2H), 4.77 (t, *J* = 5.4 Hz, 2H), 4.13 (m, 2H). ^{13}C NMR ($CDCl_3$): δ 170.9, 151.5, 148.9, 147.6, 143.8, 140.0, 137.2, 132.9, 129.0, 128.1, 128.0, 127.6, 127.3, 124.2, 123.0, 45.8.[68] HRMS: calcd 382.1668, found 336.1669, $C_{23}H_{20}N_5O$.

(4′-Fluoro-[1,1′-biphenyl]-4-yl)(3-(pyridin-2-yl)-5,6-dihydro-[1,2,4]triazolo[4,3-a]pyrazin-7(8H)-yl)methanone (***12***). Starting from **99** and 4′-fluoro-[1,1′-biphenyl]-4-carbonyl chloride as per general procedure E to obtain 29 mg. LCMS (method A) *m/z* 400 (M + 1). HPLC purity 95% (254 nm). ^{1}H NMR ($CDCl_3$): δ 8.61 (d, *J* = 4.1 Hz, 1H), 8.31 (d, *J* = 7.9 Hz, 1H), 7.83 (dt, *J* = 7.9, 1.5 Hz, 1H), 7.63−7.53 (m, 6H), 7.34 (m, 1H), 7.16 (t, *J* = 8.6 Hz, 2H), 5.10 (bs, 2H), 4.74 (t, *J* = 5.2 Hz, 2H), 4.10 (bs, 2H). ^{13}C NMR ($CDCl_3$): δ 170.8, 164.7, 161.4, 151.6, 149.0, 147.7, 142.9, 137.2, 136.2, 136.2, 133.0, 129.0 (d), 128.1, 127.5, 127.5, 124.3, 123.1, 116.1 (d), 45.8.[68] ^{19}F NMR ($CDCl_3$): −111.5. HRMS: calcd 400.1574, found 400.1577, $C_{23}H_{19}N_5OF$.

(4′-Chloro-[1,1′-biphenyl]-4-yl)(3-(pyridin-2-yl)-5,6-dihydro-[1,2,4]triazolo[4,3-a]pyrazin-7(8H)-yl)methanone (***13***). Starting from **99** and 4′-chloro-[1,1′-biphenyl]-4-carbonyl chloride as per general procedure E to obtain 50 mg (48%). LCMS (method A) *m/z* 416 (M + 1). HPLC purity 95% (254 nm). ^{1}H NMR ($CDCl_3$): δ 8.67 (d, *J* = 4.3 Hz, 1H), 8.40 (d, *J* = 8.0 Hz, 1H), 7.89 (dt, *J* = 1.7, 7.8 Hz, 1H), 7.67 (d, *J* = 8.5 Hz, 2H), 7.60 (d, *J* = 8.5 Hz, 2H), 7.56 (d, *J* = 8.7 Hz, 2H), 7.47 (d, *J* = 8.7 Hz, 2H), 7.41 (m, 1H), 5.20 (bs, 2H), 4.79 (t, *J* =

DOI: 10.1021/jm5017413
J. Med. Chem. XXXX, XXX, XXX−XXX

5.8 Hz, 2H), 4.17 (m, 2H). ^{13}C NMR ($CDCl_3$): δ 170.7, 151.5, 148.9, 147.6, 142.6, 138.5, 137.2, 134.3, 133.3, 129.2, 128.6, 128.1, 127.5, 124.2, 123.0, 45.8.[68] HRMS: calcd 416.1278, found 416.1292, $C_{23}H_{19}N_5OCl$.

*(4′-Methoxy-[1,1′-biphenyl]-4-yl)(3-(pyridin-2-yl)-5,6-dihydro-[1,2,4]triazolo[4,3-a]pyrazin-7(8H)-yl)methanone (**14**).* Starting from **99** and 4′-methoxy-[1,1′-biphenyl]-4-carbonyl chloride as per general procedure E to obtain 70 mg (68%). LCMS (method A) *m/z* 412 (M + 1). HPLC purity >98% (254 nm). ^{1}H NMR ($CDCl_3$): δ 8.66 (d, *J* = 4.4 Hz, 1H), 8.34 (d, *J* = 8.0 Hz, 1H), 7.86 (dt, *J* = 1.8, 7.8 Hz, 1H), 7.65 (d, *J* = 8.4 Hz, 2H), 7.57 (m, 4H), 7.38 (ddd, *J* = 1.0, 4.9, 7.5 Hz, 1H), 7.02 (d, *J* = 8.8 Hz, 2H), 5.17 (bs, 2H), 4.78 (t, *J* = 5.5 Hz, 2H), 4.14 (m, 2H), 3.88 (s, 3H). ^{13}C NMR ($CDCl_3$): δ 170.9, 159.8, 151.4, 149.0, 148.9, 147.6, 143.4, 137.1, 132.4, 132.2, 128.3, 128.0, 127.0, 124.1, 122.9, 114.4, 55.4, 45.8.[68] HRMS: calcd 412.1774, found 412.1760, $C_{24}H_{22}N_5O_2$.

*(4-Benzylphenyl)(3-(pyridin-2-yl)-5,6-dihydro-[1,2,4]triazolo[4,3-a]pyrazin-7(8H)-yl)methanone (**15**).* Starting from **99** and 4-benzylbenzoyl chloride as per general procedure E to obtain 57 mg (58%). LCMS (method A) *m/z* 396 (M + 1). HPLC purity 97% (254 nm). ^{1}H NMR ($CDCl_3$): δ 8.63 (d, *J* = 4.6 Hz, 1H), 8.36 (d, *J* = 8.0 Hz, 1H), 7.85 (dt, *J* = 1.7, 7.7 Hz, 1H), 7.42 (d, *J* = 8.2 Hz, 2H), 7.37−7.18 (m, 8H), 5.11 (bs, 2H), 4.74 (t, *J* = 5.5 Hz, 2H), 4.10 (m, 2H), 4.03 (s, 2H). ^{13}C NMR ($CDCl_3$): δ 170.9, 168.7, 151.3, 148.9, 148.8, 147.5, 144.3, 140.1, 137.1, 131.9, 130.2, 129.3, 129.0, 128.8, 128.6, 127.6, 126.4, 124.1, 122.9, 45.8,[68] 41.7. HRMS: calcd 396.1824, found 396.1833, $C_{24}H_{22}N_5O$.

*(3-(Pyridin-2-yl)-5,6-dihydro-[1,2,4]triazolo[4,3-a]pyrazin-7(8H)-yl)(4-(thiophen-2-yl)phenyl) methanone (**16**).* Starting from **99** and 4-(thiophen-2-yl)benzoyl chloride as per general procedure E to obtain 42 mg. LCMS (method A) *m/z* 388 (M + 1). HPLC purity >98% (254 nm). ^{1}H NMR ($CDCl_3$): δ 8.61 (d, *J* = 3.4 Hz, 1H), 8.31 (d, *J* = 7.9 Hz, 1H), 7.81 (dt, *J* = 1.5, 7.9 Hz, 1H), 7.68 (d, *J* = 8.2 Hz, 2H), 7.51 (d, *J* = 8.2 Hz, 2H), 7.39 (dd, *J* = 1.1, 3.6 Hz, 1H), 7.36 (dd, *J* = 1.1, 5.1 Hz, 1H), 7.32 (m, 1H), 7.11 (dd, *J* = 3.7, 5.1 Hz, 1H), 5.10 (bs, 2H), 4.73 (t, *J* = 5.3 Hz, 2H), 4.08 (m, 2H). ^{13}C NMR (DMSO-d_6): δ 169.5, 150.8, 149.2, 147.4, 142.3, 137.7, 135.5, 133.7, 128.8, 128.3, 126.7, 125.5, 124.8, 124.4, 122.4, 45.4.[68] HRMS: calcd 388.1232, found 388.1242, $C_{21}H_{18}N_5OS$.

*(4-(5-Methylfuran-2-yl)phenyl)(3-(pyridin-2-yl)-5,6-dihydro-[1,2,4]triazolo[4,3-a]pyrazin-7(8H)-yl) methanone (**17**).* Starting from **99** and 4-(5-methylfuran-2-yl)benzoyl chloride as per general procedure E to obtain 29 mg. LCMS (method A) *m/z* 386 (M + 1). HPLC purity >98% (254 nm). ^{1}H NMR ($CDCl_3$): δ 8.61 (d, *J* = 4.3 Hz, 1H), 8.29 (d, *J* = 7.9 Hz, 1H), 7.81 (dt, *J* = 1.5, 7.7 Hz, 1H), 7.68 (d, *J* = 8.1 Hz, 2H), 7.48 (d, *J* = 8.1 Hz, 2H), 7.32 (dd, *J* = 5.0, 7.3 Hz, 1H), 6.64 (d, *J* = 2.9 Hz, 1H), 6.09 (d, *J* = 2.9 Hz, 1H), 5.08 (bs, 2H), 4.70 (t, *J* = 5.1 Hz, 2H), 4.05 (m, 2H), 2.37 (s, 3H). ^{13}C NMR ($CDCl_3$): δ 170.9, 153.2, 151.5, 151.1, 149.1, 148.9, 147.7, 137.2, 133.6, 131.8, 128.1, 128.3, 124.2, 123.4, 123.0, 108.2, 107.9, 45.8, 13.9.68 HRMS: calcd 386.1617, found 386.1617, $C_{22}H_{20}N_5O_2$.

*(3-(4-Chlorophenyl)-1H-pyrazol-5-yl)(3-(pyridin-2-yl)-5,6-dihydro-[1,2,4]triazolo[4,3-a]pyrazin-7(8H)-yl)methanone (**18**).* Starting from **99** and 3-(4-chlorophenyl)-1*H*-pyrazole-5-carbonyl chloride as per general procedure E to obtain 30 mg (30%). LCMS (method A) *m/z* 406 (M + 1). HPLC purity >98% (254 nm). ^{1}H NMR (DMSO-d_6) 2 isomers in a 3/2 ratio: δ 13.89 (s, 0.6H), 13.85 (s, 0.4H), 8.71 (d, *J* = 4.6 Hz, 1H), 8.18 (d, *J* = 6.8 Hz, 1H), 8.00 (dt, *J* = 1.0, 7.5 Hz, 1H), 7.86 (d, *J* = 7.8 Hz, 2H), 7.57 (m, 3H), 7.19 (s, 1H), 5.61 (bs, 0.8H), 5.06 (bs, 1.2H), 4.64 (m, 2H), 4.45 (m, 0.8H), 4.15 (m, 1.2). HRMS: calcd 406.1183, found 406.1176, $C_{20}H_{17}N_7OCl$.

*(S)-(4-Fluorophenyl)(8-methyl-3-(pyridin-2-yl)-5,6-dihydro-[1,2,4]triazolo[4,3-a]pyrazin-7(8H)-yl)methanone (**19**).* Starting from **100** and 4-fluorobenzoyl chloride as general procedure E to obtain 140 mg (97%). LCMS (method A) *m/z* 338 (M + 1). HPLC purity 98% (254 nm). Chiral LC (method H) 89.6% ee ($t_{R(S)}$ = 6.0 min, $t_{R(R)}$ = 8.0 min). ^{1}H NMR (DMSO-d_6): δ 8.68 (d, *J* = 4.3 Hz, 1H), 8.17 (d, *J* = 7.9 Hz, 1H), 7.99 (dt, *J* = 1.5, 7.7 Hz, 1H), 7.60 (m, 2H), 7.51 (m, 1H), 7.33 (t, *J* = 8.8 Hz, 2H), 5.67 (m, 1H), 4.74 (m, 1H), 4.31 (m, 1H), 4.01 (bm, 1H), 3.61 (m, 1H), 1.61 (d, *J* = 6.8 Hz, 3H). ^{13}C NMR ($CDCl_3$): δ 170.1, 165.7, 162.4, 153.3, 151.1, 149.0, 147.4, 137.4, 130.9, 129.4 (d), 124.5, 123.3, 116.3 (d), 48.1, 46.1, 38.3, 20.0. ^{19}F NMR ($CDCl_3$): δ −98.1. HRMS: calcd 338.1417, found 338.1433, $C_{18}H_{17}N_5OF$.

*(R)-(4-Fluorophenyl)(8-methyl-3-(pyridin-2-yl)-5,6-dihydro-[1,2,4]triazolo[4,3-a]pyrazin-7(8H)-yl)methanone (**20**).* Starting from **101** and 4-fluorobenzoyl chloride as per general procedure E to obtain 74 mg (99%). LCMS (method A) *m/z* 338 (M + 1). HPLC purity 99% (254 nm). Chiral LC (method H) 95.4% ee ($t_{R(S)}$ = 6.0 min, $t_{R(R)}$ = 8.0 min). ^{1}H NMR (DMSO-d_6): δ 8.68 (d, *J* = 4.3 Hz, 1H), 8.17 (d, *J* = 7.9 Hz, 1H), 8.00 (dt, *J* = 1.5, 7.7 Hz, 1H), 7.60 (m, 2H), 7.51 (m, 1H), 7.33 (t, *J* = 8.8 Hz, 2H), 5.67 (m, 1H), 4.74 (m, 1H), 4.32 (m, 1H), 4.01 (bm, 1H), 3.62 (m, 1H), 1.61 (d, *J* = 6.8 Hz, 3H). ^{13}C NMR ($CDCl_3$): δ 170.0, 165.6, 162.3, 153.3, 151.2, 148.9, 147.7, 137.2, 131.0, 129.4 (d), 124.2, 123.2, 116.2 (d), 48.1, 46.1, 38.3, 20.0. ^{19}F NMR ($CDCl_3$): δ −98.1. HRMS: calcd 338.1417, found 338.1429, $C_{18}H_{17}N_5OF$.

*(R)-(4-Fluorophenyl)(8-methyl-3-(6-methylpyridin-2-yl)-5,6-dihydro-[1,2,4]triazolo[4,3-a]pyrazin-7(8H)-yl)methanone (**21**).* Starting from **102** and 4-fluorobenzoyl chloride as per general procedure E to obtain 90 mg (53%). LCMS (method A) *m/z* 352 (M + 1). HPLC purity 97% (254 nm). Chiral LC (method I) 98.4% ee ($t_{R(S)}$ = 13.7 min, $t_{R(R)}$ = 16.6 min). ^{1}H NMR ($CDCl_3$): δ 8.10 (d, *J* = 7.8 Hz, 1H), 7.71 (t, *J* = 7.8 Hz, 1H), 7.48 (m, 2H), 7.17 (m, 3H), 5.64 (m, 1H), 5.03 (dd, *J* = 3.8, 13.8 Hz, 1H), 4.61 (m, 1H), 4.34 (m, 1H), 3.49 (m, 1H), 2.57 (s, 3H), 1.74 (d, *J* = 6.9 Hz, 3H). ^{13}C NMR ($CDCl_3$): δ 170.1, 165.6, 162.3, 157.9, 153.1, 151.3, 147.0, 137.5, 131.0, 129.4 (d), 123.7, 120.2, 116.2 (d), 47.6, 45.9, 37.3, 24.5, 20.0. ^{19}F NMR ($CDCl_3$): δ −105.9. HRMS: calcd 352.1574, found 352.1588, $C_{19}H_{19}N_5OF$.

*(4-Fluorophenyl)(3-(6-methylpyridin-2-yl)-5,6-dihydro-[1,2,4]-triazolo[4,3-a]pyrazin-7(8H)-yl) methanone (**22**).* Starting from **103** and 4-fluorobenzoyl chloride as per general procedure E to obtain 32 mg. LCMS (method A) *m/z* 338 (M + 1). HPLC purity 96% (254 nm). ^{1}H NMR (DMSO-d_6): δ 7.97 (d, *J* = 7.8 Hz, 1H), 7.88 (t, *J* = 7.8 Hz, 1H), 7.64 (dd, *J* = 5.7, 8.0 Hz, 2H), 7.35 (m, 3H), 4.97 (bs, 2H), 4.60 (t, *J* = 5.3 Hz, 2H), 3.90 (m, 2H), 2.56 (s, 3H). ^{13}C NMR ($CDCl_3$): δ 170.2, 165.9, 162.5, 158.0, 151.6, 148.8, 146.7, 137.5, 130.0 (d), 123.9, 120.2, 116.2 (d), 45.7,[68] 24.5. ^{19}F NMR (DMSO-d_6): δ −107.5. HRMS: calcd 338.1417, found 338.1433, $C_{18}H_{17}N_5OF$.

*(4-Fluorophenyl)(3-(5-methylpyridin-2-yl)-5,6-dihydro-[1,2,4]-triazolo[4,3-a]pyrazin-7(8H)-yl)methanone (**23**).* Starting from **104** and 4-fluorobenzoyl chloride as per general procedure E to obtain 15 mg (22%). LCMS (method A) *m/z* 338 (M + 1). HPLC purity 98% (254 nm). ^{1}H NMR ($CDCl^3$): δ 8.44 (s, 1H), 8.19 (d, *J* = 8.1 Hz, 1H), 7.64 (d, *J* = 8.1 Hz, 1H), 7.51 (m, 2H), 7.15 (t, *J* = 7.5 Hz, 2H), 5.06 (bs, 2H), 4.70 (t, *J* = 5.0 Hz, 2H), 4.06 (m, 2H), 2.40 (s, 3H). ^{13}C NMR ($CDCl_3$): δ 170.1, 165.9, 162.5, 151.6, 149.4, 148.7, 144.8, 137.8, 134.4, 129.9 (d), 122.7, 116.2 (d), 45.7,[68] 18.6. ^{19}F NMR ($CDCl_3$): δ −105.3. HRMS: calcd 338.1417, found 338.1422, $C_{18}H_{17}N_5OF$.

*(4-Fluorophenyl)(3-(4-methylpyridin-2-yl)-5,6-dihydro-[1,2,4]-triazolo[4,3-a]pyrazin-7(8H)-yl) methanone (**24**).* Starting from **105** and 4-fluorobenzoyl chloride as per general procedure E to obtain 82 mg (50%). LCMS (method A) *m/z* 338 (M + 1). HPLC purity 98% (254 nm). ^{1}H NMR ($CDCl_3$): δ 8.48 (d, *J* = 5.0 Hz, 1H), 8.18 (s, 1H), 7.53 (m, 2H), 7.16 (m, 3H), 5.10 (bs, 2H), 4.74 (t, *J* = 5.4 Hz, 2H), 4.07 (m, 2H), 2.44 (s, 3H).^{13}C NMR ($CDCl_3$): δ 170.1, 165.9, 162.4, 151.7, 148.7, 147.2, 131.7 (d), 129.9 (d), 125.4, 123.8, 116.2 (d), 44.8,[68] 21.2. ^{19}F NMR ($CDCl_3$): δ −105.1. HRMS: calcd 338.1417, found 338.1428, $C_{18}H_{17}N_5OF$.

*(4-Fluorophenyl)(3-(3-methylpyridin-2-yl)-5,6-dihydro-[1,2,4]-triazolo[4,3-a]pyrazin-7(8H)-yl) methanone (**25**).* Starting from **106** and 4-fluorobenzoyl chloride as per general procedure E to obtain 35 mg (37%). LCMS (method A) *m/z* 338 (M + 1). HPLC purity 93% (254 nm). ^{1}H NMR ($CDCl_3$): δ 8.50 (m, 1H), 7.70 (d, *J* = 7.8 Hz, 1H), 7.53 (m, 2H), 7.28 (m, 1H), 7.16 (t, *J* = 8.5 Hz, 2H), 5.09 (bs, 2H), 4.50 (t, *J* = 5.4 Hz, 2H), 4.05 (m, 2H), 2.69 (s, 3H). ^{13}C NMR ($CDCl_3$): δ 170.1, 165.8, 162.4, 151.6, 147.9, 146.4, 145.4, 137.7, 135.1, 130.3, 130.0 (d), 123.9, 116.1 (d), 45.0,[68] 20.5. ^{19}F NMR

DOI: 10.1021/jm5017413
J. Med. Chem. XXXX, XXX, XXX−XXX

($CDCl_3$): δ −105.3. HRMS: calcd 38.1417, found 338.1424, $C_{18}H_{17}N_5OF$.

*(4-Fluorophenyl)(3-(6-(trifluoromethyl)pyridin-2-yl)-5,6-dihydro-[1,2,4]triazolo[4,3-a]pyrazin-7(8H)-yl)methanone (**26**).* Starting from **107** and 4-fluorobenzoyl chloride as per general procedure E to obtain 36 mg. LCMS (method A) m/z 392 (M + 1). HPLC purity 97% (254 nm). ^{1}H NMR ($CDCl_3$): δ 8.54 (d, J = 7.6 Hz, 1H), 8.05 (m, 1H), 7.74 (d, J = 7.2 Hz, 1H), 7.53 (m, 2H), 7.17 (t, J = 8.4 Hz, 2H), 5.10 (bs, 2H), 4.73 (m, 2H), 4.12 (m, 2H). ^{13}C NMR ($CDCl_3$): δ 170.2, 165.9, 162.5, 150.3, 149.6, 147.9, 147.7, 147.5 (d), 139.0, 130.0 (d), 125.4, 121.3 (d), 120.7 (d), 116.2 (d), 45.8.[68] ^{19}F NMR ($CDCl_3$): δ −65.3 (s, 3F), −105.0 (s, 1F). HRMS: calcd 392.1134, found 392.1168, $C_{18}H_{14}N_5OF_4$.

*(R)-(4-Fluorophenyl)(8-methyl-3-(2-methylthiazol-4-yl)-5,6-dihydro-[1,2,4]triazolo[4,3-a]pyrazin-7(8H)-yl)methanone (**27**).* Starting from **108** and 4-fluorobenzoyl chloride as per general procedure E to obtain 152 mg (35%). LCMS (method B) m/z 358 (M + 1). HPLC purity 95% (254 nm). Chiral LC (method G) 97.1% ee ($t_{R(S)}$ = 8.7 min, $t_{R(R)}$ = 11.5 min). ^{1}H NMR ($CDCl_3$): δ 7.99 (s, 1H), 7.47 (m, 2H), 7.15 (d, J = 8.4 Hz, 2H), 5.70 (m, 1H), 4.84 (dd, J = 3.2, 13.4 Hz, 1H), 4.54 (m, 1H), 4.21 (dt, J = 3.5, 12.6 Hz, 1H), 3.54 (m, 1H), 2.75 (s, 3H), 1.71 (d, J = 7.9 Hz, 3H). ^{13}C NMR ($CDCl_3$): δ 170.2, 165.6, 162.3, 152.1, 148.3, 142.7, 131.0, 129.3 (d), 119.7, 116.2 (d), 48.3, 45.0, 37.8, 20.0, 19.4. ^{19}F NMR ($CDCl_3$): δ −98.0. HRMS: calcd 358.1138, found 358.1155, $C_{17}H_{17}N_5OSF$.

*(R)-(4-Fluorophenyl)(8-methyl-3-(2-phenylthiazol-4-yl)-5,6-dihydro-[1,2,4]triazolo[4,3-a]pyrazin-7(8H)-yl)methanone (**28**).* Starting from **109** and 4-fluorobenzoyl chloride as per general procedure E to obtain 68 mg. LCMS (method A) m/z 420 (M + 1). HPLC purity >98% (254 nm). Chiral LC (method G) 91.0% ee ($t_{R(S)}$ = 7.4 min, $t_{R(R)}$ = 12.6 min). ^{1}H NMR ($CDCl_3$): δ 8.15 (s, 1H), 7.97 (m, 2H), 7.50 (m, 5H), 7.17 (t, J = 8.5 Hz, 2H), 5.71 (m, 1H), 4.96 (dd, J = 3.5, 13.8 Hz, 1H), 4.60 (m, 1H), 4.37 (m, 1H), 3.57 (m, 1H), 1.74 (d, J = 6.9 Hz, 3H). ^{13}C NMR (DMSO-d_6): δ 168.8, 168.0, 164.4, 161.2, 152.2, 147.4, 143.6, 132.5, 131.9 (d), 130.8, 129.5 (d), 129.4, 126.4, 120.3, 115.7 (d), 45.7,[68] 19.1. ^{19}F NMR ($CDCl_3$): δ −98.1. HRMS: calcd 420.1294, found 420.1278, $C_{22}H_{19}N_5OSF$.

*(R)-(8-Methyl-3-(6-methylpyridin-2-yl)-5,6-dihydro-[1,2,4]-triazolo[4,3-a]pyrazin-7(8H)-yl)(4-(thiophen-2-yl)phenyl)-methanone (**29**).* Starting from **102** and 4-(thiophen-2-yl)benzoyl chloride as per general procedure E to obtain 50 mg (23%). LCMS (method B) m/z 416 (M + 1). HPLC purity 98% (254 nm). Chiral LC (method J) 97.8% ee ($t_{R(S)}$ = 4.6 min, $t_{R(R)}$ = 5.4 min). ^{1}H NMR ($CDCl_3$): δ 8.12 (d, J = 7.7 Hz, 1H), 7.70 (m, 3H), 7.46 (m, 2H), 7.38 (dd, J = 1.1, 3.6 Hz, 1H), 7.36 (dd, J = 1.1, 5.1 Hz, 1H), 7.20 (d, J = 7.7 Hz, 1H), 7.12 (dd, J = 3.6, 5.1 Hz, 1H), 5.82 (m, 1H), 5.03 (dd, J = 3.8, 13.9 Hz, 1H), 4.65 (m, 1H), 4.36 (m, 1H), 3.51 (m, 1H), 2.58 (s, 3H), 1.77 (d, J = 6.9 Hz, 3H). ^{13}C NMR ($CDCl_3$): δ 170.7, 157.9, 153.3, 151.3, 147.0, 143.1, 137.4, 136.7, 133.6, 128.4, 127.8, 126.2, 126.1, 124.3, 123.7, 120.2, 46.0,[68] 24.5, 20.1. HRMS: calcd 416.1545, found 416.1537, $C_{23}H_{22}N_5OS$. Elementary Analysis Calcd: C, 66.48; H, 5.09; N, 16.85. Found: C, 65.90; H, 4.94; N, 16.87.

*(R)-(8-Methyl-3-(6-methylpyrazin-2-yl)-5,6-dihydro-[1,2,4]-triazolo[4,3-a]pyrazin-7(8H)-yl)(4-(thiophen-2-yl)phenyl)-methanone (**30**).* Starting from **110** and 4-(thiophen-2-yl)benzoyl chloride as per general procedure E to obtain 80 mg (25%). LCMS (method B) m/z 417 (M + 1). HPLC purity 95% (254 nm). Chiral LC (method G) 94.9% ee ($t_{R(S)}$ = 6.1 min, $t_{R(R)}$ = 10.7 min). ^{1}H NMR ($CDCl_3$): δ 9.38 (s, 1H), 8.62 (s, 1H), 7.70 (d, J = 7.8 Hz, 2H), 7.56 (d, J = 7.8 Hz, 2H), 7.35 (m, 2H), 7.10 (m, 1H), 6.00 (m, 1H), 4.98 (m, 1H), 4.55 (m, 2H), 3.81 (m, 1H), 2.64 (s, 3H), 1.97 (d, J = 6.7 Hz, 3H). ^{13}C NMR (DMSO-d_6): δ 170.0, 154.2, 153.6, 149.2, 145.3, 142.9, 141.9, 140.9, 136.1, 134.4, 130.7, 129.1, 128.3, 126.9, 125.9, 125.0, 46.2,[68] 21.1, 18.9. HRMS: calcd 417.1498, found 417.1505, $C_{22}H_{21}N_6OS$.

*(S)-(8-Methyl-3-(2-methylthiazol-4-yl)-5,6-dihydro-[1,2,4]-triazolo[4,3-a]pyrazin-7(8H)-yl)(4-(thiophen-2-yl)phenyl)-methanone (**32**).* Starting from **112** and 4-(thiophen-2-yl)benzoyl chloride as per general procedure E to obtain 16 mg (41%). LCMS (method B) m/z 422 (M + 1). HPLC purity 93% (254 nm). Chiral LC (method G) 91.6% ee ($t_{R(S)}$ = 10.8 min, $t_{R(R)}$ = 14.7 min). ^{1}H NMR ($CDCl_3$): δ 7.99 (s, 1H), 7.69 (d, J = 7.9 Hz, 2H), 7.47 (d, J = 7.9 Hz, 2H), 7.37 (m, 2H), 7.12 (m, 1H), 5.77 (m, 1H), 4.83 (dd, J = 3.4, 13.5 Hz, 1 H), 4.60 (m, 1H), 4.24 (dt, J = 4.2, 12.8 Hz, 1H), 3.50 (m, 1H), 2.70 (s, 3H), 1.73 (d, J = 6.7 Hz, 3H). ^{13}C NMR ($CDCl_3$): δ 170.6, 166.7, 152.3, 148.4, 143.2, 143.1, 136.9, 133.9, 128.4, 127.8, 126.3, 126.1, 124.3, 119.5, 119.4, 48.4, 45.2, 38.1, 20.0, 19.3. HRMS: calcd 422.1109, found 422.1110, $C_{21}H_{20}N_5OS_2$.

*(3-(2-Methylthiazol-4-yl)-5,6-dihydro-[1,2,4]triazolo[4,3-a]-pyrazin-7(8H)-yl)(4-(thiophen-2yl)phenyl)methanone (**33**).* Starting from **113** and 4-(thiophen-2-yl)benzoyl chloride as per general procedure E to obtain 462 mg (49%). LCMS (method B) m/z 408 (M + 1). HPLC purity 95% (254 nm). ^{1}H NMR ($CDCl_3$): δ 7.98 (s, 1H), 7.69 (d, J = 8.0 Hz, 2H), 7.52 (d, J = 8.0 Hz, 2H), 7.39 (d, J = 3.6 Hz, 1H), 7.35 (d, J = 4.1 Hz, 1H), 7.12 (t, J = 4.0 Hz, 1H), 5.07 (s, 2H), 4.60 (t, J = 5.4 Hz, 2H), 4.08 (m, 2H), 2.76 (s, 3H). ^{13}C NMR ($CDCl_3$): δ 170.7, 166.8, 148.8, 147.8, 143.1, 142.7, 137.0, 132.7, 128.5, 128.3, 126.2, 124.4, 119.7 45.3,[68] 19.4. HRMS: calcd 408.0953, found 408.0947, $C_{20}H_{18}N_5OS_2$.

*(R)-(8-Methyl-3-(2-(trifluoromethyl)thiazol-4-yl)-5,6-dihydro-[1,2,4]triazolo[4,3-a]pyrazin-7(8H)-yl)(4-(thiophen-2-yl)phenyl)-methanone (**34**).* Starting from **114** and 4-(thiophen-2-yl)benzoyl chloride as per general procedure E to obtain 158 mg (96%). LCMS m/z (method B) 476 (M + 1). HPLC purity 99% (254 nm). Chiral LC (method K) 96.8% ee ($t_{R(S)}$ = 40.3 min, $t_{R(R)}$ = 55.4 min). ^{1}H NMR ($CDCl_3$): δ 8.49 (s, 1H), 7.71 (d, J = 8.3 Hz, 2H), 7.49 (d, J = 8.3 Hz, 2H), 7.37 (dd, J = 1.3, 3.6 Hz, 1H), 7.35 (dd, J = 1.0, 5.1 Hz, 1H), 7.12 (dd, J = 3.6, 5.1 Hz, 1H), 5.84 (m, 1H), 4.85 (dd, J = 3.0, 13.5 Hz, 1 H), 4.59 (m, 1H), 4.30 (dt, J = 4.2, 13.1 Hz, 1H), 3.56 (m, 1H), 1.76 (d, J = 6.9 Hz, 3H). ^{13}C NMR ($CDCl_3$): δ 170.5, 156.5 (d), 153.0, 147.1 (d), 144.9, 143.0 (d), 136.9, 133.3, 128.4, 127.8, 126.2, 126.1, 124.2 (d), 121.3, 117.7, 47.7, 45.2, 38.2, 19.9. ^{19}F NMR ($CDCl_3$): δ −58.3. HRMS: calcd 476.0827, found 476.0801, $C_{21}H_{17}N_5OF_3S_2$.

*(R)-(3-(2-Isopropylthiazol-4-yl)-8-methyl-5,6-dihydro-[1,2,4]-triazolo[4,3-a]pyrazin-7(8H)-yl)(4-(thiophen-2-yl)phenyl)-methanone (**35**).* Starting from **115** and 4-(thiophen-2-yl)benzoyl chloride as per general procedure E to obtain 102 mg (60%). LCMS (method B) m/z 450 (M + 1). HPLC purity >98% (254 nm). Chiral LC (method J) 99.8% ee ($t_{R(S)}$ = 5.6 min, $t_{R(R)}$ = 8.3 min). ^{1}H NMR ($CDCl_3$): δ 7.96 (s, 1H), 7.66 (d, J = 8.1 Hz, 2H), 7.44 (d, J = 8.1 Hz, 2H), 7.35 (d, J = 3.5 Hz, 1H), 7.31 (d, J = 5.0 Hz, 1H), 7.07 (m, 1H), 5.74 (m, 1H), 4.82 (dd, J = 3.2, 13.4 Hz, 1 H), 4.53 (m, 1H), 4.22 (m, 1H), 3.49 (m, 1H), 3.30 (h, J = 6.9 Hz, 1H), 1.70 (d, J = 6.8 Hz, 3H), 1.40 (d, J = 6.9 Hz, 6H). ^{13}C NMR ($CDCl_3$): δ 178.9, 170.1, 152.1, 148.3, 142.9, 142.3, 136.9, 133.4, 128.3, 127.6, 126.1, 126.0, 124.2, 118.6, 45.0,[68] 33.3, 23.0 (2s), 20.0 HRMS: calcd 450.1422, found 450.1432, $C_{23}H_{24}N_5OS_2$.

*(R)-(3-(2-Isopropyloxazol-4-yl)-8-methyl-5,6-dihydro-[1,2,4]-triazolo[4,3-a]pyrazin-7(8H)-yl)(4-(thiophen-2-yl)phenyl)-methanone (**36**).* Starting from **116** and 4-(thiophen-2-yl)benzoyl chloride as per general procedure E to obtain 1.22 g (36%). LCMS (method B) m/z 434 (M + 1). HPLC purity 96% (254 nm). Chiral LC (method G) 94.6% ee ($t_{R(S)}$ = 8.2 min, $t_{R(R)}$ = 12.1 min). ^{1}H NMR ($CDCl_3$): δ 8.23 (s, 1H), 7.70 (d, J = 7.8 Hz, 2H), 7.47 (d, J = 7.8 Hz, 2H), 7.37 (m, 2H), 7.12 (m, 1H), 5.75 (m, 1H), 4.78 (dd, J = 2.9, 12.9 Hz, 1 H), 4.58 (m, 1H), 4.20 (dt, J = 2.5, 11.9 Hz, 1H), 3.51 (m, 1H), 3.13 (hep, J = 6.9 Hz, 1H), 1.73 (d, J = 6.8 Hz, 3H), 1.38 (d, J = 6.9 Hz, 6H). ^{13}C NMR ($CDCl_3$): δ 169.9, 152.3, 146.0, 143.0, 138.0, 136.8, 133.4, 129.2, 128.4, 127.7, 126.2, 126.1, 124.3, 48.7, 44.5, 38.1, 28.6, 20.4, 20.0. HRMS: calcd 434.1651, found 434.1667, $C_{23}H_{24}N_5O_2S$.

*(R)-(8-Methyl-3-(4-methylthiazol-2-yl)-5,6-dihydro-[1,2,4]-triazolo[4,3-a]pyrazin-7(8H)-yl)(4-(thiophen-2-yl)phenyl)-methanone (**37**).* Starting from **117** and 4-(thiophen-2-yl)benzoyl chloride as per general procedure E to obtain 60 mg (40%). LCMS (method B) m/z 422 (M + 1). HPLC purity 95% (254 nm). Chiral LC (method G) 98.6% ee ($t_{R(S)}$ = 5.9 min, $t_{R(R)}$ = 6.6 min). ^{1}H NMR ($CDCl_3$): δ 7.69 (d, J = 8.0 Hz, 2H), 7.47 (d, J = 8.0 Hz, 2H), 7.39 (dd, J = 1.0, 3.5 Hz, 1H), 7.35 (dd, J = 1.0, 5.1 Hz, 1H), 7.12 (dd, J = 3.5, 5.1 Hz, 1H), 7.00 (s, 1H), 5.82 (m, 1H), 4.95 (dd, J = 3.3, 13.6 Hz, 1 H), 4.61 (m, 1H), 4.26 (dt, J = 3.7, 12.7 Hz, 1H), 3.54 (m, 1H),

DOI: 10.1021/jm5017413
J. Med. Chem. XXXX, XXX, XXX−XXX

2.49 (s, 3H), 1.75 (d, J = 6.9 Hz, 3H). ^{13}C NMR ($CDCl_3$): δ 170.8, 154.5, 154.2, 153.3, 147.7, 143.0, 136.8, 133.4, 128.4, 127.8, 126.3, 126.2, 124.3, 115.5, 48.3, 45.3, 37.4, 19.9, 17.3. HRMS: calcd 422.1109, found 422.1093, $C_{21}H_{20}N_5OS_2$.

*(R)-(8-Methyl-3-(3-methyl-1,2,4-oxadiazol-5-yl)-5,6-dihydro-[1,2,4]triazolo[4,3-a]pyrazin-7(8H)-yl)(4-(thiophen-2-yl)phenyl)-methanone (**38**).* Starting from **118** and 4-(thiophen-2-yl)benzoyl chloride as per general procedure E to obtain 423 mg (71%). LCMS (method B) m/z 407 (M + 1). HPLC purity 97% (254 nm). Chiral LC (method L) 97.3% ee ($t_{R(S)}$ = 7.8 min, $t_{R(R)}$ = 11.9 min). ^{1}H NMR ($CDCl_3$): δ 7.70 (d, J = 8.3 Hz, 2H), 7.47 (d, J = 8.3 Hz, 2H), 7.39 (dd, J = 1.0, 3.6 Hz, 1H), 7.36 (dd, J = 1.0, 5.1 Hz, 1H), 7.12 (dd, J = 3.5, 5.1 Hz, 1H), 5.84 (m, 1H), 4.80 (dd, J = 3.3, 13.6 Hz, 1 H), 4.64 (m, 1H), 4.27 (dt, J = 4.4, 12.8 Hz, 1H), 3.55 (m, 1H), 2.51 (s, 3H), 1.77 (d, J = 6.9 Hz, 3H). ^{13}C NMR ($CDCl_3$): δ 171.1, 167.8, 164.9, 154.6, 142.9, 140.9, 137.1, 133.0, 128.5, 127.8, 126.3, 126.3, 124.4, 48.3, 45.3, 37.4, 19.9, 17.3. HRMS: calcd 407.1290, found 407.1291, $C_{20}H_{19}N_6O_2S$.

*(R)-(8-Methyl-3-(3-methyl-1,2,4-thiadiazol-5-yl)-5,6-dihydro-[1,2,4]triazolo[4,3-a]pyrazin-7(8H)-yl)(4-(thiophen-2-yl)phenyl)-methanone (**39**).* Starting from **119** and 4-(thiophen-2-yl)benzoyl chloride as per general procedure E to obtain 93 mg (40%). LCMS (method B) m/z 423 (M + 1). HPLC purity 95% (254 nm). Chiral LC (method L) 94.1% ee ($t_{R(S)}$ = 5.8 min, $t_{R(R)}$ = 7.0 min). ^{1}H NMR ($CDCl_3$): δ 7.71 (d, J = 8.4 Hz, 2H), 7.48 (d, J = 8.4 Hz, 2H), 7.39 (dd, J = 1.1, 3.6 Hz, 1H), 7.36 (dd, J = 1.1, 5.1 Hz, 1H), 7.12 (dd, J = 3.6, 5.1 Hz, 1H), 5.83 (m, 1H), 4.92 (dd, J = 3.1, 13.7 Hz, 1 H), 4.63 (m, 1H), 4.28 (dt, J = 4.3, 12.8 Hz, 1H), 3.54 (m, 1H), 2.73 (s, 3H), 1.77 (d, J = 6.9 Hz, 3H). ^{13}C NMR ($CDCl_3$): δ 174.5, 173.9, 170.8, 154.1, 145.7, 142.9, 137.0, 133.2, 128.5, 127.8, 126.3, 126.2, 124.4, 47.9, 45.3, 37.5, 19.9, 19.0. HRMS: calcd 423.1062, found 423.1057, $C_{20}H_{19}N_6O_1S_2$.

Method for LH Studies. Castrated male rat model using male Sprague–Dawley rats (150–175 g, N = 4–6/group) was used to assess circulating LH levels in the presence of test compounds. Two rats were housed per cage in a temperature-controlled room (22 ± 2 °C) and 50 ± 5% relative humidity with a 12 h/12 h light/dark cycles. After basal sampling (T_0) at a similar time (9h00 ± 1 h) each test day, a single dose of test compound was administered by iv bolus or oral gavage. Blood samples were then collected via tail vein bleed postdosing at T = 45, 90, 150, 300, and 420 min time points. The thus obtained samples were then drawn into tubes containing K_3EDTA and centrifuged immediately. Plasma samples were collected and stored in a −80 °C freezer until assayed. Serum LH levels were determined using radioimmunoassay kit from RIAZEN, rat LH, Zentech (Liège, Belgium). Baseline was defined as the initial basal blood sample.

PK Analyses. Rat PK studies were conducted on male Sprague–Dawley rats (250 ± 20 g). Three to four rats were housed per cage in a temperature-controlled room (22 ± 2 °C) and 50 ± 10% relative humidity with a 12 h/12 h light/dark cycles. For iv bolus administration, the formulated test compound was administrated at a single dose (1 mg/kg; N = 3) with blood samples drawn into tubes containing K_3EDTA at the following time points postdosing: T = 1, 5, 15, 90, 150, 210, 300, and 390 min and 24 h. For oral administration, the formulated test compound was administrated by gavage at 3 mg/kg (N = 4 rats) with blood samples drawn in EDTA tubes at the following time points postdosing: T = 5, 15, 45, 90, 150, 210, 300, and 390 min and 24 h. Plasma samples were then immediately isolated by centrifugation and stored at −20 °C prior to analysis. Plasma concentrations were determined by LCMS/MS, and data were analyzed by noncompartmental methods using PK Solutions 2.0 software (Summit Research Services, Colorado, USA).

Monkey PK studies were outsourced to PHARMARON (China) and performed on male cynomolgus monkeys castrated at sexual maturity and tested >6 months after castration (4.5 ± 0.5 kg; N = 4); monkeys tested repeatedly tested under all conditions with a minimum of 1 week washout period between treatments. Intravenous (bolus) dosing 10 mg/kg formulated in physiological saline with 9% 2-hydroxypropyl-β-cyclodextrin. Orally dosed analogue (5, 20 mg/kg) was formulated in 0.5% methylcellulose/water. Over the 8 h test period, at the time points indicated in Figure 6, blood samples were collected into centrifuge tubes containing K_3EDTA and plasma samples were then immediately isolated by centrifugation and stored at −20 °C prior to analysis. Plasma concentrations were determined by LCMS/MS, and data were analyzed by noncompartmental methods using WinNonlin Pro (Pharsight Corp., Mountain View, CA).

Plasma Protein and Brain Nonspecific Binding. Equilibrium dialysis approach was employed to determine plasma protein binding (f_u) and nonspecific brain binding (bf_u). Using a RED (Rapid Equilibrium Dialysis) device insert, which was made of two side-by-side chambers separated by an O-ring-sealed vertical cylinder of dialysis membrane (MW cutoff ca. 8000 Da), plasma or brain homogenate containing test compound (at 5 μM) was added to one chamber, while PBS pH 7.4 buffer was added to the second. After 4 h incubation at 37 °C with agitation, aliquots from both chambers were then analyzed using LCMS/MS to determine both free and bound levels.

■ ASSOCIATED CONTENT

Ⓢ Supporting Information

Additional experimental details for CYP P450 profiling, hERG patch-clamp assay, X-ray crystallographic reports (compds **31**–**33**) as well as additional data related to prototropic tautomerism in **4**. This material is available free of charge via the Internet at http://pubs.acs.org.

Accession Codes

X-ray crystallographic structures **31**, **32**, and **33** have been deposited at the Cambridge Crystallographic Data Centre (**31**, CCDC 1046850; **32**, CCDC 1046847; **33**, CCDC 1046852).

■ AUTHOR INFORMATION

Corresponding Author

*Phone: +32 71 348 502. E-mail: hhoveyda@euroscreen.com.

Notes

The authors declare no competing financial interest.

■ ACKNOWLEDGMENTS

This work was supported by the Ministry of Sustainable Development and Public Works, Walloon Region, Belgium. We thank our colleagues in the in vitro and in vivo profiling teams as well as the pharmacology team for conducting studies in support of this work. The early contributions of Dr. Vladimir Trukhan and his team, formerly at ChemBridge Corporation, Moscow, Russia, are gratefully acknowledged. Prof. Tony Plant and Dr. Suresh Ramaswamy (University of Pittsburgh) are noted for their assistance in assaying LH from monkey plasma samples. We also extend our debt of gratitude to Dr. Koen Robeyns (Université Catholique de Louvain, Belgium) for X-ray crystallographic characterization of analogues **31**–**33** and to Dr. Lisa Haigh (Imperial College, London, UK) for obtaining HRMS data on the analogues disclosed. Finally, we are grateful to Dr. Rob Scoffin (Cresset Biomolecular Discovery, UK) for help with Figure 3 as well as to Dr. Rob Scoffin and Dr. Mark Ator (Teva Pharmaceuticals) for proofreading this manuscript.

■ ABBREVIATIONS USED

ADME, absorption distribution metabolism and excretion; AUC, area under curve; bf_u, brain fraction unbound; ARC, arcuate nucleus; BMD, bone mineral density; B/P, brain-to-plasma ratio; Boc, *tert*-butyl carbamate; CL_T, total systemic clearance rate; C_{max}, maximal concentration; CVO, circumventricular organ; CYP, cytochrome P-450; %F, absolute oral availability; DMB, 2,4-dimethoxybenzyl; FSH, follicle-stimulat-

DOI: 10.1021/jm5017413
J. Med. Chem. XXXX, XXX, XXX–XXX

ing hormone; f_u, plasma fraction unbound; GnRH, gonadotropin releasing hormone; GnIH-R, gonadotropin inhibitory hormone receptor; GPCR, G-protein coupled receptor; HBA, hydrogen-bond acceptor; HBD, hydrogen-bond donor; hERG, human ether-à-go-go related gene; HLM, human liver microsomes; HPG, hypothalamic pituitary gonadal; HTS, high-throughput screening; iv, intravenous; LH, luteinizing hormone; LLE, ligand lipophilicity efficiency; iv, intravenous administration; K_i, radioligand binding equilibrium constant; KOR, κ-opioid receptor; KNDy, kisspeptin-neurokinin B-dynorphin A neuron; NKB, neurokinin B; NK_3R, neurokinin-3 receptor; PD, pharmacodynamic; PG, protective group; Pgp, P-glycoprotein; PK, pharmacokinetic; POC, proof-of-concept; RLM, rat liver microsomes; SAR, structure−activity relationship; $T_{1/2}$, elimination half-life; UF, uterine fibroids; V_{ss}, steady-state volume of distribution

REFERENCES

(1) NKB peptide = DMHDFF**V**GLM-NH_2. Neurokinins (NKs), also known as tachykinins (TAC or TK), are a family of small peptides with a common C-terminal sequence of F**X**GLM-NH_2, where **X** = branched aliphatic (V, I), or aromatic (F, Y) amino acid. Senktide = succinyl-DFMe-FGLM-NH_2. The C-terminal region is believed to be responsible for activating the receptor. Substance P (SP), NKA, and NKB have the highest affinities for the NK_1, NK_2, and NK_3 receptors, respectively. As recommended by Regoli et al., the term tachykinin refers to non-mammalian sources, whereas mammalian peptides in this family are called neurokinins. See: Regoli, D.; Boudon, A.; Fauchére, J.−L. Receptors and antagonists for substance P and related peptides. *Pharmacol. Rev.* **1994**, *46*, 551−599.

(2) Spooren, W.; Riemer, C.; Meltzer, H. NK3 receptor antagonists: the next generation of antipsychotics? *Nature Rev. Drug Discovery* **2005**, *4*, 967−975 and references cited therein.

(3) Dawson, L. A.; Porter, R. A. Progress in the development of neurokinin 3 modulators for the treatment of schizophrenia: molecule development and clinical progress. *Future Med. Chem.* **2013**, *5*, 1525−1546 and references therein.

(4) For a few recent review articles, see: (a) Navarro, V. M. New insights into the control of pulsatile GnRH release: the role of Kiss1/neurokinin B neurons. *Front. Endocrinol.* **2012**, *3*, 1−9. (b) Grachev, P.; Millar, R. P.; O'Byrne, K. T. The role of neurokinin B signaling in reproductive endocrinology. *Neuroendocrinology* **2013**, *99*, 7−17. (c) Skorupskaite, K.; George, J. T.; Anderson, R. A. The kisspeptin-GnRH pathway in human reproductive health and disease. *Hum. Reprod. Update* **2014**, *0*, 1−16.

(5) Rance, N. E.; Krajewski, S. J.; Smith, M. A.; Cholanian, M.; Dacks, P. A. Neurokinin B and the hypothalamic regulation of reproduction. *Brain Res.* **2010**, *1364*, 116−128.

(6) Note that KNDy neurons are devoid of GPR54 (or Kiss 1-R), which is mainly expressed on the GnRH neurons located in the medial preoptic area (mPOA) in hypothalamus projecting into the median eminence (ME). These observations are anatomically consistent with the downstream role of GPR54/kisspeptin vis-à-vis NKB/NK_3R (Figure 2).

(7) In this context, the colocalization within KNDy neurons of estrogen receptor alpha (ERα, or GPR30) and progesterone receptor (PR) is noteworthy based on its role in the HPG feedback loop (Figure 2), a subject that is under active investigation in this field.[5]

(8) (a) Structure **3** is the "compound **27**" (drawn incorrectly in racemic form) in the reference cited under footnote 3.. (b) Hoveyda, H.; Roy, M.-O.; Fraser, G.; Dutheuil, G. Preparation of [1,2,4]-triazolo[4,3-*a*]pyrazine compounds as selective NK-3 receptor antagonists, pharmaceutical compositions containing same, and their methods of use. PCT International Application WO121137-A1, October 6, 2011. (c) Hoveyda, H.; Dutheuil, G.; Fraser, G.; Roy, M.-O. ; El Bousmaqui, M.; Batt, F. Preparation of novel chiral 7-acyl-8-substituted-5,6,7,8-tetrahydro-[1,2,4]triazolo[4,3-*a*]pyrazines as selective NK-3 receptor antagonists, pharmaceutical composition, methods for use in NK-3 receptor mediated disorders and chiral synthesis thereof. PCT International Application WO050424-A1, April 11, 2013.

(9) Fraser, G., Khoja, Z.; Roy, M.-O.; Hoveyda, H., Blanc, S.; Tannenbaum, G. NK3 receptor signaling maintains tonic activation of the hypothalamic-pituitary-gonadal axis. Presented at ENDO Meeting, Boston, MA, 2011, P2-260.

(10) Topaloglu, A. K.; Reimann, F.; Guclu, M.; Guclu, M.; Yalin, A. S.; Kotan, L. D.; Porter, K. M.; Serin, A.; Mungan, N. O.; Cook, J. R.; Ozbek, M. N.; Imamoglu, S.; Akalin, N. S.; Yuksel, B.; O'Rahilly, S.; Semple, R. K. *TAC3* and *TACR3* mutations in familial hypogonadotropic hypogonadism reveal a key role for Neurokinin B in the central control of reproduction. *Nature Genet.* **2009**, *41*, 354−358 Note: *TAC3* = NKB and *TACR3* = NK_3R; also see footnote 1.

(11) Mice lacking functional NK_3R are capable of pubertal development and fertility in contrast with observations in humans. However, also see the following recent studies related to the latter point: Yang, J. J.; Caligioni, C. S.; Chan, Y.-M.; Seminara, S. B. Uncovering novel reproductive defects in neurokinin B receptor null mice: closing the gap between mice and men. *Endocrinology* **2012**, *153*, 1498−1508.

(12) For a recent review, see: Kim, J. J.; Kurita, T.; Bulun, S. E. Progesterone action in endometrial cancer, endometriosis, uterine fibroids and breast cancer. *Endocr. Rev.* **2013**, *34*, 1−33.

(13) See Engel, J. B.; Schally, A. V. Drug Insight: clinical use of agonists and antagonists of luteinizing-hormone-releasing hormone (LHRH). *Nature Clin. Pract.* **2007**, *3*, 157−167 and references therein..

(14) For a review, see: Betz, S. F.; Zhu, Y.-F.; Chen, C.; Struthers, R. S. Non-peptide gonadotropin-releasing hormone receptor antagonists. *J. Med. Chem.* **2008**, *51*, 3331−3348.

(15) (a) Pierce, S. J.; Gazvani, M. R.; Farquharson, R. G. Long-term use of gonadotropin-releasing hormone analogs and hormone replacement therapy in the management of endometriosis: a randomized trial with a 6-year follow-up. *Fertil. Steril.* **2000**, *74*, 964−968. (b) Riggs, M. M.; Bennetts, M.; van der Graaf, P. H.; Martin, S. W. Integrated pharmacometrics and systems pharmacology model-based analyses to guide GnRH receptor modulator development for management of endometriosis. *Pharmacometrics Syst. Pharmacol.* **2012**, *1*, e11. (c) The FDA guidance related to BMD loss with plasma estradiol E_2 < 20 pg/mL is supported by literature reports such as: Barbieri, R. L. Hormone treatment for endometriosis: the estrogen threshold hypothesis. *Am. J. Obstet. Gynecol.* **1992**, *166*, 740−745.

(16) Guo, S.-W. Recurrence of endometriosis and its control. *Hum. Reprod. Update* **2009**, *4*, 441−461 and references therein.

(17) (a) Marshall, J. C.; Griffin, M. L. The role of changing pulse frequency in the regulation of ovulation. *Hum. Reprod.* **1993**, *8*, 57−61. (b) Thompson, I. R.; Kaiser, U. B. GnRH pulse frequency-dependent differential regulation of LH and FSH gene expression. *Mol. Cell. Endocrinol.* **2014**, *385*, 28−35 To recall, in males, the GnRH pulse frequency is constant, whereas in females, it is variable during menstrual cycle with the characteristic GnRH surge just prior to ovulation.

(18) Francou, B.; Bouligand, J.; Voican, A.; Amazit, L.; Trabado, S.; Fagart, J.; Meduri, G.; Brailly-Tabard, S.; Chanson, P.; Lecomte, P.; Guiochon-Mantel, A.; Young, J. Normosomic congenital hypogonadotropic hypogonadism due to *TAC3/TACR3* mutations: characterization of neuroendocrine phenotypes and novel mutations. *PLoS One* **2011**, *6*, e25614.

(19) For a recent review, see: Solozarno, C. M.; Beller, J. P.; Abshire, M. Y.; Collins, J. S.; McCartney, C. R.; Marshall, J. C. Neuroendocrine dysfunction in polycystic ovary syndrome. *Steroids* **2012**, *77*, 332−337.

(20) Blank, S. K.; McCartney, C. R.; Marshall, J. C. The origins and sequelae of abnormal neuroendocrine function in polycystic ovary syndrome. *Hum. Reprod. Update* **2006**, *4*, 351−361.

(21) Millar, R. P.; Newton, C. L. Current and future applications of GnRH, kisspeptin and neurokinin B analogues. *Nature Rev. Endocrinol.* **2013**, *9*, 451−466.

DOI: 10.1021/jm5017413
J. Med. Chem. XXXX, XXX, XXX−XXX

(22) Emonds-Alt, X.; Bichon, D.; Ducoux, J. P.; Heaulme, M.; Miloux, B.; Poncelet, M.; Proietto, V.; Van Broeck, D.; Vilain, P.; Neliat, G.; Soubrié, P.; Le Fur, G.; Brelère, J. C. SR142801, the first potent non-peptide antagonist of the tachykinin NK3 receptor. *Life Sci.* **1995**, *56*, PL27−PL32.
(23) Sarau, H. M.; Griswold, D. E.; Potts, W.; Foley, J. J.; Schmidt, D. B.; Webb, E. F.; Martin, L. D.; Brawner, M. E.; Elshourbagy, N. A.; Medhurst, A. D.; Giardina, G. M.; Hay, D. W. P. Nonpeptide tachykinin receptor antagonists: I. Pharmacological and pharmacokinetic characterization of SB223412, a novel, potent and selective neurokinin-3 receptor antagonist. *J. Pharmacol. Exp. Ther.* **1997**, *281*, 1303−1311.
(24) Malherbe, P.; Ballard, T. M.; Ratni, H. Tachykinin neurokinin 3 receptor antagonist: a patent review (2005−2010). *Expert Opin. Ther. Pat.* **2011**, *21*, 637−655 and references cited therein.
(25) (a) Litman, R. E.; Smith, M. A.; Desai, D. G.; Simpson, T.; Sweitzer, D.; Kanes, S. J. The selective neurokinin 3 antagonist AZD2624 does not improve symptoms or cognition in schizophrenia: A proof-of-principle study. *J. Clin. Psychopharmacol.* **2014**, *34*, 199−204. (b) Gilmour, P. S.; Tony, H. O.; Rahul, K.; Webber, L. NK3 receptor antagonist compound for use in a method for the treatment of polycystic ovary syndrome. PCT International Application WO170648-A1, October 23, 2014.
(26) Hoveyda, H. R.; Roy, M.-O.; Blanc, S.; Noël, S.; Salvino, J. M.; Ator, M. A.; Fraser, G. Discovery of 3-aryl-5-acylpiperazinyl-pyrazoles as antagonists to the NK_3 receptor. *Bioorg. Med. Chem. Lett.* **2011**, *21*, 1991−1996.
(27) Le Poul, E.; Hisada, S.; Mizuguchi, Y.; Dupriez, V. J.; Burgeon, E.; Detheux, M. Adaptation of aequorin functional assay to high throughput screening. *J. Biomol. Screening* **2002**, *7*, 57−65.
(28) ^{1}H NMR spectroscopic data for **4** clearly suggested presence of prototropic tautomerism. See Supporting Information for further details.
(29) Cheesright, T.; Mackey, M.; Rose, S.; Vinter, A. Molecular field extrema as descriptors of biological activity: definition and validation. *J. Chem. Inf. Model.* **2006**, *46*, 665−676.
(30) Hoveyda, H. R.; Fraser, G. L.; Dutheuil, G.; El Bousmaqui, M.; Korac, J.; Lenoir, F.; Lapin, A.; Noël, S. Discovery and optimization of novel antagonists to the human neurokinin-3 receptor for the treatment of sex-hormone disorders (Part II). *ACS Med. Chem. Lett.*, to be submitted for publication.
(31) See for example: (a) Nelson, P. J.; Potts, K. T. 1,2,4-Triazoles VI. The synthesis of some *s*-triazolo[4,3-*a*]pyrazines. *J. Org. Chem.* **1962**, *27*, 3243−3248. and (b) McCort, G. A.; Pascal, J. C. A rapid and efficient synthesis of imidazo [1,2-*a*] and 1,2,4-triazolo[4,3-*a*]-piperazine carboxylic acids. *Tetrahedron Lett.* **1992**, *33*, 4443−4446.
(32) (a) Kende, A. S.; Fan, J.; Chen, Z. A concise total synthesis of (±)-alantrypinone by a novel hetero-Diels−Alder reaction. *Org. Lett.* **2003**, *5*, 3205−3208. (b) Sánchez, J. D.; Ramos, M. T.; Avendano, C. Intramolecular Friedel−Crafts-type reactions involving *N*-acyliminium ions derived from glycine templates. *J. Org. Chem.* **2001**, *66*, 5731−5735.
(33) Meerwein, H. Triethyloxonium fluoroborate. *Org. Synth.* **1966**, *46*, 113 Other related reagents such as Me_3OBF_4, Me_2SO_4, and Et_2SO_4 were investigated and found to be less effective.
(34) Lipinski, C. A.; Lombardo, F.; Dominy, B. W.; Feeney, P. J. Experimental and computational approaches to estimate solubility and permeability in drug discovery and development settings. *Adv. Drug Delivery Rev.* **1997**, *23*, 3−25.
(35) Hann, M. Molecular obesity, potency and other addictions in drug discovery. *MedChemComm* **2011**, *2*, 349−355.
(36) (a) High safety risk space defined as molecules with clogP > 3 and TPSA < 75 Å^2 based on data for 245 preclinical Pfizer compounds. See: Hughes, J. D.; Blagg, J.; Price, D. A.; Bailey, S.; DeCrescenzo, G. A.; Devraj, R. V.; Ellsworth, E.; Fobian, Y. M.; Gibbs, M. E.; Gilles, R. W.; Greene, N.; Huang, E.; Krieger-Burke, T.; Loesel, J.; Wager, T.; Whiteley, L.; Zhang, Y. Physicochemical drug properties associated with in vivo toxicological outcomes. *Bioorg. Med. Chem. Lett.* **2008**, *18*, 4872−4875. (b) A more recent Pfizer study reports that the low predictability of the so-called 3/75 rule in exploratory toxicology studies (ETS) is due to the lack of consideration of the therapeutic index and human efficacious concentration (C_{eff} levels). However, these authors also pointed out that compounds that were most potent in vitro and had high LLE, were the most likely to survive ETS. See: Wager, T.; Kormos, B. L.; Brady, J. T.; Will, Y.; Aleo, M. D.; Stedman, D. B.; Kuhn, M.; Chandrasekaran, R. Y. Improving the odds of success in drug discovery: choosing the best compounds for in vivo toxicology studies. *J. Med. Chem.* **2013**, *56*, 9771−9779.
(37) Stating that compounds with clogP < 4 and MW < 400 on average possess a more favorable ADMET profile, based on analysis of approximately 30000 neutral, basic, acidic and zwitterionic molecules at GSK. See: Glesson, M. P. Generation of a set of simple, interpretable ADMET rules of thumb. *J. Med. Chem.* **2008**, *51*, 817−834.
(38) (a) Leeson, P. D.; Empfield, J. R. Reducing the risk of drug attrition associated with physicochemical properties. *Annu. Rep. Med. Chem.* **2010**, *45*, 381−391. and references therein. (b) Gleeson, M. P.; Hersey, A.; Montanari, D.; Overington, J. Probing the links between in vitro potency, ADMET and physicochemical parameters. *Nature Rev. Drug Discovery* **2011**, *11*, 197−208.
(39) (a) Leeson, P. D.; Springthorpe, B. The influence of drug-like concepts in decision-making in medicinal chemistry. *Nature Rev. Drug Discovery* **2007**, *6*, 881−890. (b) Hopkins, A. L.; Keserü, G. M.; Lesson, P. D.; Rees, D. C.; Reynolds, C. H. The role of ligand efficiency metrics in drug discovery. *Nature Rev. Drug Discovery* **2014**, *13*, 105−121.
(40) (a) Lovering, F.; Bikker, J.; Humblet, C. Escape from flatland: increasing saturation as an approach to improving clinical success. *J. Med. Chem.* **2009**, *52*, 6752−6756. (b) Ritchie, T. J.; Macdonald, S. J. F. The impact of aromatic ring count on compound developability—are too many aromatic rings a liability in drug design? *Drug Discovery Today* **2009**, *14*, 1011−1019. (c) Luker, T.; Alcaraz, L.; Chohan, K. K.; Blomberg, N.; Brown, D. S.; Butlin, R. J.; Elebring, T.; Griffin, A. M.; Guile, S.; St-Gallay, S.; Swahn, B.-M.; Swallow, S.; Waring, M. J.; Wenlock, M. C.; Leeson, P. D. Strategies to improve in vivo toxicology outcomes for basic candidate drug molecules. *Bioorg. Med. Chem. Lett.* **2011**, *21*, 5673−5679.
(41) Hill, A. P.; Young, R. J. Getting physical in drug discovery: a contemporary perspective on solubility and hydrophobicity. *Drug Discovery Today* **2010**, *15*, 648−655.
(42) Klabunde, T. Chemogenomics approaches to ligand design. In *Ligand Design for G Protein-Coupled Receptors*; Rognan, D., Ed.; Wiley-VCH: Darmstadt, Germany, 2006; pp 115−135 and references therein.
(43) ΔLLE values throughout this report are calculated using log $D_{7.4}$-derived LLE values, except when noted as ΔLLE_{clogP}, indicating that clogP-derived LLE values were used.
(44) For a review, see: Barreiro, E. J.; Kümmerle, A. E.; Fraga, C. A. The methylation effect in medicinal chemistry. *Chem. Rev.* **2011**, *111*, 5215−5246.
(45) For example, ΔpK_a values for mono-methyl substituted pyridines (vs unsubstituted pyridine) in water are as follows: 2-Me (ΔpK_a = 0.8), 3-Me (0.5), 4-Me (0.8). Hence, analogues **21** (2-Me) and **24** (4-Me), although similar in terms of their basicity (ΔpK_a = 0) were 1.1−log apart in bioactivity (ΔpK_i, ΔpIC_{50} = 1.1; **21** > **24**). (ΔpK_a values cited from: Katritzky, A. R.; Pozharskii, A. F. *Handbook of Heterocyclic Chemistry*; Pergamon: Amsterdam, 2000; p 178.).
(46) Jamieson, C.; Moir, E. M.; Rankovic, Z.; Wishart, G. Strategies and tactics for hERG optimization. In *Antitargets*; Vaz, R. J., Klabunde, T., Eds.; Wiley-VCH: Darmstadt, Germany, 2008; pp 423−456.
(47) The 2-methylpyridine moiety (pK_a ca 5.2) in **29** represents the most basic Ring D among analogues discussed herein. Comparative pK_a values for *unsubstituted* heteroaryl rings in question are as follows: pyrazine $pK_a \approx 0.6$ (**30**), thiazole $pK_a \approx 2.5$ (**31**−**35**), thiadiazole $pK_a \approx -4.9$ (**39**) (pK_a values were obtained from the CommonOrganicChemstry.com resources web page http://www.commonorganicchemistry.com/Sidebar/Resources.htm (accessed February 24, 2015).

DOI: 10.1021/jm5017413
J. Med. Chem. XXXX, XXX, XXX−XXX

(48) In a survey of crystallographic data, only 86 (4.75%) of the 1811 Y−S−Z substructures that occur with N−H or O−H donors were found with S···H−N,O within S···H < 2.9 Å. See: Allen, F. H.; Bird, C. M.; Rowland, R. S.; Raithby, P. R. Hydrogen-bond acceptor and donor properties of divalent sulfur (Y−S−Z and R−S−H). *Acta Crystallogr., Sect. B: Struct. Sci.* **1997**, *B53*, 696−701.

(49) The degree of amino acid sequence identity within human receptors shows the following trend: 51% between (NK_1R vs NK_3R) > 47% (NK_1R vs NK_2R) > 41% (NK_1R vs NK_2R). See: Almeida, T. A.; Rojo, J.; Nieto, P. M.; Hernandez, M.; Martin, J. D.; Candenas, M. L. Tachykinins and tachykinin receptors: structure and activity relationships. *Curr. Med. Chem.* **2004**, *11*, 2045−2081.

(50) Smith, J. T.; Clarke, I. J. Gonadotropin inhibitory function in mammals. *Trends Endocrinol. Metab.* **2009**, *21*, 255−260.

(51) Of the two gold standards, osanetant (**1a**) displayed a particularly poor off-target selectivity profile. For instance, even at 1 μM it displayed ≥ 50% inhibition vs muscarinic (M3, M4 and M5), dopamine D3, opioid (δ, κ and μ), serotonin ($5HT_{1A, 2A, 2B}$ and $5HT_7$ subtypes), histamine H2, as well as on norepinephrine and dopamine transporters. Talnetant (**2a**) showed ≥60% inhibition against adenosine (A1, A3), benzodiazepine, CCK2 and prostanoid (EP4).

(52) Kerns, E. H.; Di, L. *Drug-Like Properties: Concepts, Structure Design and Methods: from ADME to Toxicity Optimization*; Elsevier: Burlington, MA, 2008; p 233.

(53) See for example: (a) Ward, K. M.; Hardy, L. B.; Kehler, J. R.; Azzarano, L. M.; Smith, B. R. Apparent absolute oral bioavailability in excess of 100% for a vitronectin receptor antagonist (SB-265123) in rat. II. Studies implicating transporter-mediated intestinal secretion. *Xenobiotica* **2004**, *34*, 367−377. (b) Roffey, S. J.; Cole, S.; Comby, P.; Gibson, D.; Jezequel, S. G.; Nedderman, A. N. R.; Smith, D. A.; Walker, D. K.; Wood, N. The disposition of voriconazole in mouse, rat, rabbit, guinea pig, dog and human. *Drug Metab. Dispos.* **2003**, *31*, 731−741. (c) Godbole, A. M.; Ramalingam, S.; Ramamurthy, V. P.; Khandelwal, A.; Bruno, R. D.; Upreti, V. V.; Gediya, L. K.; Purushottamachar, P.; Mbatia, H. W.; Addya, S.; Ambulos, N.; Njar, V. C. O. VN/14-1 induces ER stress and autophagy in HP-LTLC human breast cancer cells and has excellent oral pharmacokinetic profile in female Sprague−Dawley rats. *Eur. J. Pharmacol.* **2014**, *734*, 98−104 and references therein.

(54) Benet, L.Z.; Perotti, B. Y. T. Drug absorption, distribution and elimination. In *Burger's Medicinal Chemistry and Durg Discovery, Vol. 1: Prinicples and Practice*; Wolf, M. E., Ed.; John Wiley & Sons: New York, 1995; p 122.

(55) Kerns, E. H.; Di, L. *Drug-Like Properties: Concepts, Structure Design and Methods: From ADME to Toxicity Optimization*; Elsevier: Burlington, MA, 2008; pp 122−135 and references therein.

(56) Trainor, G. L. The importance of plasma protein binding in drug discovery. *Expert Opin. Drug Discovery* **2007**, *2*, 51−64 and references therein.

(57) (a) Di, L.; Rong, H.; Feng, B. Demystifying brain penetration in central nervous system drug discovery. *J. Med. Chem.* **2013**, *56*, 2−12. (b) Liu, X.; Wright, M.; Hop, C. E. C. A. Rational use of plasma protein and tissue binding data in drug design. *J. Med. Chem.* **2014**, *57*, 8238−8248.

(58) Kratochwil, N. A.; Huber, W.; Muller, F.; Kansy, M.; Gerber, P. R. Predicting plasma protein binding of drugs: a new approach. *Biochem. Pharmacol.* **2002**, *64*, 1355−1374.

(59) Hitchcock, S. A.; Pennington, L. D. Structure−brain exposure relationships. *J. Med. Chem.* **2006**, *49*, 7559−7583 and refs 17 18, and 19 cited therein.

(60) Although compartmental equilibrium (including influences of transporters) has not been formally established herein, given the good agreement between $(B/P)_u$ values at 10 min and 1 h time points, the measured values likely reflect a state of equilibrium.

(61) In case of talnetant (**2a**), the $(B/P)_u$ > 1 reflects its 33-fold higher bf_u (0.01) against f_u (0.0003). With compd **3**, due to its poor solubility, DMA/PEG-400 formulation had to be used (as footnoted in Table 6) that may impact the values discussed herein.

(62) Fraser, G. L.; Hoveyda, H. R.; Roy, M.-O.; Ramaswamy, S.; Plant, T. M.; Smith, J.; Clarke, I. NK3 receptor signaling maintains LH pulse secretion, mean plasma LH levels and induces testicular testosterone release; studies in cynomolgus monkey (*Macaca fascicularis*) and Corriedale ewe. Presented at ENDO Meeting, San Francisco, CA, 2013, SAT-146.

(63) (a) Morita, S.; Miyata, S. Accessibility of low-molecular-mass molecules to the median eminence and arcuate hypothalamic nucleus of adult mouse. *Cell Biochem. Funct.* **2013**, *3*, 668−677. (b) Ciofi, P. The arcuate nucleus as a circumventricular organ in the mouse. *Neurosci. Lett.* **2011**, *487*, 187−190.

(64) Boron, W. F.; Boulpaep, E. L. *Medical Physiology: A Cellular and Molecular Approach*; Saunders: Philadelphia, 2003; pp 408−409.

(65) Pinilla, L.; Aguilar, E.; Dieguez, C.; Millar, R. P.; Tena-Sempere, M. Kisspeptins and reproduction: physiological roles and regulatory mechanisms. *Physiol. Rev.* **2012**, *92*, 1235−1316.

(66) Fraser, G. L.; Hoveyda, H. R.; Rao, A.; Clarke, I. J.; Ramaswamy, S.; Plant, T. M.; Rose, C.; Millar, R. P. The NK3 receptor antagonist ESN364 slows pulsatile LH secretion and moderates levels of ovarian hormones throughout the menstrual cycle. *Endocrinology*, to be submitted for publication.

(67) Fraser, G. L. Discovery and development of ESN364, a novel NK3 antagonist for the treatment of hormone-dependent pathologies. Presented at ENDO Meeting, Chicago, IL, 2014, S44-2.

(68) Due to slow relaxation, two of three Csp^3 carbons in the piperazine Ring B were not readily detectable.

DOI: 10.1021/jm5017413
J. Med. Chem. XXXX, XXX, XXX−XXX